Fall 2014

Development of planar patch clamp with potentiometric calcium ion-selective electrode

Kul Inn
Purdue University

Graduate School Form 30
(Updated 11/20/2014)

PURDUE UNIVERSITY
GRADUATE SCHOOL
Thesis/Dissertation Acceptance

This is to certify that the thesis/dissertation prepared

By Kul Inn

Entitled
DEVELOPMENT OF PLANAR PATCH CLAMP WITH POTENTIOMETRIC CALCIUM ION-SELECTIVE ELECTRODE

For the degree of Doctor of Philosophy

Is approved by the final examining committee:

Jenna L. Rickus

D. Marshall Porterfield

Jong Hyun Choi

Laurent L. Couetil

To the best of my knowledge and as understood by the student in the Thesis/Dissertation Agreement, Publication Delay, and Certification/Disclaimer (Graduate School Form 32), this thesis/dissertation adheres to the provisions of Purdue University's "Policy on Integrity in Research" and the use of copyrighted material.

Jenna L. Rickus

Approved by Major Professor(s): _____

Approved by: Bernard Engel 12/02/2014

Head of the Department Graduate Program Date

DEVELOPMENT OF PLANAR PATCH CLAMP WITH POTENTIOMETRIC CALCIUM ION-SELECTIVE ELECTRODE

A Dissertation

Submitted to the Faculty

of

Purdue University

by

Kul Inn

In Partial Fulfillment of the

Requirements for the Degree

of

Doctor of Philosophy

December 2014

Purdue University

West Lafayette, Indiana

To my parents

ACKNOWLEDGEMENTS

I wish to express my greatest gratitude to my Ph.D. advisory committee. I sincerely wish to thank Prof. D.Marshall Porterfield for his support, encouragement, and patience in guiding me throughout my Ph.D. program, Prof. Jenna Rickus for her advices and technical support, Prof. Laurent Couetil for his support and extra research opportunities in Veterinary Clinical Science, and Prof. Jong Hyun Choi for serving on my committee.

I wish to thank my colleagues, Joon Hyeong Park, Matt Stensberg, Rajtarun Madangopal, Jun Hyeong Park, Albert Kim, Manuel Ochoa, Ilchung Park, Hyoungsoon Lee, Taegon Cha, and many others for their valuable suggestions and help. I also would like to thank all Birck Nanotechnology Center staff members for providing training and technical supports.

I would like to offer my sincere gratitude to Dr. Seyoung An at University of Illinois – Chicago for guiding me through microfabrication process.

Lastly, I would like to pay my gratitude to my parents and my friends for their love, care, and support. I would like to dedicate this dissertation to my parents.

TABLE OF CONTENTS

Page

LIST OF TABLES

LIST OF FIGURES

Figure Page

Appendix Figure

Figure Page

ABSTRACT

Inn, Kul. Ph.D., Purdue University, December 2014. Development of Planar Patch Clamp with Potentiometric Calcium Ion-Selective Electrode. Major Professor: D.Marshall Porterfield & Jenna Rickus.

Ion channels are proteins in cell lipid bilayer membranes and act as pores which can adopt closed and open states, thus gating the flow of ions in and out of the cell. Patch clamp technology has been the proven standard for fundamental studies of ion channel activities. However, the technique has some basic limitations: low throughput, time consuming nature of its process, need of highly skilled personnel and inability to identify ionic composition of electrophysiological events. Many different materials and fabrication methods have been introduced to replace traditional patch clamp setup to overcome limitations.

In this dissertation, a planar patch clamp device with calcium ion-selective electrode is developed in miniaturized form for high throughput cell electrophysiology, and screening of ion channel modulators as potential drug targets in an *in vitro* format. Femtosecond laser-drilling technique is newly introduced to fabricate the patch-pore and new design of planar ion-selective electrode is suggested for calcium ion measurement. By integrating a standard patch clamp electrophysiological interface with calcium ion-selective electrode on a single platform, it is possible to directly identify the ionic component of a whole-cell potential recording. This system is innovative because the

focus is not entirely on increasing experimental throughput, but instead offers information on user specified target ion activities through ion channels.

CHAPTER 1. INTRODUCTION

1.1 Ion Channels and Patch Clamp Technology

Ion channels are proteins in the lipid bilayer of cell membranes. They act like doors which can be closed and open, to control the flow of ions in and out of the cell membrane. Ion channels are very important in cell studies, because ionic flux through the channels provides the foundation for membrane excitability and neurotransmission that is essential for the proper functioning of neurons, cardiac and muscle cells. Figure 1.1 shows the basic layout of ion channel functioning as a gate for ion flow. Many researchers in biomedical and pharmatheutical field are focusing at ion channels to better understand cell activities once it is treated with newly formulated drugs, and to eliminate any misinterpretations in previous cell monitoring technique [1,2]. It is now estimated that approximately 15% of all newly developed drugs being screened are generally classified as “ion channel modifiers”. The technologies for high throughput screening (HTS) at an early stage of the drug discovery process for compounds with activities as ion channel modifiers have been quite successful. Because drug screening needs to digest the large number of available compounds, accelerated kinetics of ion channels and the demand of data outputs per day, automated methods to measure ionic potential or fluxes from ion channels are highly desired for current experimental conditions.

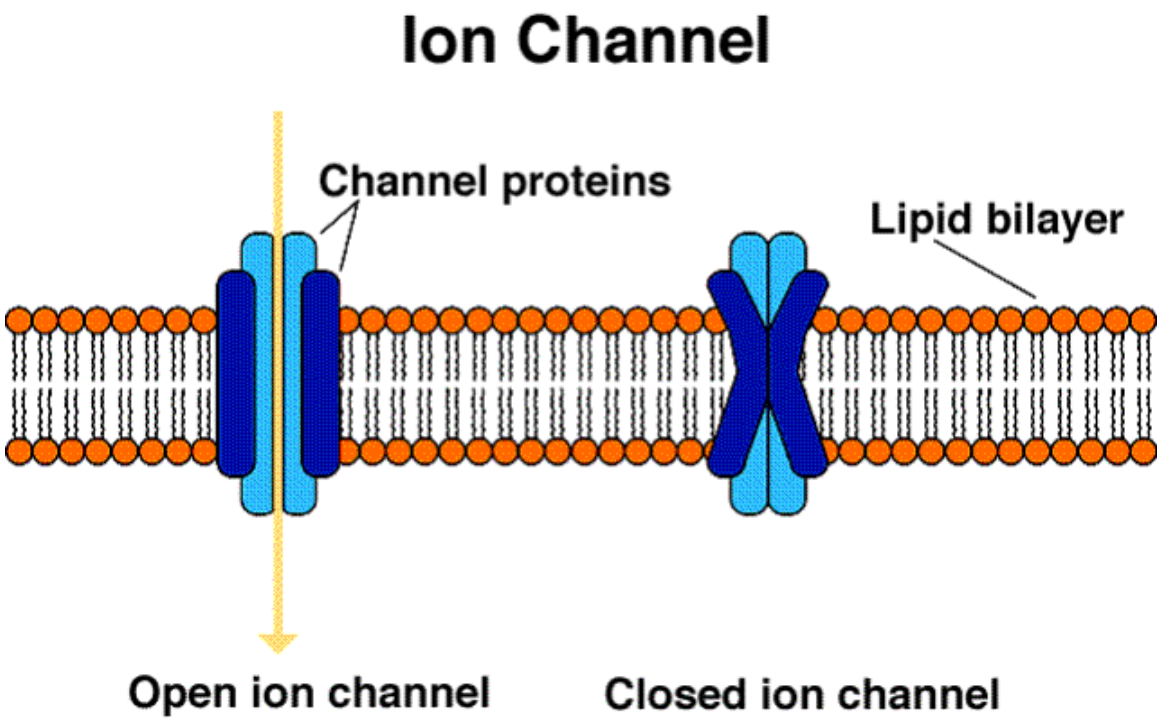

Figure 1.1 Open and closed state of ion channel. Figure adopted from [3].

Patch clamp technology has been widely accepted as the standard method [4] to monitor ion channels in cell membrane. Established by Neher and Sakmann [5], the system uses fire-polished glass micropipette with a 1 ~ 2 μm tip, which is attached to a micromanipulator. The glass micropipette contains a Ag/AgCl electrode, which acts as a working electrode for potential measurement. A cell membrane can be carefully pulled onto the micropipette tip and this maneuver can be observed under microscope. Once pressure is applied for solid seal between cell membrane and the micropipette tip, it creates electrical isolation creating above giga ohm resistance, "gigaseal", for a measurement [6,7]. Because of the size of micropipette tip, this technique has an

advantage towards measuring very small mammalian cells. Figure 1.2 shows the typical setup of patch clamp station and schematic of patch clamp experiment.

There are four major patch clamp techniques that can be performed on a single cell [8,9]. The techniques are called cell-attached recording, whole-cell recording, inside-out patch, and outside-out patch. The inside-out and outside-out patch are known as "excised patch" method. In both cases, patched membrane portion is "excised" from the cell membrane. These two "excised patch" methods and cell-attached recording are performed to monitor the behavior of single ion channels in the part of membrane attached to the tip of micropipette. Whole-cell recording, as its name would suggest, is method that allows monitoring ion channels activities of the entire cell. While all other methods focus their technique to create suction seal and electrical isolation, whole-cell recording takes one step further. Once cell membrane is attached to the tip of the micropipette and creates gigaseal, more suction is applied to rupture the membrane. This procedure provides a connection to the intracellular space of the cell. The whole-cell recording is notably suitable to small cells with 5 to 20 μm in size.

Even though the patch clamp technology is "gold standard" of cell study, it has its limitations: low throughput, time consuming nature of its process, demand of highly skilled personnel and inability to identify ionic composition of electrophysiological events. Also, patch clamp system requires expensive equipments such as amplifier and digitizer for signal recording.

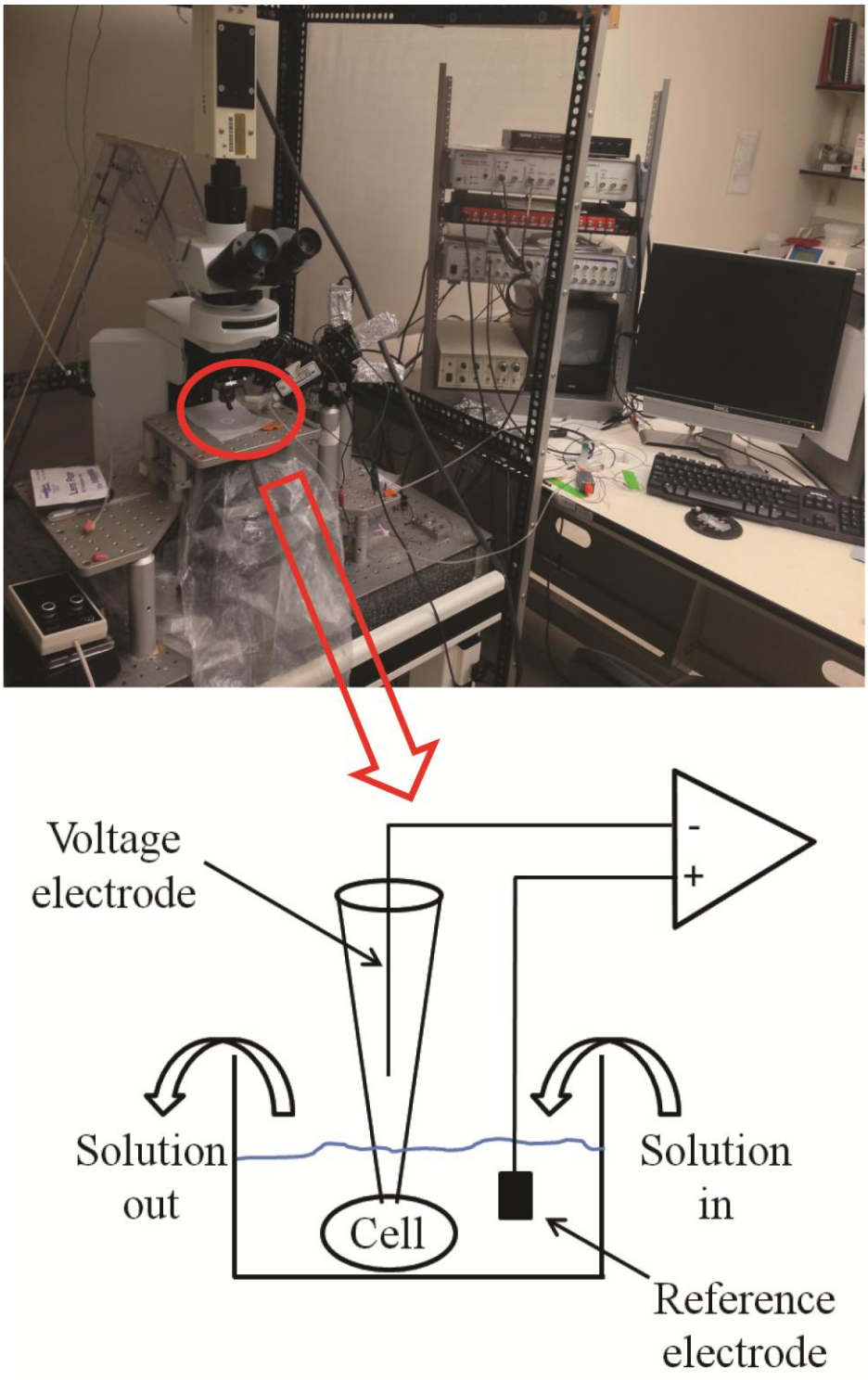

Figure 1.2 Traditional patch clamp system.

1.2 Current Status of Patch Clamp Technique

In order to overcome the limitations and process high throughput screening in traditional patch clamp technique, countless attempts have been made in recent years for improvements [10-16]. To eliminate extensive labors in patch clamp technique, planar form, replacing micropipette, has been introduced to patch a cell with capillary flow created by electromechanically controlled pump. These planar patch clamp devices need less equipment than traditional patch clamp workstation an, is less sensitive to any vibrations from environments, and is easier for user to take long-term measurement.

Planar patch clamp has been fabricated with different types of materials such as, polyimide films [17], SiO_2 nozzle [18], Polydimethylsiloxane (PDMS) treated with O_2 plasma [19], nitride membrane coated with SiO_2 [20], deep reactive ion etching (DRIE) applied silicon holes coated with oxide [21], track-etched quartz [10], and glass substrates [23,24]. Silicon, quartz, PDMS and glass are highly popular materials and have been extensively researched for last two decades. Crystal, electrical, and thermal properties of four popular materials are shown in Table 1.1. The main difference between quartz and glass (fused silica) is that glass is made of non-crystalline silica, while quartz is composed of crystalline silica. The dielectric constant is the ratio of the permittivity of a substance to the permittivity of free space. If the dielectric constant increases, the electric flux density increases. A high dielectric constant is not desired for electrical insulation. Electrical resistivity is a property that shows how strongly a material opposes the flow of electric current. Higher resistivity means higher resistance is formed when a material is within an electrical circuit. Thermal conductivity is property to conduct heat. The

materials are temperature dependant, so it creates thermal resistivity, which is reciprocal of thermal conductivity.

Table 1.1 Properties of materials used in planar patch clamp [29-33]

Material	Crystal	Electrical		Thermal
	Density (g/cm^3)	Dielectric Constant	Resistivity (Ω-m)	Conductivity (W/(m-K))
Silicon	2.329	11.9	2.5×10^2	148
Quartz	2.203	3.75	10^{18}	1.3
PDMS	0.00097	2.3 ~ 2.8	4×10^{13}	0.15
Glass	2.2	3.82	$10^{10} \sim 10^{14}$	1.38

Among above materials, fabrication using planar silicon substrate has been highly favorable in last decade. On silicon substrate, micro to nano sized patch-pore can be fabricated [20]. Despite simplicity of fabrication, planar silicon substrate exposed some issues. Because it has a high density of free charge carries, a transient parasitic current occurs within the system. Silicon surface also has photoelectric effect, which decreases possibility of forming gigaseal resistance with a cell. Still, silicon has great potential when it is assembled with microfluidic channels [14].

A number of research groups have employed the use of silicon-based patch clamp devices. Schmidt *et al.* introduced a unique method for trapping and positioning the biological sample under investigation on a planar silicon substrate. By applying a small electric field (<200mV) through the aperture, Schmidt was able to attract the negatively charged specimen [59]. Although Schmidt and colleagues were able to obtain gigaseal, other scientists who develop planar patch clamp chips have not used this method of trapping. The hesitation of using this method may be attributed to the lack of

implementation on mammalian cell-lines and the similarity of the trapping technique to electroporation; however in electroporation, the electric field is strong enough to tear the cell membrane.

Among the first to implement a planar patch on living cells was Lehnert *et al.* [18], who sought to maintain the 3-dimensional structure of the traditional patch clamp pipette tip. To achieve this feature, Lehnert *et al.* designed silicon oxide apertures that protruded from the surface of the silicon substrate, much like a nozzle. The design allowed them to trap cells via suction, but the seal was not tight enough to allow gigaseal formation because of the rough inner surface of the nozzle [18]. The authors then improved the design by deposition and reflow of phosphosilicate glass (PSG) to obtain a smoother surface. This new smoothing technique yielded gigaseal in 40% of tested planar patch clamp chips [60]. While the PSG deposition approach yielded promising results, no report was made on the relative ease of fabrication or the product yield. Therefore, this design, while successful, indicates a complicated process requiring further characterization.

Alberti *et al.* recently developed a Si-based planar patch clamp device called "Patch Clamp Micro-Channel Array" (PCμCA). PCμCA consists of an array of six patch-pores with individual microfluidic channels for perfusion and suction [61]. Each aperture is 400 μm away from the next. The PCμCA is housed in a microfluidic chamber, making it a compact system. PCμCA is made completely in silicon and thus is subject to the limitations of silicon-based devices. These limitations include high device capacitance (100pF) and very low seal formation resistance, about 40 MΩ. As a result of these

limitations, Alberti and colleagues were unable to perform whole-cell recordings to establish proof-of-concept.

Despite the ability to fabricate complex structures in silicon, the material has not been able to allow researchers to achieve high success rate in gigaseal formation and high quality whole cell recordings on mammalian cells. Silicon is relatively easy to fabricate but its quality as a poor dielectric, despite insulation, preclude the use of silicon as the base substrate for patch clamping. Currently available silicon-based planar patch clamp devices are reported as table form in Appendix A.

PDMS and glass, both show good insulating qualities. Their transparency brings ability to adopt fluorescence measurement and convenience of observation throughout patch clamp procedure. PDMS might have the simplest way to fabricate patch-pore and it can be made within micro-sized level [25,26]. O_2 plasma treatment can modify hydrophobicity of PDMS surface to help forming gigaseal resistance with a cell. It is relatively cheaper to buy and process than other materials. However, it also comes with a disadvantage. The flexibility of PDMS can prevent a cell to attach onto patch-pore by closing its pore when suction pressure is applied. Recently, PDMS was reinforced with SU-8 to fabricate patch-pore that could sustain suction pressure [27].

In 2002, Klemic *et al.* reported on the fabrication of two types of PDMS-based patch clamp tools [19], which were made from a direct mold of a glass micropipette and a silicon mold. The patch-pores were fairly large, 4-20 μm and could only be applied to large cells such as *Xenopus Oocytes* and not to most mammalian cells. Also, no whole-cell experiments were reported. The authors were able to obtain 13% success rate in

gigaseal formation in oocytes, which is higher than the success rate obtained with the silicon-based devices.

In 2005, the Sigworth group published an improved PDMS design with smaller patch-pore (~ 2.5μm) that were created using an air molding technique in which streams of nitrogen are used to define patch-pore [25]. In their design, whole cell recordings were performed on Chinese Hamster Ovary (CHO) cells and Rat Basophilic Leukemia (RBL) cells with success rates of 7% and 10%. In addition to the low yield of gigaseal formation, the fabrication process flow resulted in low yield (about 20 chips per day), which limits this design's potential use in commercial applications. After slight modification in process flow in which the PDMS plasma treatment was extended from 1 to 4 hours to increase the hydrophilicity of the surface, the researchers were able to increase their device yield to 60 chips per day.

Glass is naturally hydrophilic with good mechanical properties. Because gigaseal formation takes place more readily with glass in comparison to silicon and PDMS [62], there are companies that manufacture glass planar patch clamp chips. Nanion developed one such chip that is part of the Patchliner and the Port-a-Patch automated patch clamp system. For their patch chip, the glass substrate is first thinned down via a wet etch process, then a particle accelerator shoots a heavy ion-beam (gold) through the thinned glass substrate to produce an ion track that can be etched chemically to create the aperture (1-2μm) [10, 22,63-65]. With an average access resistance of approximately 5 MΩ and capacitance of <1pF, the electrical properties of the glass chip are comparable to that of the glass micropipette in traditional patch clamping. The success rate for gigaseal formation is about 50% [10]. The major limitation with applying this chip design to study

neuronal networks is the limited access to a particle accelerator and the chip's inability to manipulate individual cells/channels on a single chip. Ion-tracked etching was utilized to fabricate micro-sized patch-pore [28], but this still had an issue of tapered patch-pore which brings down success rate of gigaseal.

To improve volume of data collection, automated patch technique has been in development. The automated patching systems are introduced and reviewed elsewhere [34,35]. The first automated system was introduced in late 90s and it used the classical glass microelectrodes to gain the electrical contact with a cell [34]. In order to commercialize the automated patch system, planar form was adopted. Planar automated patch system was originally developed in 1970s [36]. But the noise level was not in satisfying range. In 90s, Klemic et al. adopted ultra-low-noise recording in planar patch clamp system [19]. The glass substrate with multi-well replaces traditional microelectrode with 1 to 2 μm patch-pore in bottom of every well. Once cells are placed into wells, suction is applied to form electrical seal, and enables whole-cell recording.

The latest, commercially available, automated system is able to measure and record data up to 64 cells in a well [35], and this is called population patch. This technique shows better quality of data by reducing cell-to-cell variability [37]. Currently available automated patching systems are illustrated in Figure 1.3.

Even though automation has been successful in patch clamp technique, seal resistance shows in MΩ range, and voltage control can be limited. The technical limitations lead to limitations in precise recording, and collected data are closer to estimative. It can only used for example study in the early drug screening [38,39]. However one recent study shows good correlation between traditional patch clamp

technique and automated patch system [40]. If solutions to other technical limitations can be found, measurements from automated system can be an effective for ionic current analysis.

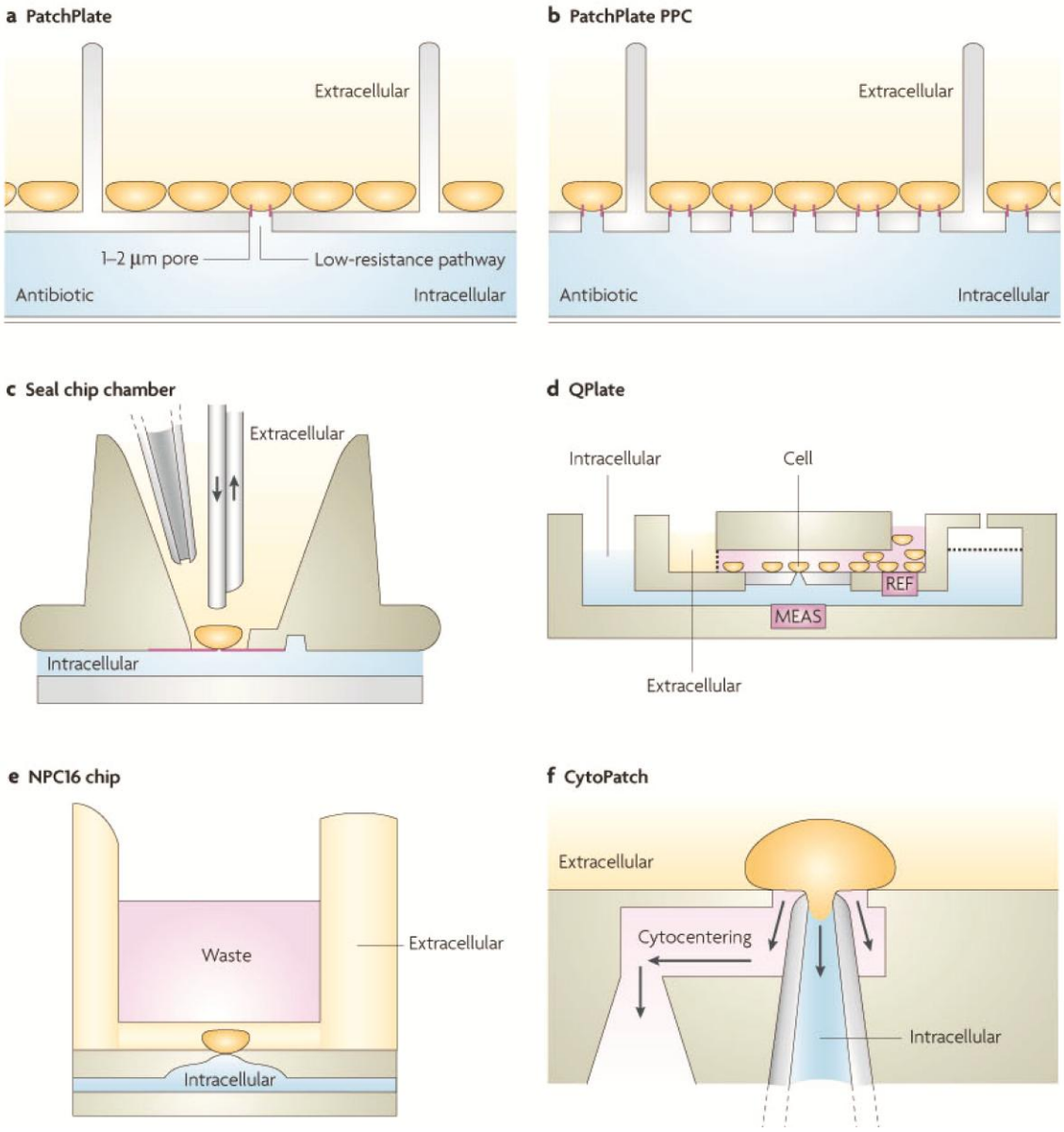

Figure 1.3 Automated planar patch clamp technologies. (a) Ion Works HT PatchPlate (molecular Devices); (b) IonWorks Quattro Population Patch clamp (PPC) PatchPlate (Molecular Devices); (c) Molecular Devices SealChip used in PatchXpress; (d) Sophion Qplate, where MEAS-measurement electrode and REF is reference electrode; (e) Nanion planar patch chip; (f) Cytopatch by Cytocentrics. Figure adopted from [66].

1.3 Calcium Ion-Selective Electrode

Calcium ion is an intracellular messenger, which controls many cellular processes, such as fertilization, gene transcription, muscle contraction, neural signaling, and proliferation [41-44]. In recent reviews, calcium signaling has been key factors in asthma [45], cardiac arrhythmias [46], immune system diseases [47], embryonic development [48], and cancer [49]. Studies confirm the significance of calcium signaling in disease mechanism and cell studies. This leads us to determine calcium ion as a target of cell intercellular studies.

Since 1920s, science researchers attempted to measure calcium ion, but only few of them were successful. The first dependable measurements of calcium ion concentration were done by Ridgway and Ashley [50]. They injected the photoprotein aequorin into the single muscle fiber to measure calcium ion concentration. In 1980s, various kinds of chemical fluorescent indicators were developed to measure calcium ion [51-56]. Since the indicators were introduced, studies involving calcium ion concetration studies within intracellular level have rapidly increased.

The other popular method to measure ionic activities is using ion-selective electrode. This device allows direct measurement of ionic activities, which is not possible for other mechanisms [57]. This system requires no addition of chemicals in the sample, which brings minimum interference to the physiology of the cell in study. To improve its ability, the electrode can be fabricated in micro-size for local measurement in cells [57,58]. In 1970s and 80s, many researchers, studying ionic activities in cells, developed glass capillary ion-selective electrodes. For intracellular measurements, cells were

manually punctured with micro-pulled tip of glass capillary. Five different configurations for glass capillary ion-selective electrode are shown in Figure 1.4.

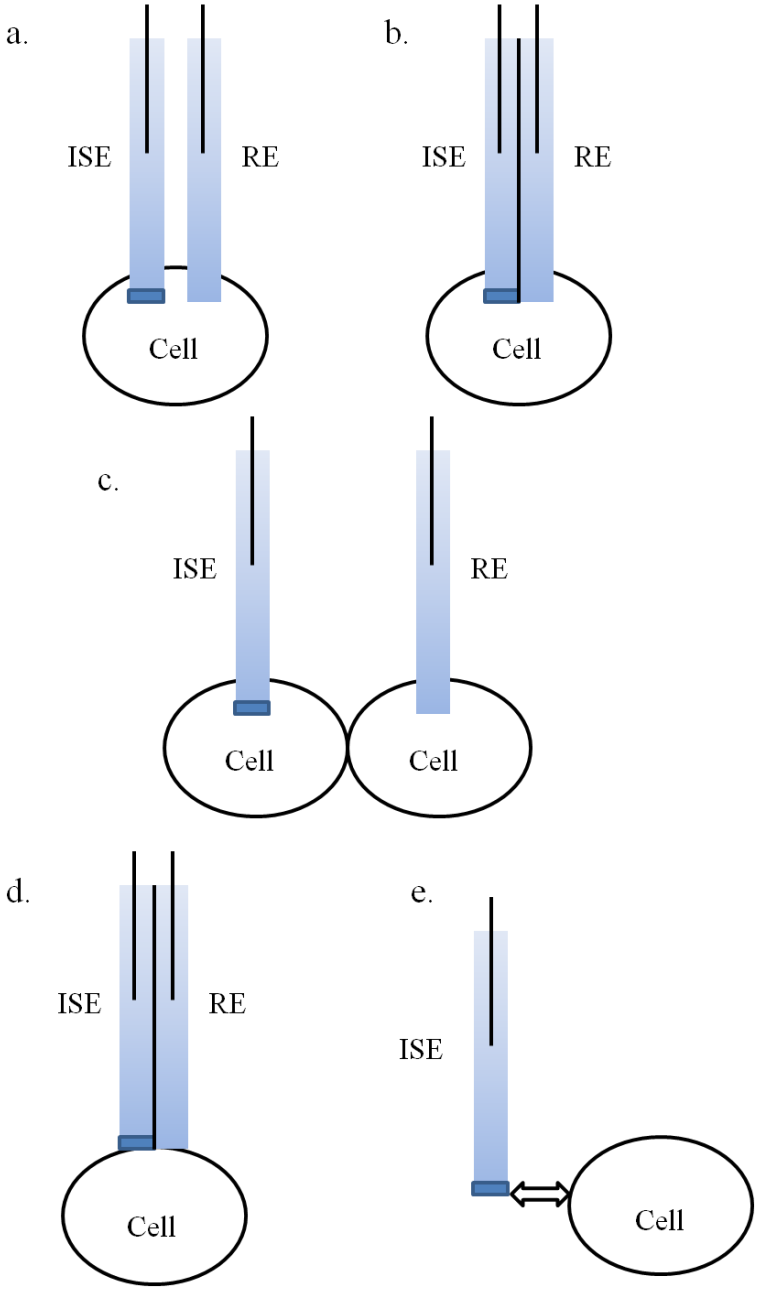

Figure 1.4 Five different methods of glass capillary ion-selective electrodes in ion measurement in a cell. (a) ion-selective electrode (ISE) and reference electrode (RE) pierce a cell; (b) Single glass capillary divided into two sections for ISE and RE; (c) ISE and RE pierce two different cells with same trans-membrane potential; (d) Patch clamp configuration using glass capillary electrode; (e) Self-referencing ISE.

The membrane sealing quality around the ISE tip is verified from the signal difference in ISE and RE. This insures the signal dependability of a real intracellular change [67]. Self-referencing ISE in Figure 1.4e is vibrating electrode. The signal difference between two different positions (away from cell and close to cell) of ISE gives a recording of ion concetration or ion flux [68]. This technique has been in use with patch clamp to measure ionic fluxes through ion channels [69].

The key feature of ISE is ion-selective membrane (ISM). Ideally, Liquid polymeric ISM can extract target ion. The traditional ISM is composed with following components:

Plasticizer

This is also called "membrane solvent". This is a lipophilic liquid solution with low vapor pressure. The polarity of this solution can change the selectivity of ISM. Higher percent of polar solvent will boost the selectivity of divalent over monovalent ions [57]. Bis (2-ethylhexyl) sebacate (DOS) and 2-nitrophenyl octyl ether (o-NPOE) are most common plasticizers.

Ionophore

The term indicates a compound that enforces the transmission of an ion across a lipid barrier by combining with the ion. Increasing the permeability of the barrier also facilitates the transmission. In ISE, the properties of an ionophore to compose a hydrophobic complex with a target ion are manipulated to allow the solubilization of the ion in the ISM layer. In ideal situation, ISM forms a strong complex with the target ion, yet reversible. The concentrations of typical ionophore in ISM are 10^{-2} mol / kg to 10^{-1} mol / kg, but sometimes it goes down to around 10^{-4} mol / kg [57].

Lipophilic ion exchangers

In order to gain an ideal response, the permselectivity of the ISM should be assured. This phenomenon is called Donnan exclusion and it means that no considerable amount of ions of opposite charge to the target ion may penetrate the membrane [70]. In neutral carrier-based membranes, permselectivity is granted by counter ions confined to the membrane layer. Early ISE with liquid membrane were realized with no addition of lipophilic ionic sites [71], but response was improved when these components were present. For cation-selective electrode, a tetraphenylborate is added, and a tetraalkylammonium is added for anion-selective electrode [70].

An excess of ionic sites correspond to the complexing capacity of the ionophore must be avoided [72]. As the lipophilic ionic sites have also ion-exchanger properties [26,27], an excess of ionic site will penetrate in competition with the ionophore and extract cation into the membrane layer. If the selectivities of the lipophilic sites are dissimilar than those of the ionophore, the selectivity will be dominated by the properties of ion exchanger. The addition of the ionic sites can decrease the electrical resistance of the membrane.

Matrix

Mechanical stability in the membrane is provided by matrix. The most common matrix is PVC. For biocompatibility, polyurethanes and silicone are also used as PVC substitute [73-76]. These two materials do not require additional plasticize, so their diffusion coefficients are several orders of magnitude lower than PVC-based ISE. Porous glassy carbon [77] and porous silicon [78] have been introduced in recent years to

substitute PVC in ISM. Matrix is one of most important component because it has a great influence on the polarity of the membrane.

Extra additives

In order to improve the electrode performance, mixture of lipophilic cations and anions can be added [79]. This mixture eliminates anionic interference and decreases the electrical resistance of the membrane and increase upper detection limit. Lipophilic inert nano-particles can also be added to the membrane layer for lowering the ionic fluxes.

The details of calcium ISM fabrication procedure used in this research is introduced in CHAPTER 3 and Appendix B.

The basic schematic of potentiometric ISE system is shown in Figure 1.5.

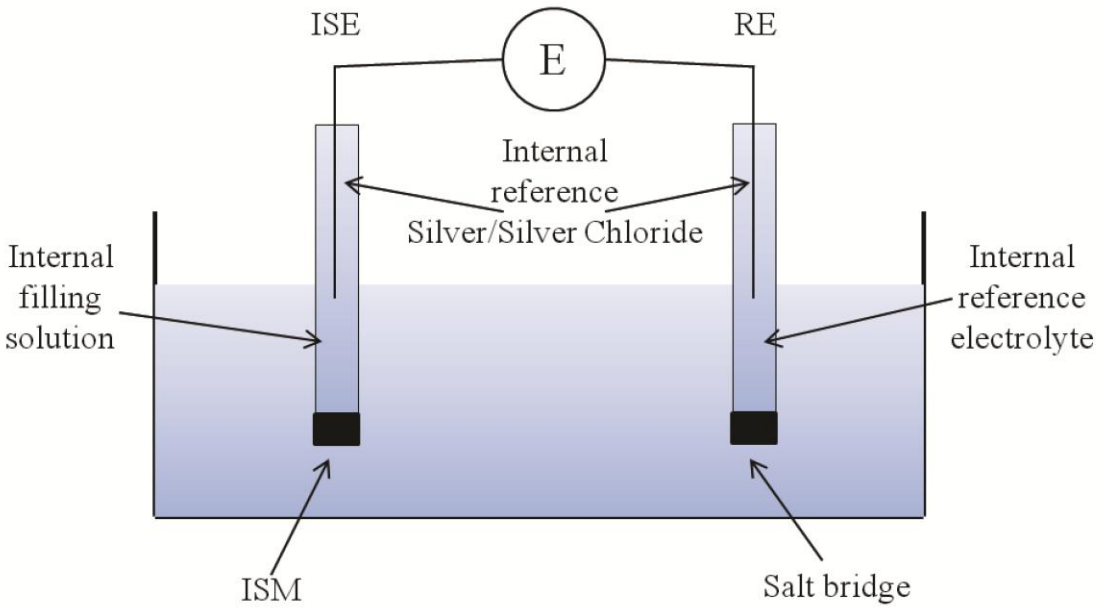

Figure 1.5 Schematic of general potentiometric ISE system.

In Figure 1.5, internal reference electrolyte is potassium chloride (KCl), and potential energy diagram can be laid out in following order:

Ag | AgCl | KCl | salt bridge | sample | ISM | internal solution | AgCl | Ag

E_1 E_2 E_3 E_R E_M E_4 E_5

And this diagram can be transferred to mathematical equation:

$$E = (E_1 + E_2 + E_3 + E_4 + E_5) + E_R + E_M \quad (1.1)$$

The sum of all boundary local potentials equals to potential response of the electrochemical cell. At given temperature, E_1 - E_5 are consistent, and the electrolyte usually has no potential, so E_R can be neglected. The membrane potential, E_M, is divided into 3 parts. First potential is $E_{M,\ sample}$, which is potential between sample and ISM. Second potential is diffusion potential, E_D, which is internal potential, and third potential is boundary potential between ISM and electrolyte, $E_{M,\ internal\ solution}$.

$$E_M = E_{M,sample} + E_{M,internal\ solution} + E_D \quad (1.2)$$

If we take steady state (zero current) as assumption, E_D can be neglected [80]. The membrane potential becomes potentials acting on two membrane boundaries with target ions. Then, Equation 1.2 can be transformed to following equation:

$$E_M = \frac{RT}{z_I F} \ln \frac{a_I^{sample}}{a_I^{internal\ solution}} \quad (1.3)$$

Z_I is the charge of ion I, R is ideal gas constant, T is the temperature (in K), F is the Faraday constant, and a_I^{sample} and $a_I^{internal\ solution}$ are the activities of the I in the sample and internal solution. Equation 1.3 is called the Nernst equation. If the internal solution composition is constant, theoretical potential response can be expected:

$$E = E_I^0 + \frac{RT}{z_I F} \ln a_I^{sample} = E_I^0 + \frac{S}{z_I} \log a_I^{sample} \quad (1.4)$$

For temperature equals to 25 ˚C, S is 59.16 mV. For constant temperature, 4% of Z_I change in a_I^{sample} is equal to 1 mV.

1.4 Motivation for Planar Patch Clamp with Calcium Ion-Selective Electrode

Patch clamp system has been evolved with technological advance in microfabrication and different types of materials. Still, current patch clamp technique suffers from basic limitations: low throughput, need of highly skilled personnel, and inability to identify ionic composition of electrophysiological events. In order to overcome current limitations, we have employed technique to assemble parts made from different materials, rather than developing a system from a single material in a planar form. Considering its unique material properties, fused silica (glass) is inherently capable

of serving as a substrate for fabricating planar patch-pore to replace glass micropipette tip. This provides security to form a gigaseal while ion activities are recorded throughout a cell study. PDMS solution chamber is designed and molded for applying suction pressure and intracellular solution exchange. Finally, planar calcium ISE is newly introduced in patch clamp system to enable target-monitoring without post process.

The assembled system can provide an easy-to-use technology for HTS cell electrophysiology, and screening of ion channel modulators as potential drug targets in an in vitro format. This technology is highly innovative because the focus is not entirely on increasing electrophysiological experimental throughput, but instead offers information on user specified target ion activities through ion channels.

CHAPTER 2. PLANAR TRANSFORMATION

The novel part of this research, which separates from previous studies, is integrating patch clamp system with calcium ion-selective electrode. In order to miniaturize the total volume of integrated system, each part needs to be on planar surface. Therefore, tip of glass micropipette needs to be fabricated on a surface where cells can be loaded and survive for recording period. The material should have excellent electrical resistance properties and structural stability. In order to meet the requirements of this research, we have employed different types of substrate to three different parts: patch-pore, intracellular exchange chamber, and calcium ISE. In this CHAPTER, material for the research is carefully selected and examined for fabrication process.

2.1 Patch-Pore

2.1.1 Material Selection

The patch-pore layer is the most important part of planar patch clamp system. It is impossible to begin measuring cell activities without having proper patch-pore. Once cell is patched on to the pore, resistance higher than GΩ needs to be achieved for electric isolation and mechanical stability. In order to replace current glass micropipette, many materials have been suggested throughout planar transformation. Two most commonly used materials were chosen as candidates for our research: silicon and fused silica.

Silicon

As mentioned in introduction, silicon is an appealing candidate of material for wafer-based patch clamp systems. It is common semiconductor material used in microelectromechnical systems (MEMS) fabrication. A common microfabrication method employed for insulation of silicon-based systems is growth/deposition silicon dioxide (SiO_2). Silicon nitride (Si_3N_4) has also been used, but only to support SiO_2 [59,81]. Figure 2.1 shows the fabrication process of patch-pore on silicon substrate. The advantage of using silicon as a substrate is that it has been researched for long period of time and it brings industrial and mature technologies for constructing and modifying its surface properties. But as the name "semiconductor" suggests, silicon alone is a poor insulator due to freely moving charges that increase the overall capacitance [28]. This is also can cause slow voltage transients and high noise across the partition.

The one of main goal for this research is to achieve consistent gigaseal resistance once cell is patched onto pore. However, the overall success rate for high gigaseal resistance formation using insulated silicon-based systems still remains low. Silicon is relatively easy to fabricate as planar substrate for patch-pore, but its quality as a poor dielectric, despite insulation, preclude the use of silicon as the planar patch-pore substrate for our study.

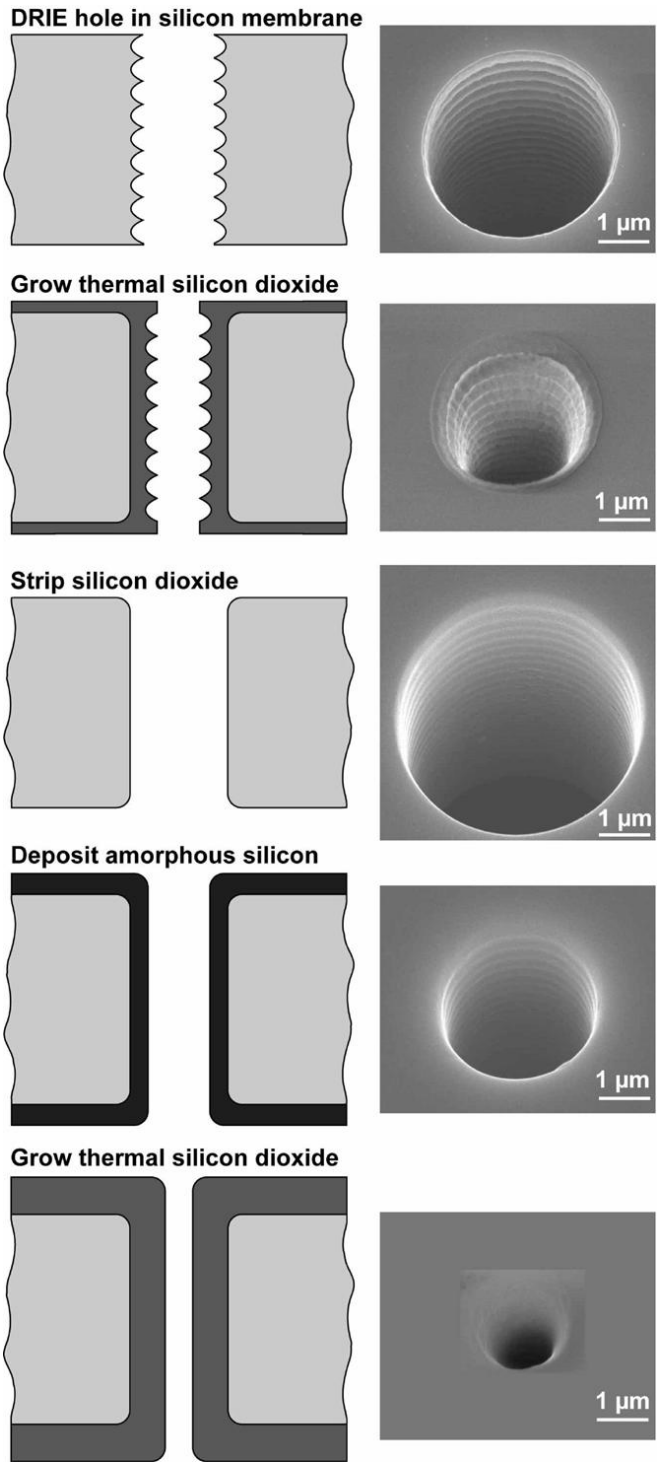

Figure 2.1 Cell patch-pore fabrication process on silicon substrate. Figure adopted from [14].

Fused silica

After careful review of silicon as a substrate, we have decided to find other substrate that could meet the electrical requirement for our patch-pore. We had to find a material that is an excellent insulator and provides good seal with membranes. Fused silica brings both excellent insulation and reduction of signal noise. Fused silica is also transparent; therefore it can be coupled with an imaging technique such as Confocal or Two-Photon microscopy to observe cells under investigation. Only one obstacle would be fabrication process; compare to silicon, fused silica is more difficult to etch a hole through substrate once the thickness gets increased. A solution to this problem is thinning the substrate before fabricating the patch-pore. One-sided etch using hydrofluoric acid (HF) can locally thin the fused silica wafer. Then, a single ion can be blasted and leave ion track of 1-2 μm aperture. One more step of one-sided HF etching can create conical patch-pore with clean edges [65]. Figure 2.2 shows a microfabricated patch-pore on fused silica (glass) substrate.

This etching process has enabled fused silica as a patch-pore substrate. The whole-cell [10] and single channel [22] recordings were performed on planar glass substrate. It is suggested in Table 1.1 that fused silica has much lower dielectric constant than silicon, which provides better electric insulation and lower capacitances. We have chosen our patch-pore substrate as fused silica because gigaseal formation takes place more readily with fused silica substrate in comparison to silicon and PDMS [62]. Thinning might be an issue at the fabrication since substrate can be easily cracked or broken in such thickness. Our study has come up with laser-drilling technique rather than traditional etching technique to overcome the difficulty of microfabrication.

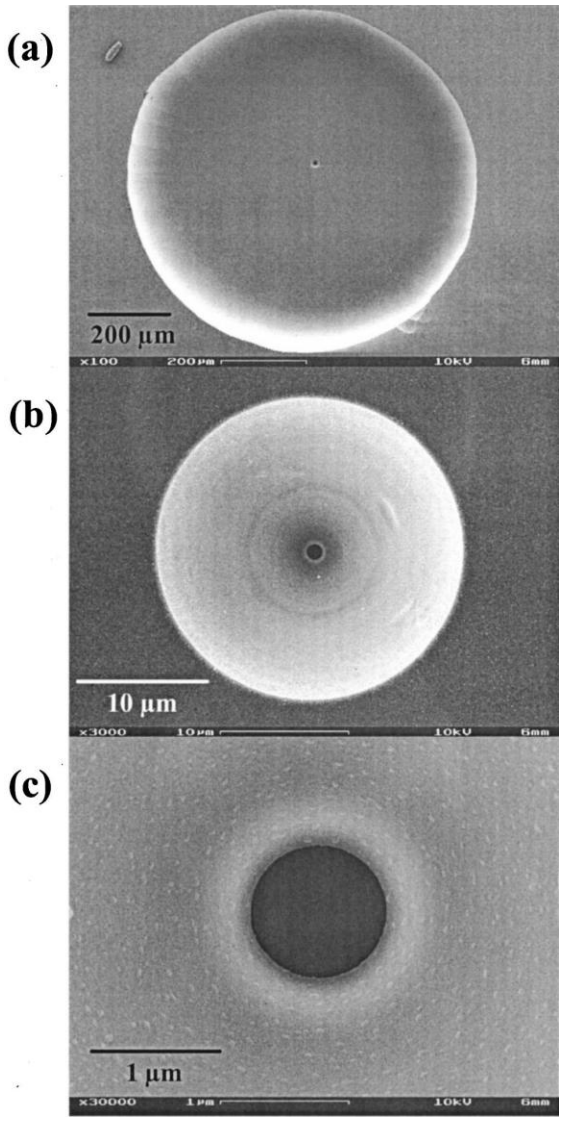

Figure 2.2 Patch-pore fabrication sequences on fused silica (glass); (a) Pre-etched groove; (b) Etched ion track in the substrate; (c) Finished patch-pore. Figure adopted from [28].

2.1.2 Etching and Laser-drilling

Etching

Etching is a technique that used in microfabrication to chemically remove layers from target surface during manufacturing. Typical process starts with coating the surface with photoresist, "masking material", and makes patterns with photolithography. Some

situations require a durable silicon nitride mask. There are two main etching techniques widely used in microfabrication: Wet-etching and plasma etching.

Wet-etching commonly uses liquid etchants. The substrate is immersed in etchant bath, which needs to be stirred to accomplish process control. Buffered hydrofluoric acid (BHF) is common etchant solution to SiO_2 on silicon substrate. Depends on the surface materials, different liquid etchant can be employed.

Since fused silica has impurity of less than 1%, it is challenging to be etched via wet-etching. It needs long wet etch time and the requirement for robust mask. Cr-Au-photoresist multilayer is used as the mask. Cr maintains mask adhesion to substrate, and Au resists hydrofluoric acid (HF) etchant. Photoresist (AZ5214E-IR), with high resistance to HF was hard-baked on top of Au, which the hydrophobic layer prevents pinhole formation on Au layer. A thin layer of 1.4 μm is sufficient to withstand HF etch. This is superior to the previous usage of AZ9260 photoresist, which fails to withstand HF etching even at 10 μm thickness. To increase the etch rate (1 μm/min), HF (49%) was used. Our process shows that HF (49%) destroys mask layer within 2 hours. This hinders deep channel etch. For etching channel deeper than 100 μm, HF buffered with ammonium fluoride (BHF or BOE) was used. However, the etch rate of BHF was found to be sensitive to temperature. The etch rate at 18 ˚C is 0.095 μm/min, and at 38 ˚C it is increased to 0.31 μm/min. Temperature higher than 40 ˚C can weaken the photoresist layer. For etching purposes, BHF (BOE 1:6) at 38 ˚C was used.

The problem with wet-etching in our study was the thickness of fused silica substrate, 150 μm. The size of the patch-pore should remain less than 5 μm to match traditional glass micropipette in patch clamp system. By using wet-etching technique,

patch-pore shape becomes isotropic, which shows large bias for thickness of our substrate. In order to reduce the bias, plasma etching technique was employed for patch-pore fabrication.

Plasma etching involves bombardment of energetic ions onto substrate which etch atoms from the surface by transferring momentum. Because it has ion travelling in one direction, the process is very anisotropic. For deep narrow features, deep reactive ion etching (DRIE) is employed for highly anisotropic etching. Due to its purity, fused silica substrate does not react with plasma gases used in DRIE process, in comparison with silicon. Hence, DRIE on fused silica depends on strong ion bombardment rather than reaction with gas. In addition, strong ion bombardment produced by high-power inducted coupled plasma (ICP) can etch the mask; fused silica DRIE needs thicker metal mask, if compared with silicon DRIE. Since electroplating can make thicker mask than evaporation, electroplated Nickel with Cr-Cu seed layer was used as a mask. Figure 2.3 shows DRIE process of patch-pore fabrication. For micro-channel #2 in Figure 2.3, DRIE characterization was performed with circle feature of different diameters. When increasing ICP power and etching gas (C_4H_8), mask peeling was prevented and the etching rate increased to 0.5 μm per min. But for longer than 2 hour DRIE etching, continuous increase of reflection power from ICP power, can halt the plasma formation and can heat the mask and substrate. Programming the DRIE machine to provide 5 minute cooling for every 5 minute of DRIE etch process, can increase the plasma stability and mask life time.

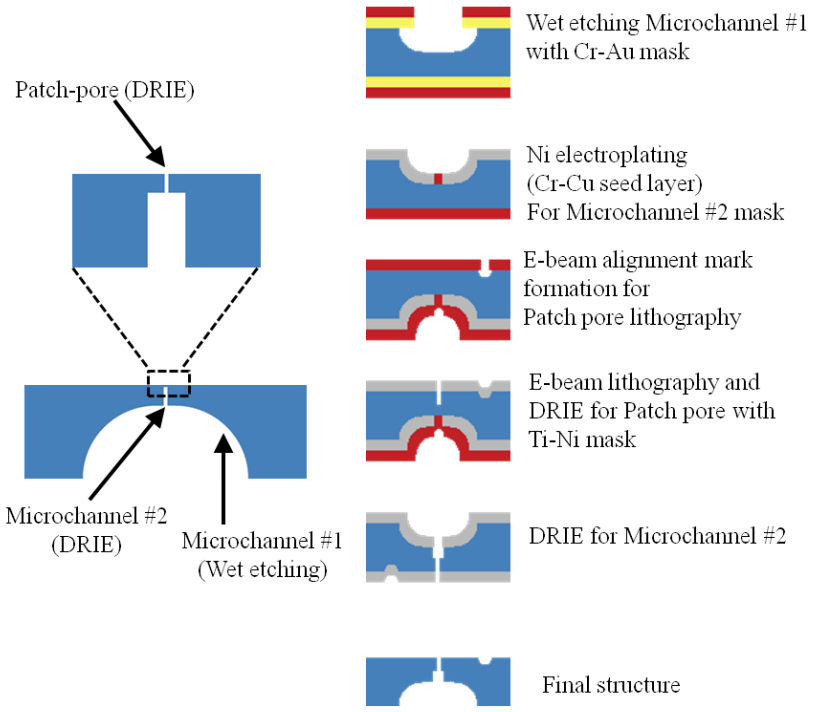

Figure 2.3 Cross-section schematic of patch-pore fabrication using DRIE.

Figure 2.4 and Table 2.1 show the DRIE results of fused silica and parameter used in DRIE characterization.

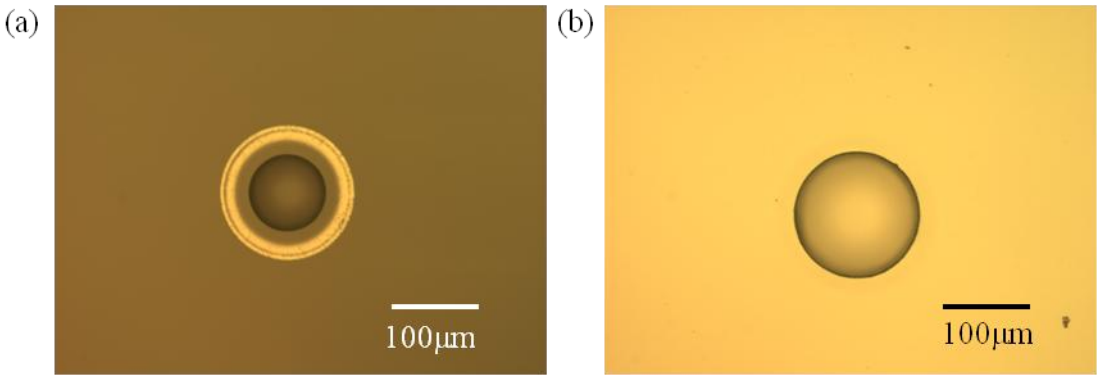

Figure 2.4 DRIE characterization results; (a) ϕ = 100 μm, depth = 70μm; (b) ϕ = 150 μm, depth = 105μm.

Table 2.1 Parameter used in fused silica DRIE characterization.

Parameter	(a)	(b)
ICP Power (W)	1200	1600
RF Power (W)	350	250
Gas (sccm)	Butene: 60 Oxygen: 5	Butene: 80 Oxygen: 5
Pressure (mTorr)	9	11
Ni thickness (μm)	7	13

Because of time consuming nature of DRIE on fused silica and lack of rigidity of mask, it was not possible to fabricate patch-pore without thinning the fused silica substrate at the first step before DRIE. But fused silica substrate thinner than 150 μm is impossible to handle and easily broken as soon as it is grabbed by tweezers. Main problem is that fused silica isn't DRIE-friendly like silicon substrate. We have sought solution to fabricate patch-pore and reached few dead ends along the way, but finally found a solution in different fabrication method: laser-drilling.

Laser-drilling

Ultra-short laser pulses have been introduced to microfabrication in recent years. When a laser beam is focused inside a transparent target material, only localized region in focal volume absorbs laser energy by nonlinear optical breakdown, and rest of the target specimen is unaltered [82]. From this advantage, many applications have been developed; 3-D optical storage [83], 3-D structure by photopolymerization [84,85], fabrication of

optical waveguides [86,87], and 3-D drilling [88]. Femtosecond lasers are known for precise abscission of material with no significant heat effect [89]. Femtosecond laser drilling has reported that it is more controllable and reproducible than longer laser pulses, such as nanosecond laser [90-93]. With Femtosecond laser, many different optical devices ranging from straight waveguides to more sophisticated features can be fabricated. The process can be fully automated and controlled electromechanically with precision, implementing a highest order of flexibility to users for sophisticated designs compared to traditional lithographic methods. Example of holes drilled on fused silica glass is shown in Figure 2.5.

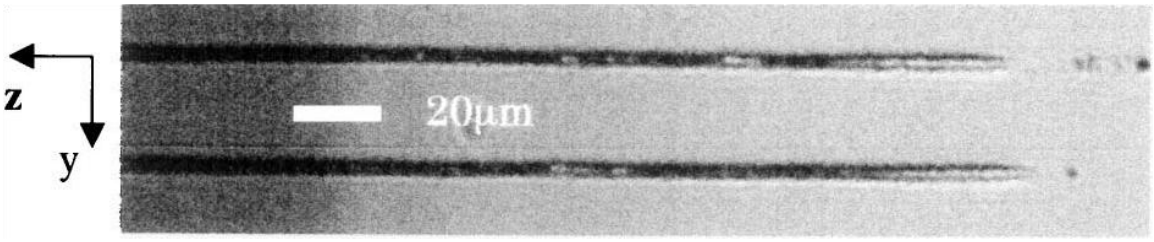

Figure 2.5 Two holes drilled on silica glass with pulse energy of 1 μJ. Figure adopted from [88]

By changing incident pulse energy, the diameter of hole can be controlled. Greater incident pulse energy increases the size of diameter. Table 2.2 shows the difference in size of diameter by different incident energy pulse. As Figure 2.5 suggests, the hole is highly anisotropic, and can drill up to the depth greater than 600 μm.

Table 2.2 Hole diameter size corresponding to different incident pulse energy [88].

Incident pulse energy (μJ)	Diameter size (μm)
1	4
4	7
10	21

2.1.3 Why Laser Drilling?

Fused silica (glass) has many useful properties, such as its inertness and transparency, and is commonly used in industrial and academic research. However, conventional wet-etching and plasma etching (DRIE) technique on fused silica suffers from isotropic profile and time consumption of process. The isotropic profile can be modified by thinning the area around the patch-pore, but it still requires thicker masking for protection, much of manual labor, and cost along the way.

The laser drill process discussed in previous part (2.1.2) is feasible at low cost compared to etching process. Femtosecond laser increases the precision and flexibility in microfabrication without compromising vicinity of target area. With its capability of drilling micro-sized pore on fused silica, our study could add another advanced technology to device fabrication. This also brings us an ability to mass-produce fused silica substrate with multiple patch-pores for planar patch clamp device. It is also commercially available at relatively low cost with highest surface quality.

2.2 Inner Filling Solution for Calcium ISE

The critical issue in fabricating planar calcium ISE is replacing liquid internal electrolyte solution. In order to minimize the volume of the device, planar transformation of calcium ISE is inevitable. The quickest method to solve the problem is removing the internal electrolyte solution layer. But if electrode and ISM are in direct contact without internal solution layer, the measurement signal suffers from drift. This might require re-calibration of the sensor at the time of measurement. All-solid-state ion sensor concept has been introduced to solve this issue. This platform replaces liquid interface into solid layer, such as hydrogel [94] and conducting polymers [95,96], which provides a transducer layer between metallic electrode and ISM. This all-solid-state ion sensor provides stability and microfabrication capability of ISE. But hydrogel tends to change its volume when it is placed in bath solution and it could create ISM expansion, which might damage the ISM in process. From its proven ability, conducting polymer was initially chosen as transducer layer for calcium ISE in this study.

2.2.1 Conducting Polymer

Conducting polymers are favorable as transducer layer in solid-state ISE for multiple reasons: (a) they create “ohmic contact” with carbon, platinum and gold, (b) they can be electrodeposited on the conductor by electro chemical polymerization, (c) they are soluble, therefore solution deposit is possible, (d) since they are electroactively composed, ionic signal can be transuded into an electronic signal [95]. These features are excellent conditions for conducting polymers to be a transducer layer in the solid state.

Potentiometric ISE with oxidized (p-doped) conducting polymer set up is shown in Figure 2.6. One of the favorite conducting polymer used in solid contact ISE is poly(3,4-ethylenedioxythiophene) doped with poly(styrene Sulfonate) – PEDOT/PSS. PEDOT/PSS is well-known for forming a benzoid or coiled structure [97], which decreases electrical conductivity due to electrostatic interactions between positive charges on the PEDOT and free sulfonic of PSS.

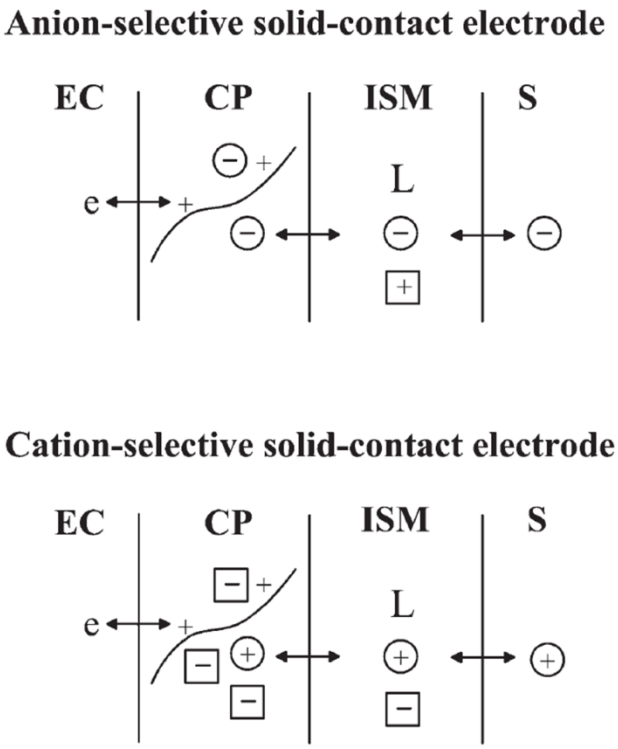

Figure 2.6 Operating setup of solid condact ISE with an oxidized (p-doped) conducting polymer as transducer; EC - electronic conductor; CP – conducting polymer; ISM – ion-selective membrane; S – sample solution. Figure adopted from [95].

We have calibrated potentiometric calcium ISE with transducer layer of PEDOT/PSS and super-Nernstian slope was observed (65.63 ± 1.28 mv per decade of

increase). Super-Nernstian slope is usually observed due to uptake of primary ions into ISM phase. Figure 2.7 shows calibration of potentiometric calcium ISE with solid contact PEDOT/PSS.

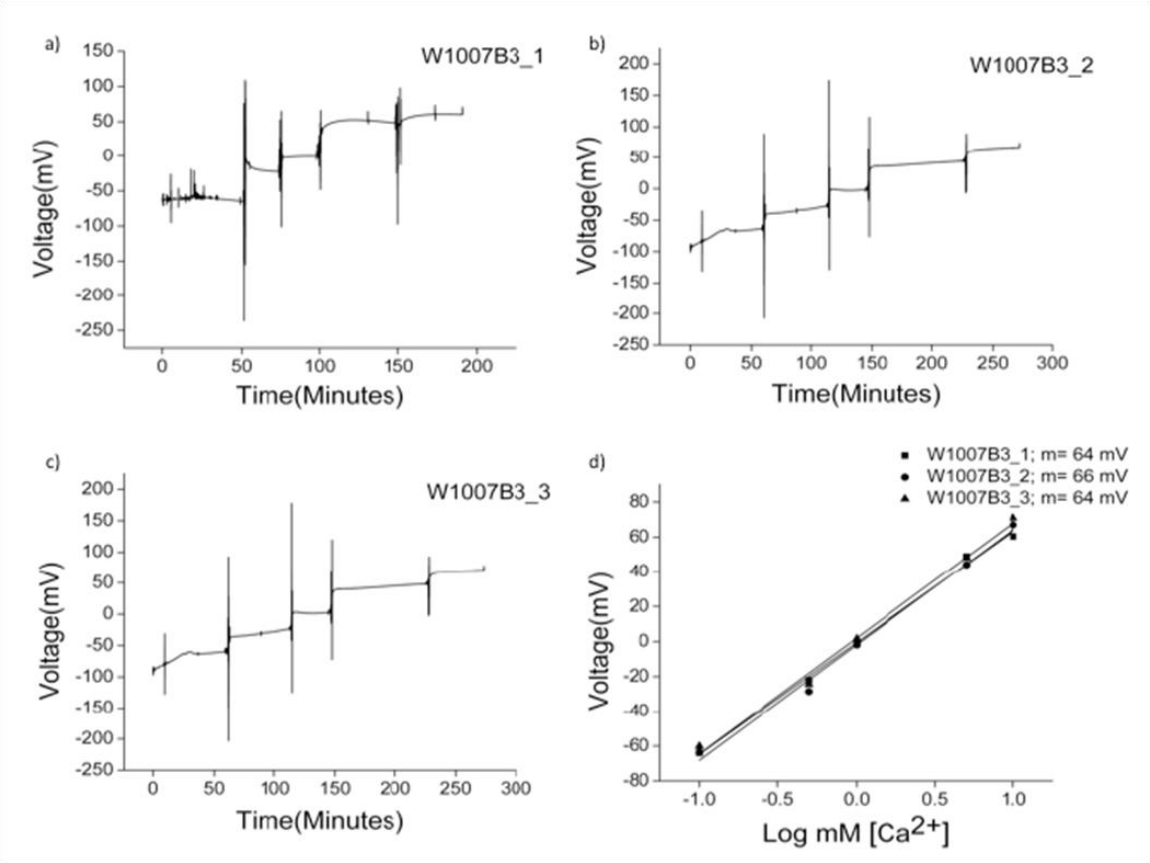

Figure 2.7 Real-time potentiometric response of calcium ISE with PEDOT/PSS transducer layer; (a-c) calibrations from 0.01 mM to 10 mM; (d) sensor calibration fit with super-Nernstian behavior (Courtesy of Michael Zeitchek).

The excess negative charges on PSS promote binding of calcium ions to transducer layer to build up positive charge and this can result in super-Nernstian behavior in Figure 2.7. The area of concern would be the long response times associated with PEDOT/PSS calcium ISE. A possible reason for the elevated response time could exist in the inherent nature of conducting a potentiometric measurement. Potentiometry is

a diffusion-limited process that depends on a change of potential generated by the diffusion of ions at the boundary layer between the liquid-electrode interfaces. In terms of detection limit, PEDOT/PSS calcium ISE showed reasonable performance. The detection limit was 0.018 ± 0.003 μM according to the calibration.

Even though conducting polymer (PEDOT/PSS) showed linear performance and good detection limit, conducting polymer can't be a solution to planar transformation of calcium ISE in patch clamp system. This is because measurement in patch clamp requires immediate response time of the sensor. Also, a target cell would not survive such a long period of time and it would be perished before any detection of calcium from the sensor.

2.2.2 Why ISE without Inner Filling Solution?

It was mentioned in previous section that conducting polymer is very attractive solution to replace inner filling solution into solid-state for minimize ISE volume and planar transformation. Hydrogel-based electrolyte is also another promising candidate to replace liquid inner electrolyte of traditional ISE [98]. The main problem with hydrogel is liquid (mainly water) uptake/release and parallel volume changes of the layer, depending on concentration of salt in hydrogel layer. Volume change can cause the deformation of ISM in solid contact layout shown in Figure 2.6.

As mentioned before, having no internal electrolyte solution would cause drift in measurement signal. Instability would cause frequent recalibration before any measurement can take a place. In order to solve this issue, different composition of calcium ISM is proposed to replace previously used calcium ISM with PEDOT/PSS. Ratios between ionophore & lipophilic ion exchangers and plasticizer & matrix are same

as previous calcium ISM, but weight % of each component is carefully adjusted for optimal linear calibration from 1 μM to 100 mM of calcium on the planar calcium ISE without internal electrolyte solution. Detailed composition change and fabrication process are introduced in CHAPTER 3.3. In this study, newly developed calcium ISM can perform as linearly calibrated sensor with minimum drift, which can be also predicted.

CHAPTER 3. FABRICATION OF PLANAR PATCH CLAMP DEVICE

3.1 Planar Patch-Pore with Cell Well

Fabricating patch-pore is most intrigued and crucial part of planar patch clamp device, because the patch clamp measurement cannot carry on without proper patch-pore with gigaseal formation. Another thing to consider in the fabrication is to create cell loading area, "cell well", above the patch-pore.

To drill a patch-pore, Femtosecond laser pulses of 120-fs (FWHM) duration are generated from a amplified Ti:sapphire laser system with λ = 800 nm with repetition rate of 1 kHz. With 1 μJ (single pulse) of incident energy, fluence is around 60 J / cm^2. A schematic laser setup is shown in Figure 3.1.

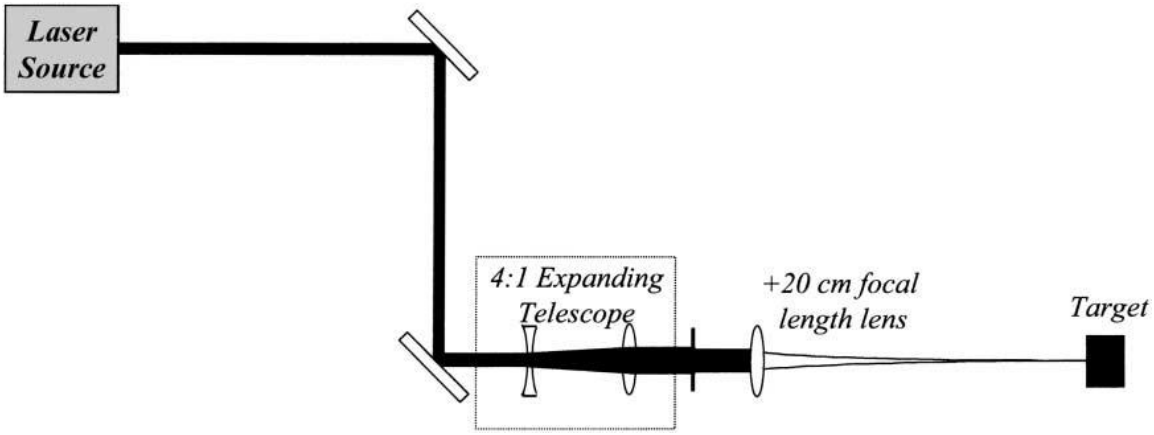

Figure 3.1 Schematic of laser drill setup. Figure adopted from [100]

4 inch 150 μm thick fused silica wafers were purchased from Mark Optics (Santa Ana, CA) for patch-pore fabrication. Fused silica wafer thinner than 300 μm is highly fragile and it could break or crack just by holding it with tweezers, so extra attention is required in handling the wafers. Before any fabrication process, each wafer is carefully Piranha-cleaned with mixture of H_2SO_4:H_2O_2 (3:1) to remove any metals and organic residues. This procedure creates hydrophilic surface condition, which is favorable for maintaining extracellular solution with target cells. Because the mixture is exothermic, it can heat up to 120 ˚C. Mixture needs to be cool down before cleaning process.

Since Purdue University doesn't have Femtosecond laser, we had to find outside resources for patch-pore fabrication. Translume (Ann Arbor, MI) and Lenox Laser (Glen Arm, MD) provide Femtosecond laser drilling with rapid process and precision. Piranha-cleaned fused silica wafers were divided into two batches and each batch was sent two service providers for laser drilling.

In Figure 3.2b "cell well" locations are indicated. The patch-pores were fabricated on the center of the "cell wells". Each wafer contains twenty patch-pores enabling to make twenty patch clamp devices. The 4 mm circular "cell wells" were fabricated on 4 inch 500 μm fused silica wafer. Since "cell wells" were relatively bigger and required less of accuracy, it could use laser-cut technique rather than using laser-drill technique. PLS6MW Multi-Wavelength Laser Platform (Figure 3.2a) by Universal Laser Systems (Scottsdale, AZ) was used for cutting out "cell wells". It has capability of cutting glass with CO_2 laser source with λ = 10.6 μm and 2.0" MW standard focusing lens. Laser power and speed were manually controlled with programmable software for entire cutting process. The main key is to start the cutting at low laser power (20 %) with high speed

(100%). If the cutting process starts with high power (100%), there is a possibility that fused silica wafer can be cracked or even broken. Laser power was increased by 10% and speed was decreased by 10% after 15 repeated cuts until circular "cell wells" were removed from the wafer.

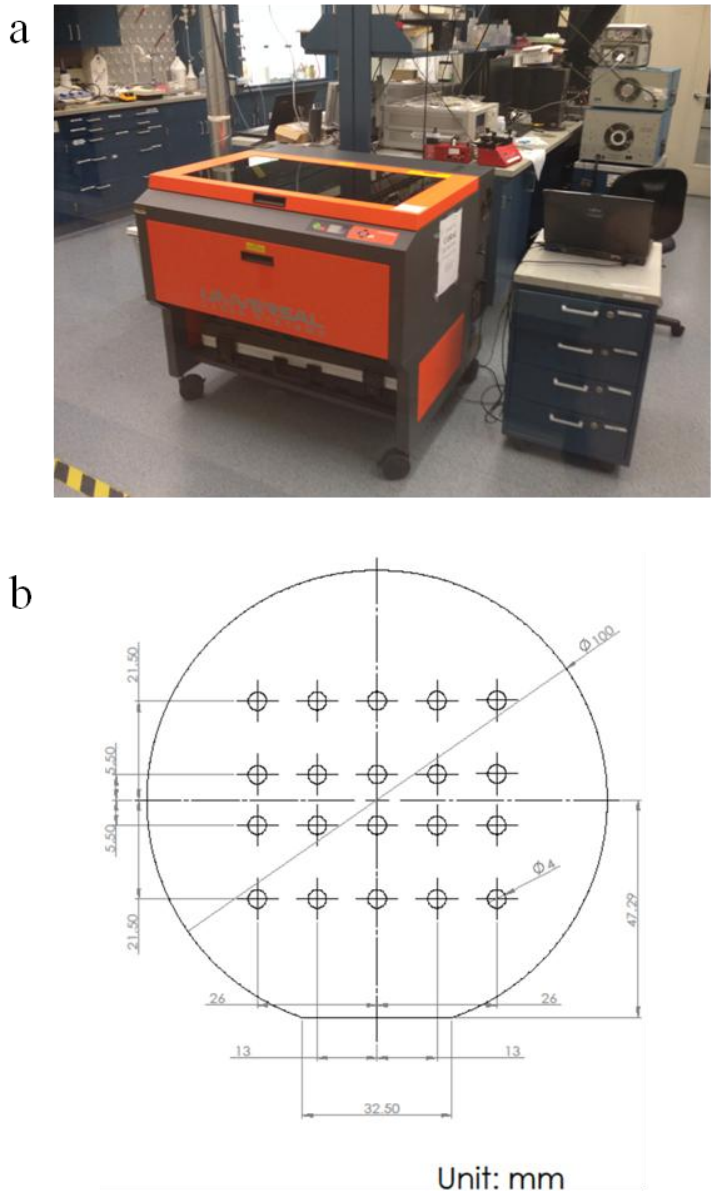

Figure 3.2 "Cell well" laser cut layout; (a) PLS6MW Multi-Wavelength Laser Platform by Universal Laser Systems; (b) cell well locations on fused silica wafer are drawn. Center of cell well is where patch-pore is located.

After cell wells were fabricated, laser-drilled fused silica wafers were examined under microscope. Figure 3.3 shows patch-pores on fused silica wafer. Laser drill done by Translume had relatively larger patch-pore compare to Lenox Laser. Most of patch-pores from Translume were larger than 5 µm which would not be suitable for cell sized less than 10 µm. Lenox Laser provided with average of 4 µm patch-pores. The smallest patch-pore was 3 µm, which would be suitable for patch clamp technique.

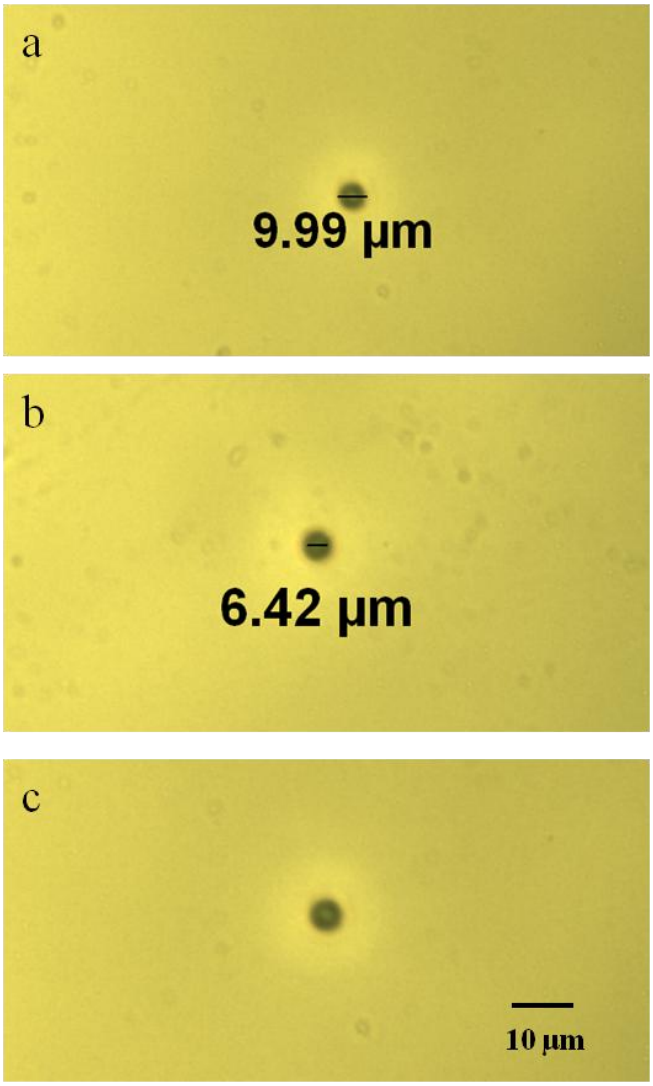

Figure 3.3 Patch-pores drilled on fused silica wafers; (a-b) patch-pores drilled by Translume; (c) patch-pore drilled by Lenox Laser with 3 µm in diameter.

After both patch-pores and cell wells were fabricated on fused silica wafers, bonding procedure was performed. Anodic bonding [101] and direct bonding [102] are common techniques to bond wafers together. Anodic bonding requires heat and electric current between two bonding wafers. It is usually applied to bond silicon to silicon and silicon to glass. Direct bonding uses pressure and heat for the process, and it is used to bond same materials. Direct bonding would be ideal technique for our bonding process. However, bonder in Birck Nanotechnology Center, Purdue University, would not operate up to the temperature where fused silica surface can be bonded. Also, even if temperature can reach melting point, there is a possibility of patch-pore deformation from the heat. To simplify the bonding procedure, 3M adhesive transfer tape was applied to bond patch-pore wafer and cell well wafer. This tape could also protect wafer from cracks might be caused by wafer dicing. Figure 3.4 shows diced planar patch-pore layer with cell well. Size of diced part is 11 mm x 14 mm x 0.74 mm.

This bonding provides structural reinforcement to the layer, so that it can be easily handled and treated with oxygen plasma for final assembly of planar patch clamp device. The accomplishment from patch-pore layer fabrication in this research is that patch-pore is drilled with laser rather than using conventional etching technique, which requires thinning of the substrate before the patch-pore can be fabricated. It makes users to handle the substrate easier than thinned substrate for further fabricate of planar patch clamp device. Also the thickness (150 μm) can maintain patching pressure when suction is applied through the patch-pore.

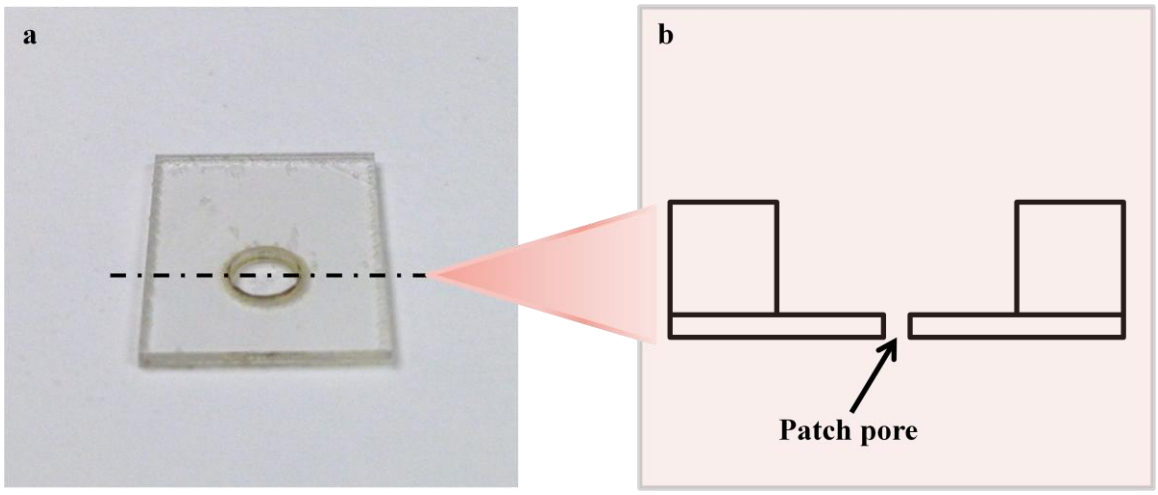

Figure 3.4 Patch-pore with cell well layer replacing glass micropipette; (a) Two fused silica wafers are bonded together with adhesive transfer tape after laser treatment. (b) Cross section from Figure 3.4a (not in scale)

3.2 Intracellular Solution Exchange Chamber

Polydimethylsiloxane (PDMS) has been favorite material to fabricate microfluidic devices [12,19,21,25,27]. It is biocompatible, cheap, transparent, and it can be mold with a resolution down to nano-size. All the advantages led us to choose PDMS as our supporting structure while serving as intracellular solution exchange chamber. This chamber provides connection between planar patch-pore layer and planar calcium ISE layer.

The mold design for intracellular solution exchange chamber is shown in Figure 3.5a. The chamber mold is made from 2 mm thick acrylic sheet. Hollow chamber part is cut from acrylic sheet by CO_2 laser and attached to other acrylic sheet with UV curable glue (Loctite 3301). Once acrylic parts are attached together, the entire mold is cleaned with isopropyl alcohol to remove any residues from surfaces. Cleaning the acrylic mold is crucial because residues can cause irregular surface quality, which could cause and a

problem when PDMS is bonded with other layers. Only the flat surface of PDMS can guarantee the bond between PDMS chamber and other layers without leakage.

After acrylic mold is made, two solution exchange tubes are place within the mold before PDMS mixture is poured. Ends of each tube are treated with UV curable glue to prevent any penetration of PDMS mixture when it's placed in vacuum desiccator. This is very important because solution can't enter or exit if there is no tube connected to the chamber. Syringe puncture method was originally planned after PDMS fabrication, but we realized that puncture would cause a leakage. UV cured glue can be removed once PDMS is cured and provide patching pressure and solution exchange.

Dow Corning SYLGARD 184 Silicone Elastomer Kit was purchased through Dow Corning for PDMS chamber fabrication. To begin to make intracellular solution exchange chamber, the elastomer and curing agent are mixed at weight ratio of 10:1. Constant stir-mixing needs to be done for at least 3 minutes for fine mixture. Once mixture is ready, it can be gently pour into the acrylic mold and wait until mixture can settle. The mixture needs to be slightly over poured since there will be air bubbled form within the mixture. To completely remove this air bubbles, acrylic mold with the mixture is placed inside vacuum desiccator for 30 minutes. When there is no visual of air bubble within PDMS mixture, it can be taken out of vacuum desiccator. In order to ensure the flat surface on top surface, transparent sheet is placed with weight on the top. The sheet needs to be rolled from one edge with angle to prevent any bubble formation. PDMS mold is cured for 24 hours at room temperature (24 ˚C). Baking PDMS in an oven can accelerates cure, but it also causes deformation of the acrylic mold. This creates deformation of PDMS and surface becomes uneven for oxygen plasma bonding in device

assembly. Figure 3.5b shows PDMS intracellular solution exchange chamber integrated with PTFE tubes (ID = 100 μm). Final size of the chamber is 11 mm x 12 mm x 2 mm.

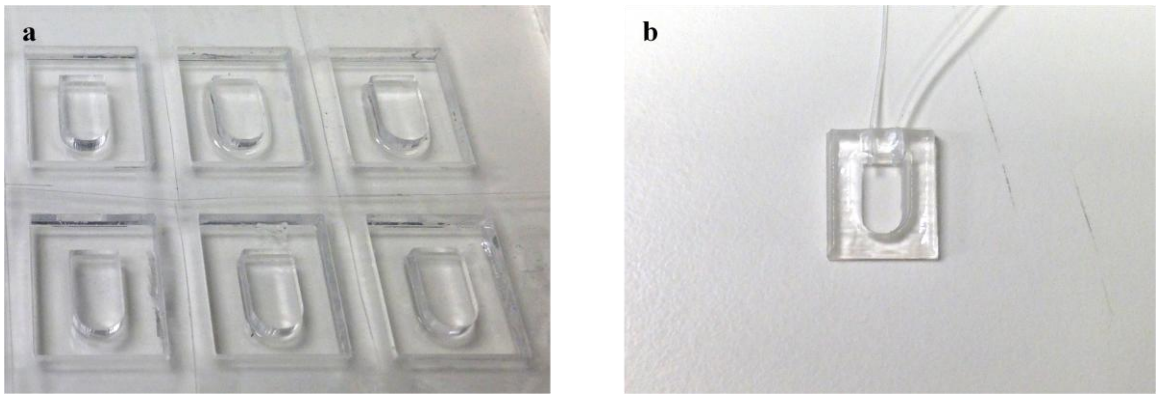

Figure 3.5 The PDMS mold design for intracellular solution exchange chamber;
(a) Acrylic PDMS mold; (b) PDMS chamber integrated with PTFE tubes

The thickness of the PDMS chamber can be adjusted by acrylic thickness. We found that 2 mm is optimal since thinner chamber caused formation of air bubbles within chamber during solution exchange. Epoxy glue can be applied around PTFE tubes for extra seal to prevent any leakage during solution exchange and patching.

3.3 Ag/AgCl Based Planar Calcium Ion-Selective Electrode

Ag/AgCl electrode is a reference electrode used in electrochemical sensing scheme [103]. Following equation shows the electrochemical reaction at the electrode.

$$AgCl_{(s)} + e^{-} \Leftrightarrow Ag_{(s)} + Cl^{-} \quad (3.1)$$

Potential related at the steady state comes from reactant and dissociation activities. This can be represented with Nerst equation [104].

$$E = E^0 - 2.303\left(\frac{RT}{nF}\right)\log_{10}[Cl^-]^{\alpha} \quad (3.2)$$

E^0 is standard potential which is a constant; n is the number of electrons; R is gas constant; T is absolute temperature; F is the Faraday constant; $[Cl^-]$ is the concentration of chloride; α is ion coefficient for chloride.

KCl solution is common chloride salt (inner filling solution) to protect Ag/AgCl electrode in classical reference electrode. This provides a low impedance path for ionic current between Ag/AgCl and target solution. The transient response of reference electrode is also improved by high ion mobility.

As it was discussed in planar transformation in CHAPTER 2, we have decided to eliminate inner filling solutions in our device to simply the calcium ISE fabrication process. Graphical detail of fabrication process is shown with mask designs in Appendix B.

4 inch 500 μm thick silicon wafer is purchased from Mark Optics to fabricate calcium ISE. Before any fabrication procedure, silicon wafers are Piranha-cleaned to remove any dusts or organic residues. Figure 3.7 shows 4 major steps in calcium ISE fabrication. Titanium (30 nm) is deposited as an adhesive between silicon wafer and platinum (150 nm) layer. This platinum is used as wire for signal transfer from Ag/AgCl electrode with calcium ISM. Silicon dioxide (500 nm) is deposited using plasma-enhanced chemical vapor deposition (PECVD) to protect platinum layer from signal

noise and corrosion. Reactive-ion etching (RIE) opened up the area where silver is deposited. After passivation, silver (1 ~ 2 μm) is deposited for final microfabrication process. Figure 3.6 shows result of microfabrication and details of electrode design.

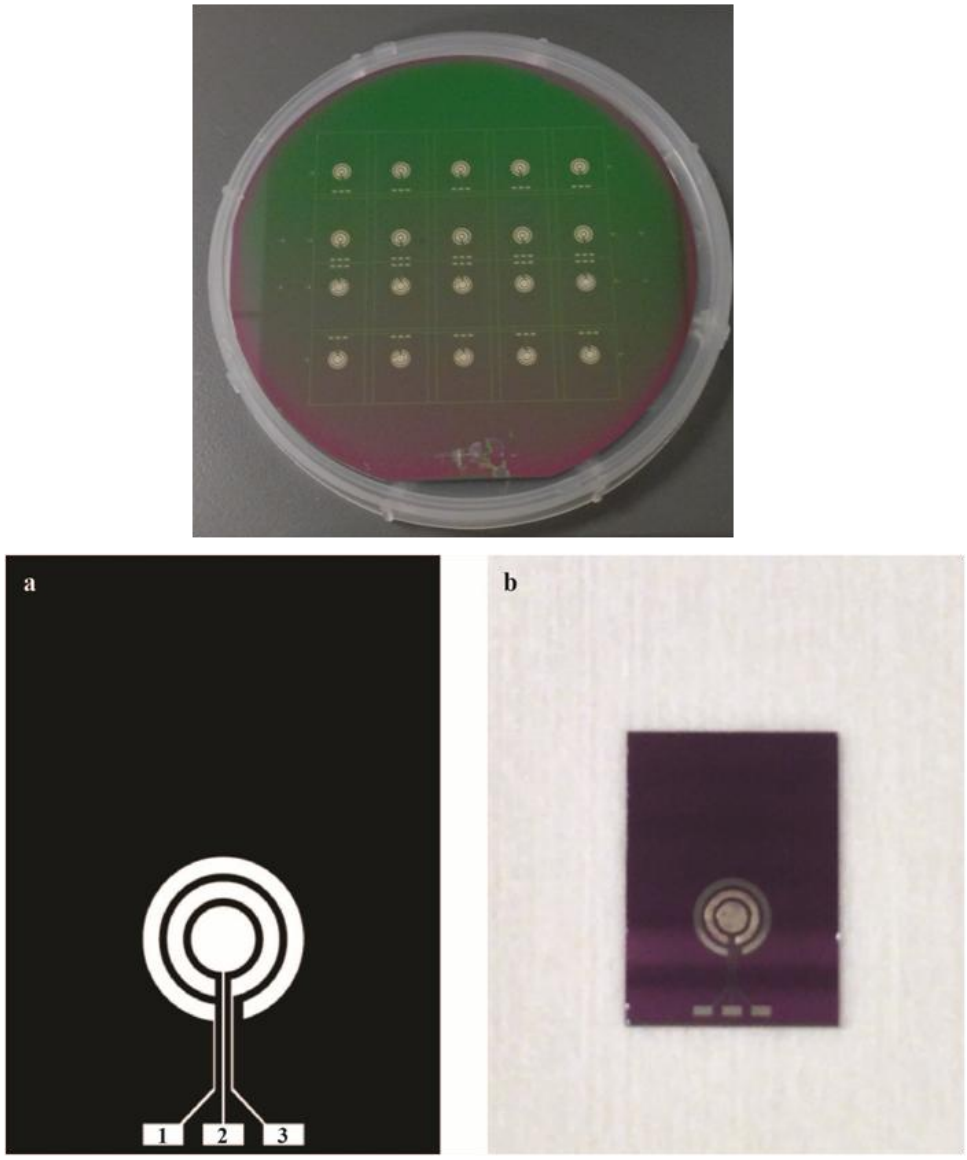

Figure 3.6 Twenty calcium ISE fabricated on silicon wafer; (a1) Pt wire for gigalseal measurement; (a2) Working Ag/AgCl electrode coated with calcium ISM (2 mm^2); (a3) Reference Ag/AgCl electrode (2.8 mm^2); (b) Calcium ISE electrode image. Chip size of 11 mm x 14 mm.

In order to form silver chloride layer, following redox reaction is needed.

$$4Ag_{(s)} + 2NaOCl_{(aq)} + H_2O_{(l)} \longrightarrow 2AgCl_{(s)} + Ag_2O_{(s)} + 2NaOH_{(aq)} \quad (3.3)$$

After silver deposition, electrode is dipped into diluted sodium hypochlorite (10:1) to form silver chloride layer on surface. The surface color changes as a redox reaction takes a place (Figure 3.8).

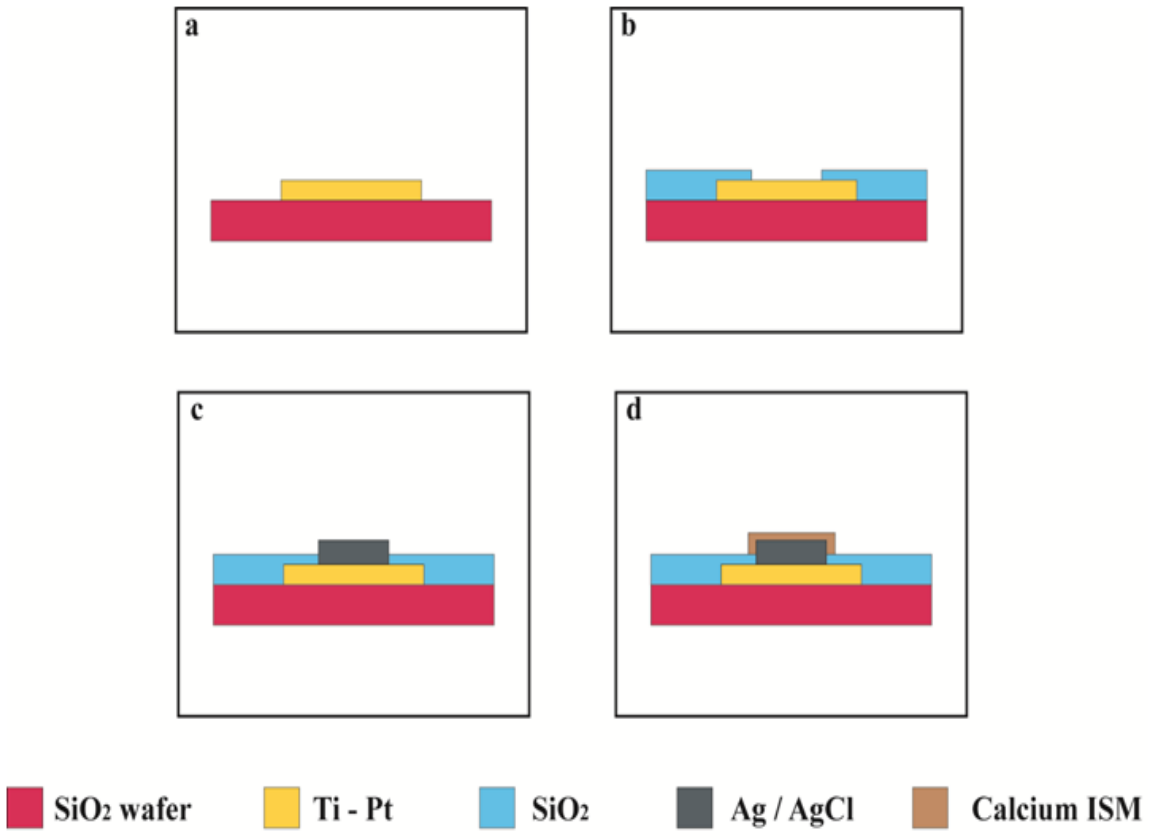

Figure 3.7 Calcium ISE fabrication on silicon wafer; (a) Ti – Pt are deposited on silicon wafer; (b) Silicon dioxide is deposited to protect Ti – Pt layer; (c) Silver is deposited

above Ti – Pt and sodium hypochlorite treatment is performed to form AgCl layer on the surface; (d) Calcium ISM is coated to Ag/AgCl surface for final process.

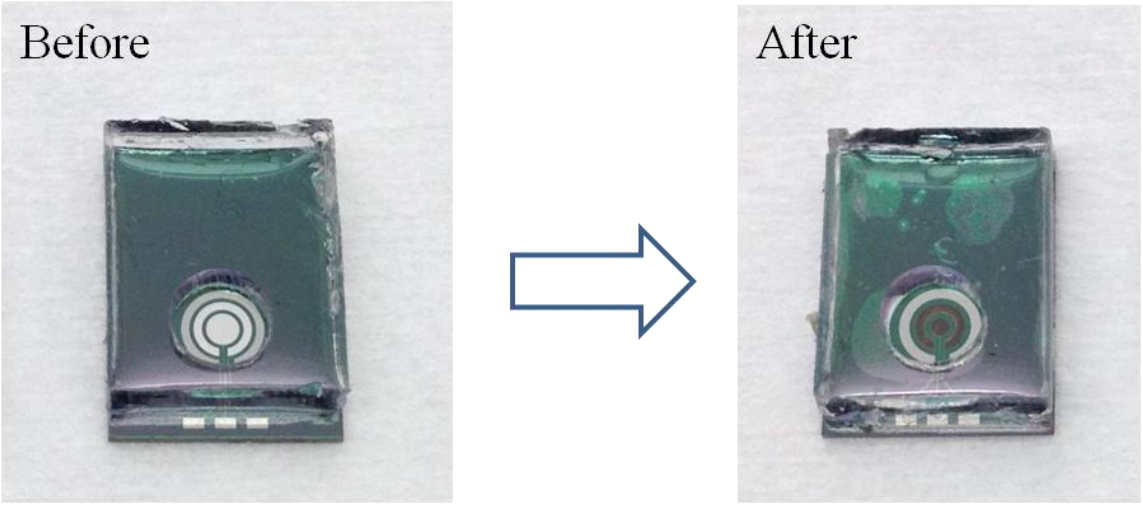

Figure 3.8 Before and after of silver layers treated with diluted sodium hypochlorite.

Final step of calcium ISE fabrication is ISM coating on working electrode. SU-8 photolithography process is applied around working Ag/AgCl electrode before calcium ISM loading to prevent connection between working and reference Ag/AgCl electrodes. Thin layer of photoresist is applied onto silicon wafer to protect electrode area before dicing procedure. The silicon wafer is carefully diced following the dicing line shown in Figure 3.6 using dicing saw (DISCO-DAD). After dicing, the protective photoresist is removed with acetone and isopropanol. Individual chip is carefully dried with nitrogen blow, and scanned under microscope to verify if there is any defect or SU-8 deformation after dicing. Calcium ISM is updated from previous PEDOT/PSS calcium ISE for increase detection capability. Polyurethane (PU) is removed from mixture and higher percentage of PVC is added. Plasticizer, DOS, is replaced with o-NPOE. Table 3.1 shows membrane recipes for PEDPT/PSS and current study.

Table 3.1 Calcium ISM chemical compositions

Componet	Previous weight %	Current weight %
ETH 129 (Calcium ionophore II)	1	3
KTpclPB	0.7	1.8
PVC	19	31.733
PU	10	N/A
DOS	69.3	N/A
o-NPOE	N/A	63.467

The weight ratio between ETH 129 and potassium tetrakis [3, 5-bis (trifluoromethyl) phenyl] borate (KTpclPB) is 1:0.6. The weight ratio between polyvinyl chloride and 2-Nitrophenyl octyl ether (o-NPOE) is 1:2. These two ratios have to be met to produce highly selective membrane. The amount of membrane components added is calculated using a total solution weight of 500 mg.

Calcium ISM fabrication starts with dissolving PVC in cyclohexanone with constant stir for overnight. Parafilm needs to be placed to prevent evaporation of cyclohexanone. After PVC is completely dissolved, remaining components are added and mixed overnight with constant stir. Stirring is required forming a homogenous mixture. Finished ISM is stored in the refrigerator (4 ˚C) for use.

Calcium ISM can be drop-coated on working electrode (1.6 mm in diameter) with micropipette (1 to 2 μL). In order to finish the coating process, solvent (cyclohexanone) evaporation is required. The chip loaded with calcium ISM is placed inside vacuum

desiccator for at least 12 hours to evaporate solvent. This process ensures the adhesion of calcium ISM to Ag/AgCl electrode.

3.4 Assembly

To ensure strong bonding between PDMS and other two layers (fused silica patch-pore and calcium ISE), oxygen plasma-activated treatment is required. Oxygen plasma etcher is shown in Figure 3.9.

Figure 3.9 Oxygen plasma etcher

The bonding mechanism is very similar to the hydrophilic bonding process. Only difference between two is oxygen plasma bonding doesn't require heating in the process for bonding strength. With no extra heat applied, spontaneous reactions within sequential activated surfaces provides in higher bonding strength. Oxygen plasma bonding has two

activation step process. First, oxygen plasma removes native oxide from bonding surface by sputtering and grows oxide on silicon surface. In next step, nitrogen makes surfaces thermodynamically and chemically unstable. Therefore, surfaces become much more hydrophilic after activation. After these two steps, surfaces have increased porosity.

This assembly process is very critical since chamber needs to hold pressure while patching and recording. Bonding surfaces are carefully examined for its flatness before cleaning. Once they are cleaned with acetone and methanol, parts are sonicated in isopropanol bath. Bonding surfaces are carefully placed inside plasma etcher chamber. Once parts are in place, pressure needs to be decreased down to 30 Pa. Oxygen plasma is activated at 200 watts for 60 seconds. After oxygen plasma treatment, parts are removed from chamber for physical bonding. Physical bonding should take less than 60 seconds because treated surfaces can react with air and lose its hydrophilicity and bonding strength. Assembly device is cured on hot plate (60 ˚C) for an hour to increase bond strength between surfaces. Figure 3.10 shows bonding process of planar patch clamp with calcium ISE device for final assembly.

Oxygen plasma can be also replaced with air plasma. Air plasma can be applied without any vacuum. It has advantage of eliminating transition time after applying plasma. Oxygen plasma etcher can take time to increase pressure from vacuum and that gives shorter time for user to physically bond surfaces. Air plasma can eliminate this problem because it can be applied in open-air condition. Since air plasma gun doesn’t bring high volume of plasma like oxygen plasma etcher, surface needs to be treated up to 5 minutes to gain high bond strength.

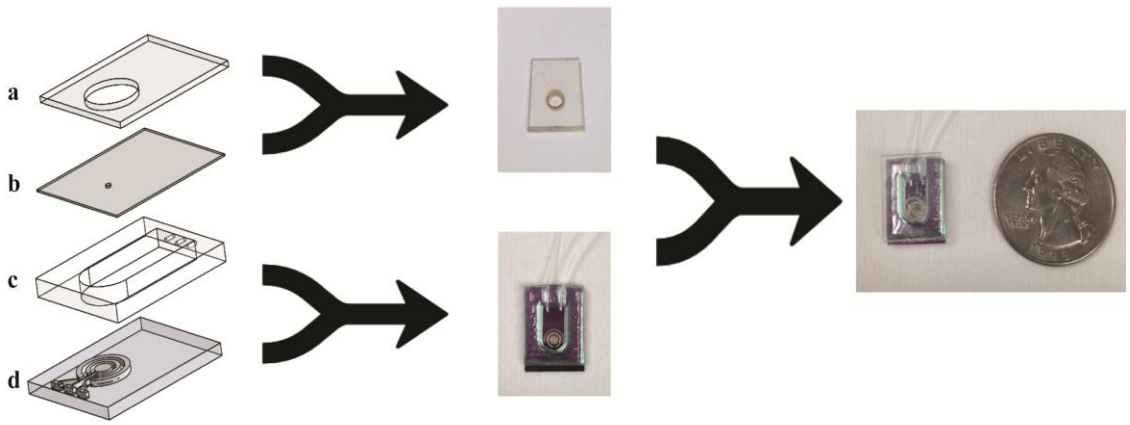

Figure 3.10 Planar patch clamp assembly layout. Assembled device is 11 mm x 14 mm x 22 mm. (a) 500 µm thick fused silica with 4 mm hole "cell well"; (b) 150 µm thick fused silica with ≤ 5 µm patch-pore; (c) PDMS intracellular solution exchange chamber; (d) Calcium ISE

3.5 Measurement Setups

Target monitoring has been always a goal for drug screening and measurement of cell activities. Conventional patch clamp only uses a single Ag/AgCl electrode, so measurement can be recorded through a single patch clamp amplifier. In this way, Ag/AgCl monitors all ion activities within recording time. However, it requires post analysis to identify activities of specific ion after measurement. In this study we have fabricated planar patch clamp device with planar calcium ISE, which can target-monitor ion activities without post-process. This requires simple setup in measurement setups and patch clamp amplifier can be replaced with digital or analog ohmmeter.

There are two important measurement setups in this study. Seal resistance measurement shows the performance of patch-pore. The goal is to reach beyond 1 GΩ to securely patch cell onto laser-drilled planar patch-pore on fused silica substrate. The other measurement setup is for potentiometric calcium concentration measurement for

whole cell recording. Schematic measurement setups are shown in Figure 3.11. To verify the compatibility with current system, we have used patch-clamp amplifier to measure seal resistance of patch pore. Potentiostat is connected to calcium ISE (WE & RE) to monitor calcium ion activities in whole-cell recording experiment.

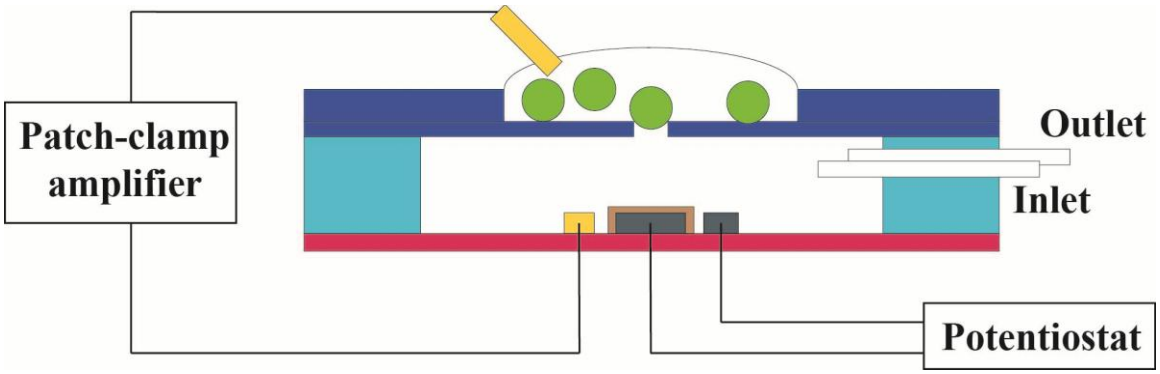

Figure 3.11 Schematic measurement setup for planar patch clamp device.

3.5.1 Seal Resistance Measurement

Conventional patch clamp uses membrane test to measure seal resistance between micropipette tip and a target cell. Membrane test allows user to control the holding potential, which is applied to hyperpolarize a cell to support in membrane seal formation. Typical set up of patch clamp data input system is shown in Figure 3.12. This setup is usable through permission of Dr. Ed Bartlett in Department of Biomedical Engineering, Purdue University. Main components of the system are MultiClamp 700B amplifier (Molecular Devices, Sunnyvale, CA) and Digidata 1440A digitizer (Molecular Devices, Sunnyvale, CA). User input can be controlled with computer software, pCLAMP (Molecular Devices, Sunnyvale, CA).

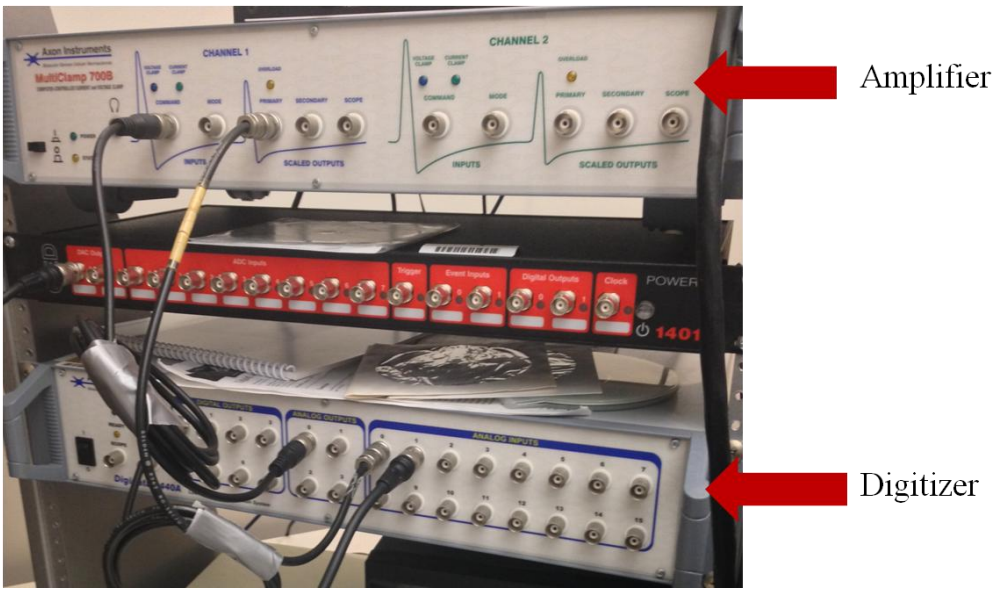

Figure 3.12 Patch clamp amplifier and digitizer.

In this setup, the resistance from an electrode is called electrode resistance, R_e. This resistance is also termed as the patch-pore (pipette in traditional setup) resistance, R_p. It is common that additional resistance appears due to unknown environmental conditions near the electrode. The environmental factors can be air bubbles, debris from cell, and solution conductivity. This can be expressed as R_{debris}. When R_e and R_{debris} are added together, it becomes access resistance, R_{access}. This is also called series resistance, R_s, in patch clamp. The resistance across the cell membrane is termed membrane resistance, R_m. When the cell is in contact with the electrode, there are two paths from electrode to the ground: traversing the membrane and bypassing. Depends on access condition of electrode, only one path is calculated ignoring another. Two paths are drawn in Figure 3.13.

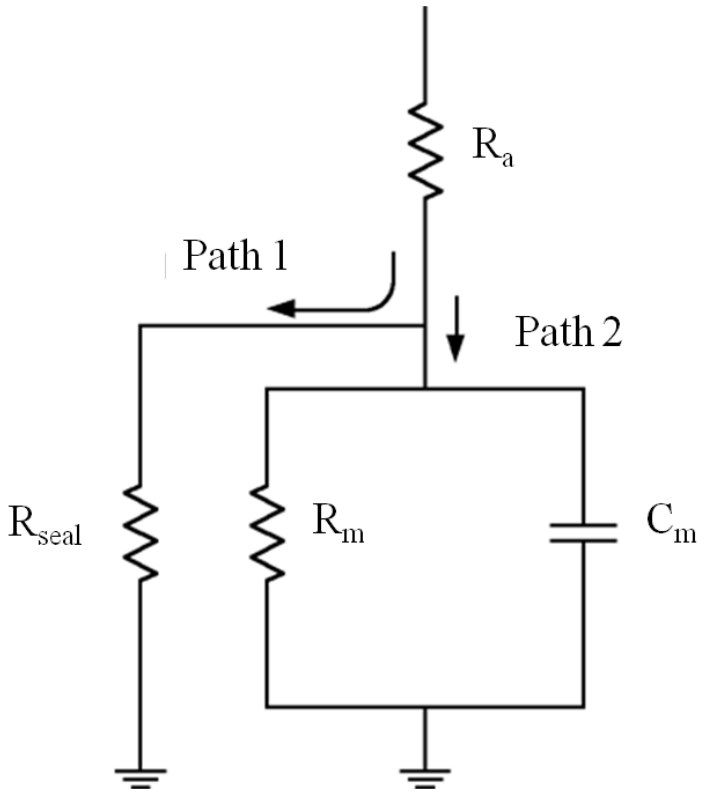

Figure 3.13 Circuit with two paths from electrode to ground.

When a seal is created between the membrane and patch-pore, the resistance is very high, so current would leak through the membrane/patch-pore seal. This is equal to the circuit Path 1 in Figure 3.13. The resistance to this leak, determined by the quality of the seal attained, is commonly called the seal resistance, R_{seal}. In successful seal formation through cell patching, the seal resistance is much higher than access resistance, and it becomes the total resistance, R_t. In this study, we would like to carry out the resistance measurement from planar patch-pore beyond GΩ to verify the technological compatibility of laser-drilling technology.

In this study, PDMS chamber is filled with intracellular solution, Ringer's solution (116 mM NaCl, 2.9 mM KCl, 1.8 mM $CaCl_2$, 1.8 mM $CaCl_2$, 5.0 mM HEPES,

pH = 7.2), before cell is loaded onto planar patch-pore layer. Programmable syringe pump is used to feed the solution through PTFE tube until no air bubble is visible within the chamber. After cells are loaded, outlet tube can be closed and suction pressure can be applied by withdrawing solution from inlet tube. Seal resistance can be observed by connecting Pt wire within the chamber and Pt wire attaching to cell well.

3.5.2 Calcium Measurement

Open circuit potentiometric measurement is performed to measure calcium concentration change within intracellular solution. The open circuit potential is the potential with no current. The core of potentiometric measurements is the Nerst equation, which has a relationship between the concentration of electroactive species on the electrode surface and the potential of the electrode. The potential is measured between working and reference electrode. The working electrode is sensitive to the concentration of the target analyte in solution, calcium in our case. The reference electrode supplies a stable reference potential for the potential of the working electrode. Major parameters used in calcium concentration measurement for open circuit potential verses time is introduced in CHAPTER 4.

For open circuit potentiometric measurement, Ag/AgCl based calcium ISE and reference electrode are connected to BASi C3 Cell Stand (BASi, West Lafayette, IN). Intracellular solutions with different background ion concentrations are tested to validate performance of the calcium ISE. The calibration is performed from 1 μM to 100 mM of calcium. BASi Cell Stand is connected with EC epsilon (BASi, West Lafayette, IN) potentiostat/galvanostat to correct potentials as the calcium concentration changes

through recording. Figure 3.14 show potentiostat setup with Cell Stand for calcium measurement.

Figure 3.14 Cell stand (left) and EC epsilon potentiostat (right) for open circuit potential measurement of calcium concentration.

CHAPTER 4. RESULTS AND DISCUSSION OF EXPERIMENTAL DEVICE

4.1 Seal Resistance Performance

In order to achieve whole cell recording, gigaseal condition is a must. Without a steady gigaseal, quality of data from whole cell recording becomes unreliable. Not only resistance formation matters to patch clamping, monitoring transient current response are critical for seal formation. Collected current data can provide general information about patching pressure range.

Constant potential (voltage) is applied during resistant recording. Both current (A) and resistance (Ω) are recorded to confirm the seal resistance between cell and planar patch-pore. Current recording is important in seal resistance measurement because transient current shapes can identify rupture and whole cell recording condition.

GBAM1 cell line of human glioblastoma stem cells (CD133+ > 98% from passage 18-25) are used to examine seal resistance of planar patch clamp device. Cells are cultured in liquid media DMEM/F12 (Life Technologies, Carlsbad, CA, USA) supplemented with B27 without vitamin A (Life Technologies, Carlsbad, CA, USA) and growth factor EGF, bFGF (50 ng/ml each, Peprotech, Rocky hill, NJ, USA), at 37 ˚C in an atmosphere of 5% CO_2. Cells were cultured up to 100 μm in diameter before seal resistance measurement.

4.1.1 Current Measurement

The current measurement is carried out with voltage pulse of 5 mV filtered at 10 kHz, and digitized at 25 kHz. Setup of current measurement can be found in Figure 3.11. Lower starting resistance (2 ~ 4 MΩ) is preferred for whole-cell recording. If the starting resistance is lower than 2 MΩ, it is difficult to form gigaseal. Our planar patch-pores meet the requirement with average of 2.9 MΩ from 20 patch-pores tested. The starting currents are collected from 20 patch-pores with patch-pore diameter smaller than 5 μm to compare starting current. Figure 4.1 is capture from pCLAMP software at start of current measurement. Figure 4.2 show the relationship between current flowing through planar patch-pore and patch-pore diameter. In conventional glass micropipette, a tip with higher quality and smaller diameter creates higher resistance and lower current at the start of measurement. Our planar patch-pores show similar relationship with conventional glass micropipette. As the planar patch-pore increases its diameter size, current increases its magnitude with constant voltage input across two Pt wires located inside intracellular solution chamber and cell well. Even though planar patch-pore sizes are verified for exact measurement, currents can be quite different from each other. The main reason for this difference might come from the debris in intracellular solution in exchange chamber. Also quality of laser-drilled planar patch-pore edge can create minor noise and extra resistance to current flow. The average planar patch-pore diameter is 3.98 μm with standard deviation of 0.57 μm. The size range of the patch-pore is from 3.12 μm to 4.9 μm. The average starting current is 1.755 nA with standard deviation of 0.31 nA. Specifications of laser-drilled patch-pore provide suitable environment for patch clamp technique.

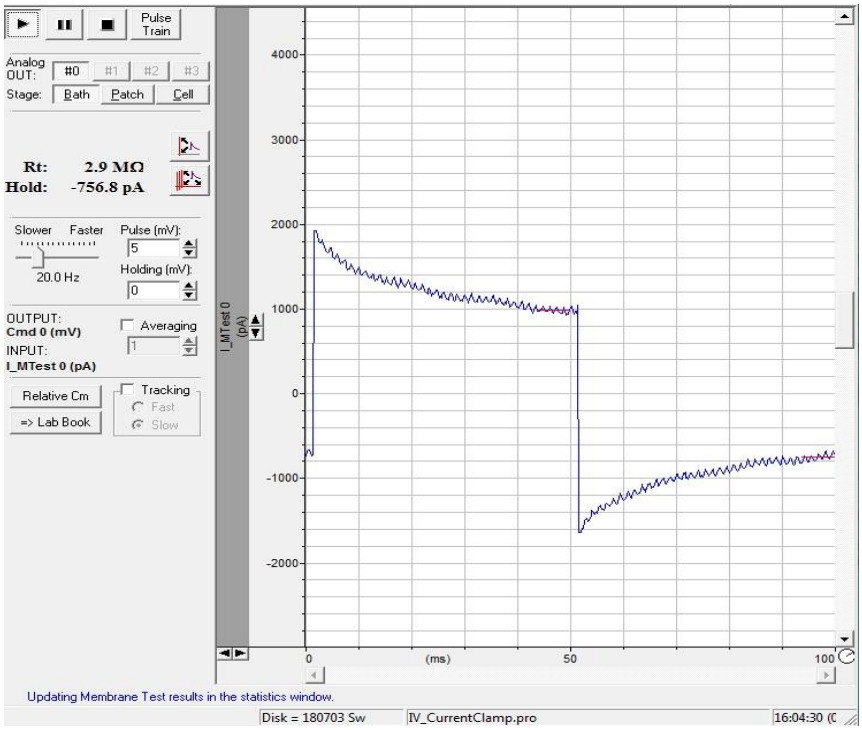

Figure 4.1 Current measurement at bath condition.

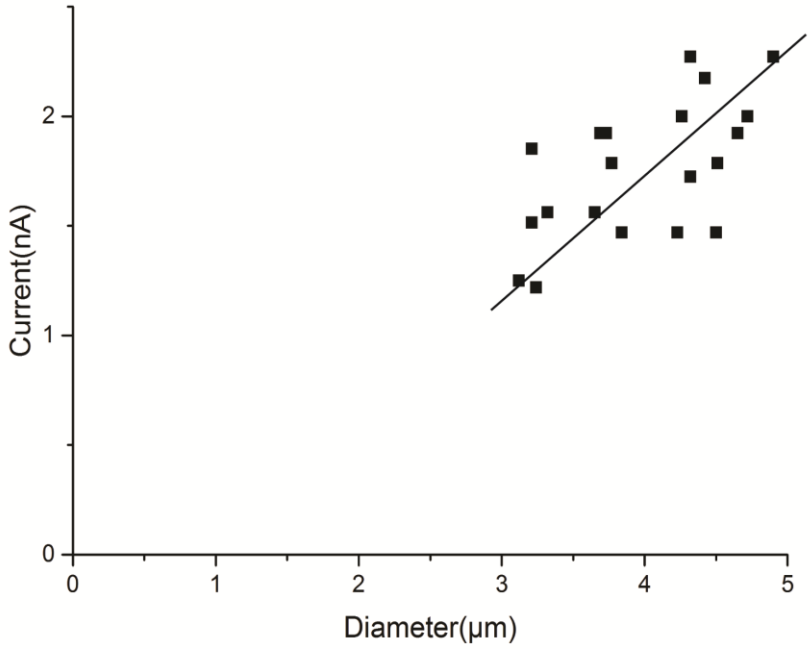

Figure 4.2 Current (nA) vs. patch-pore diameter (μm).

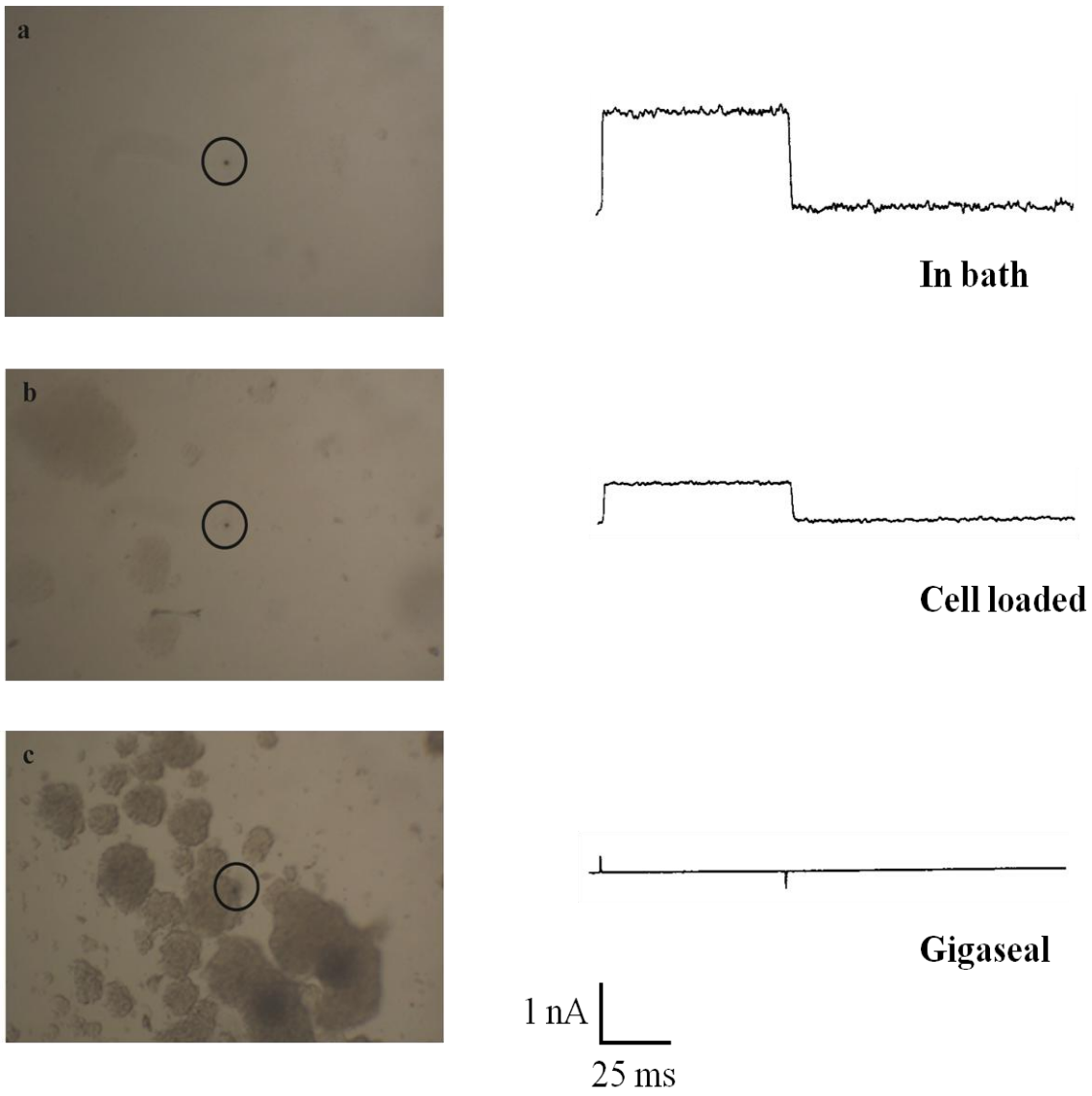

Figure 4.3 Current measurements for seal resistance. Circle in each image shows the location of the planar patch-pore; (a) Current measurement before cells are loaded onto cell well; (b) Current measurement after cells are loaded onto cell well and suction pressure is being applied; (c) Cell is patched onto pore to form gigaseal between intracellular chamber and extracellular area.

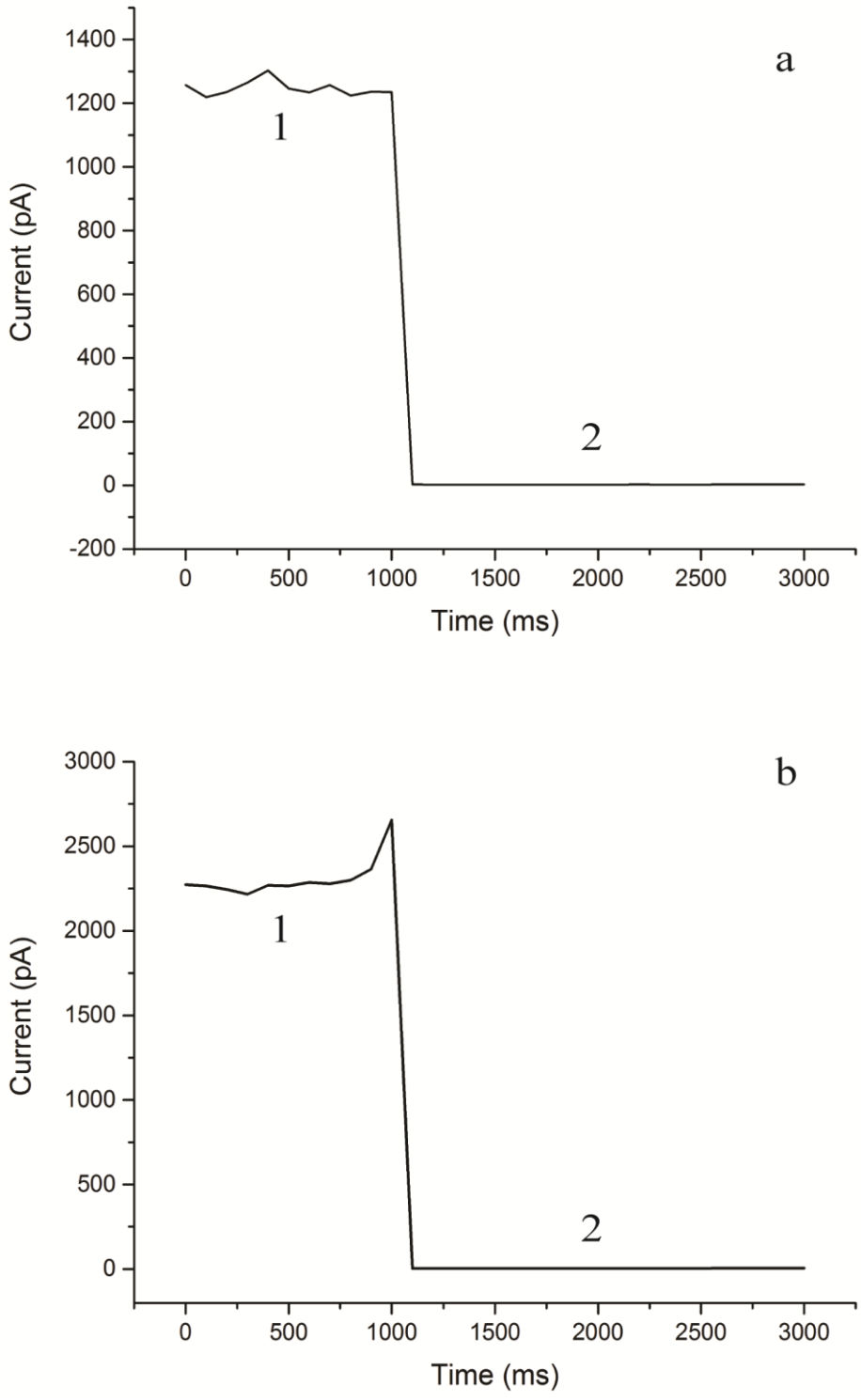

Figure 4.4 Monitored continuous current in cell gigaseal formation. 1:In bath, 2: Cell patched; (a) Patch-pore with 3.12μm. (b) Patch-pore with 4.9 μm

Figure 4.4 shows the behavior of current during gigaseal formation. Smaller planar patch-pore starts at lower current value around 1200 pA (1.2 nA). For our membrane test setting, a gigaseal is achieved when leakage current is reduced to lower than 5 pA. For smaller planar patch-pore, average of 2.128 pA is achieved, which is suitable transition before whole-cell recording. For patch-pore with diameter of 4.9 μm starts at 2300 pA (2.3 nA) and reduced its current to average of 4.3 pA when cell is patched. This confirms a gigaseal formation for the patch-pores and provides good transition stage before whole-cell recording can occur.

Once a gigaseal is achieved, extra 30 to 50 mbar of suction pressure can be applied for membrane rupture. This creates connection to intracellular volume for whole-cell recording. Typical whole-cell recording current trend is shown in Figure 4.5. The current through membrane is usually greater than 0.25 nA for 5 mV input, and sealing current is slightly increased to 6 pA.

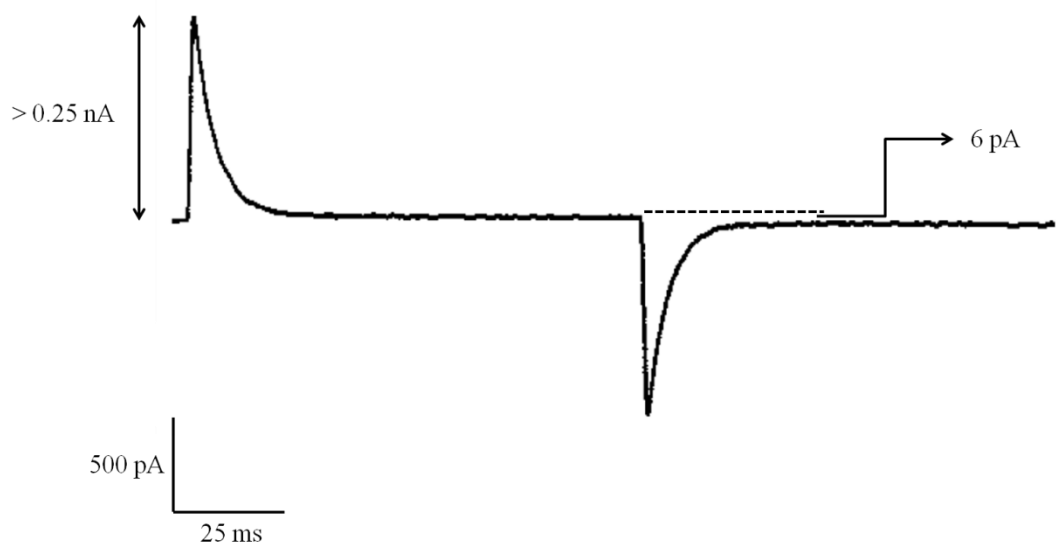

Figure 4.5 Current trend for whole-cell recording at 5 mV voltage-clamp.

4.1.2 Resistance Measurement

Along with current measurement, resistances are recorded throughout cell patching trials. The key to this measurement is to verify if the device can hold its sealing resistance throughout the experiment. It is very crucial factor for the patch clamp experiment because only gigaseal resistance can assure the quality of obtained data during patch clamp experiment. Losing a gigaseal formation within recording time can compromise entire experiment. Starting resistance is measured for 20 planar patch-pores to verify their whole-cell patch ability (Figure 4.6). Planar patch-pores with diameter greater than 5 μm are excluded from measurement since their starting resistance is lower than 2 MΩ. It shows inverse relationship between resistance and size of diameter.

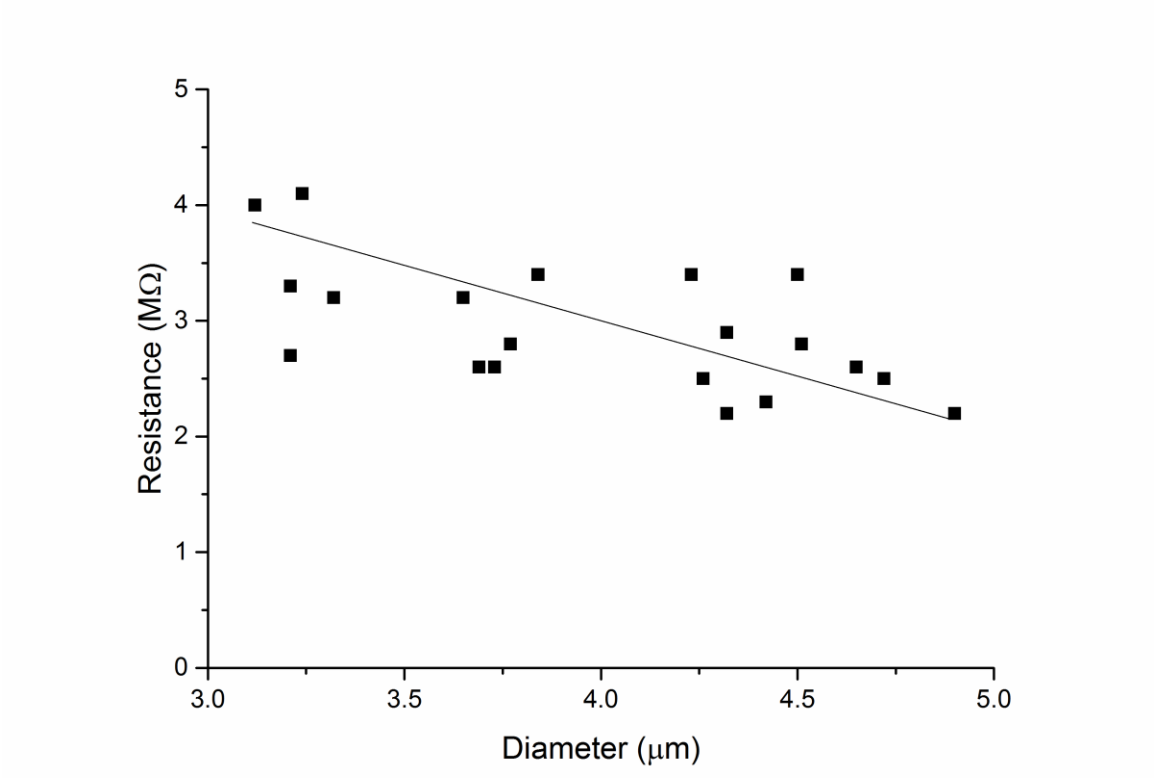

Figure 4.6 Starting resistance vs. planar patch-pore diameter.

Cells are attached to planar patch-pore by applying negative pressure within intracellular solution exchange chamber. 6 out of 20 patch-pores are successfully achieved gigaseal formation. This rate is close to traditional glass micropipette (40~50%) in whole-cell recording [105]. Figure 4.7 illustrates resistance measurement in gigaseal formation for 10 minutes of experiment time.

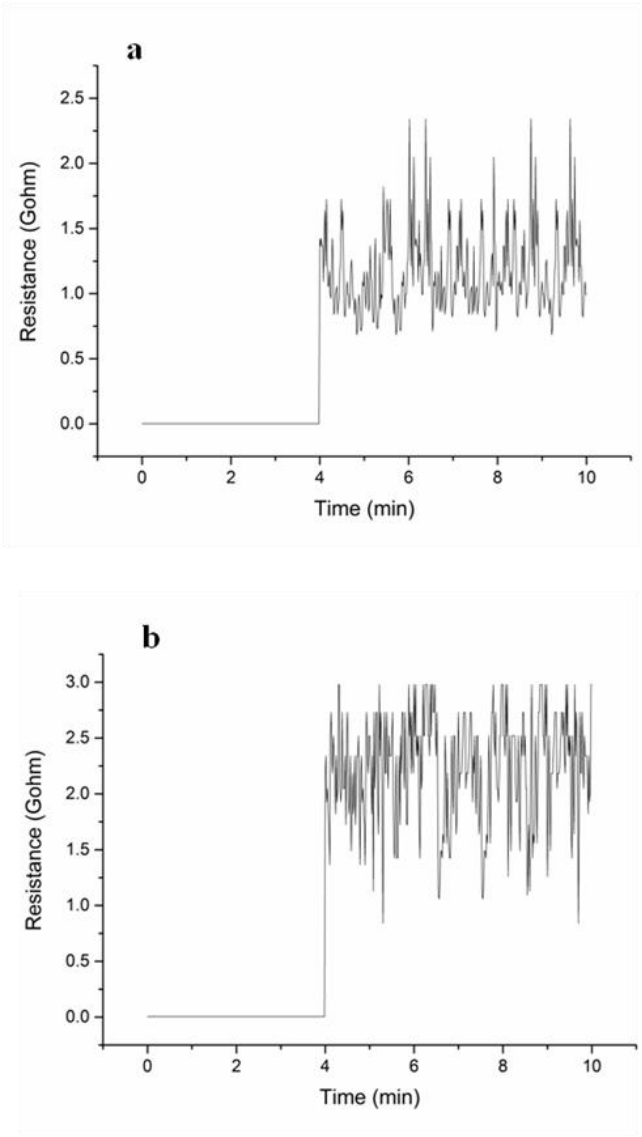

Figure 4.7 Gigaseal formation graphs; (a) Starting at 2.05 MΩ, average of 1.17 GΩ seal is achieved; (b) Starting at 3.91 MΩ, average of 2.23 GΩ is achieved.

The average sealing resistance is 1.17 GΩ and higher sealing resistance, 2.23 GΩ, is achieved on finer patching-pore (3.12μm). At the patching stage, current stays around pico-amp level, so tiny movement of cell or fluidic motion could drastically change the seal resistance. This is why we see oscillations in Figure 4.7 graphs. Syringe pump is used to hold pressure within the chamber after a cell is patched to the pore. Resistance is measure between platinum wire (Figure 3.6 (a1)) on planar calcium ISE and platinum wire dipped into cell well on cell well.

This resistance measurement confirms the performance of patch-pore fabricated using laser-drilling technology. It has advantage over silicon based patch-pore by providing stable and higher gigaseal formation. It is also comparable to traditional glass micropipette as success patching rate can be matched each other.

PDMS intracellular solution exchange chamber provides an excellent seal while negative pressure is applied to patch a cell onto patch-pore. Bonded surfaces have no sign of leak during resistance measurement and hold pressure during experiment.

As a fabrication method, Femtosecond laser drilling is introduced to microfabrication of patch-pore in planar patch clamp device. This technique provides rapid fabrication time over traditional etching technique introduced in the introduction. It still needs some improvement on surface finish, but thinning is not required within the process, which could decrease the structural strength of patch-pore layer. Oxygen plasma bonding technique is verified through seal resistance measurement for its stability and adhesion. No visual leakages or air penetrations are observed while measurements are in progress. This is a huge step forward for planar patch clamp device that provides whole-cell recording.

4.2 Calcium ISE Performance

In this study, planar ion-selective electrode is introduced to patch clamp device for the first time. In order to verify its performance, planar calcium ISEs with different calcium ISMs are tested for approval to use whole-cell patch clamp experiment.

Two different ISMs are applied to Ag/AgCl working electrode: ISM with calcium ionophore IV and ionophore II (modified).

All ISMs are tested for its performance in H_2O and solution with major background ions (5 mM K^+ and 150 mM Na^+). Results are compared for different ISMs to choose best available ISM for planar calcium ISE in our patch clamp device.

4.2.1 Calibration

ISM with Calcium Ionophore IV

Calcium ISM with ionophore IV recipe has been available to PSF for ISE fabrication. This recipe is start point of our ISM verification to make compatible calcium ISE in patch clamp device. Table 4.1 shows the component of the ISM.

Fabricated calcium ISE is calibrated and checked for its sensitivity and drift.

Table 4.1 Calcium ISM recipe using ionophore IV

Component	Weight %
Polyurethane (PU)	10
Polyvinylchloride (PVC)	19
Bis (2-ethylhexyl) sebacate	69.3
Calcium ionophore IV	1
Potassium tetrakis [3, 5-bis (trifluoromethyl)phenyl] borate (KTpCIB)	0.7
Cyclohexanone	10 wt%/vol

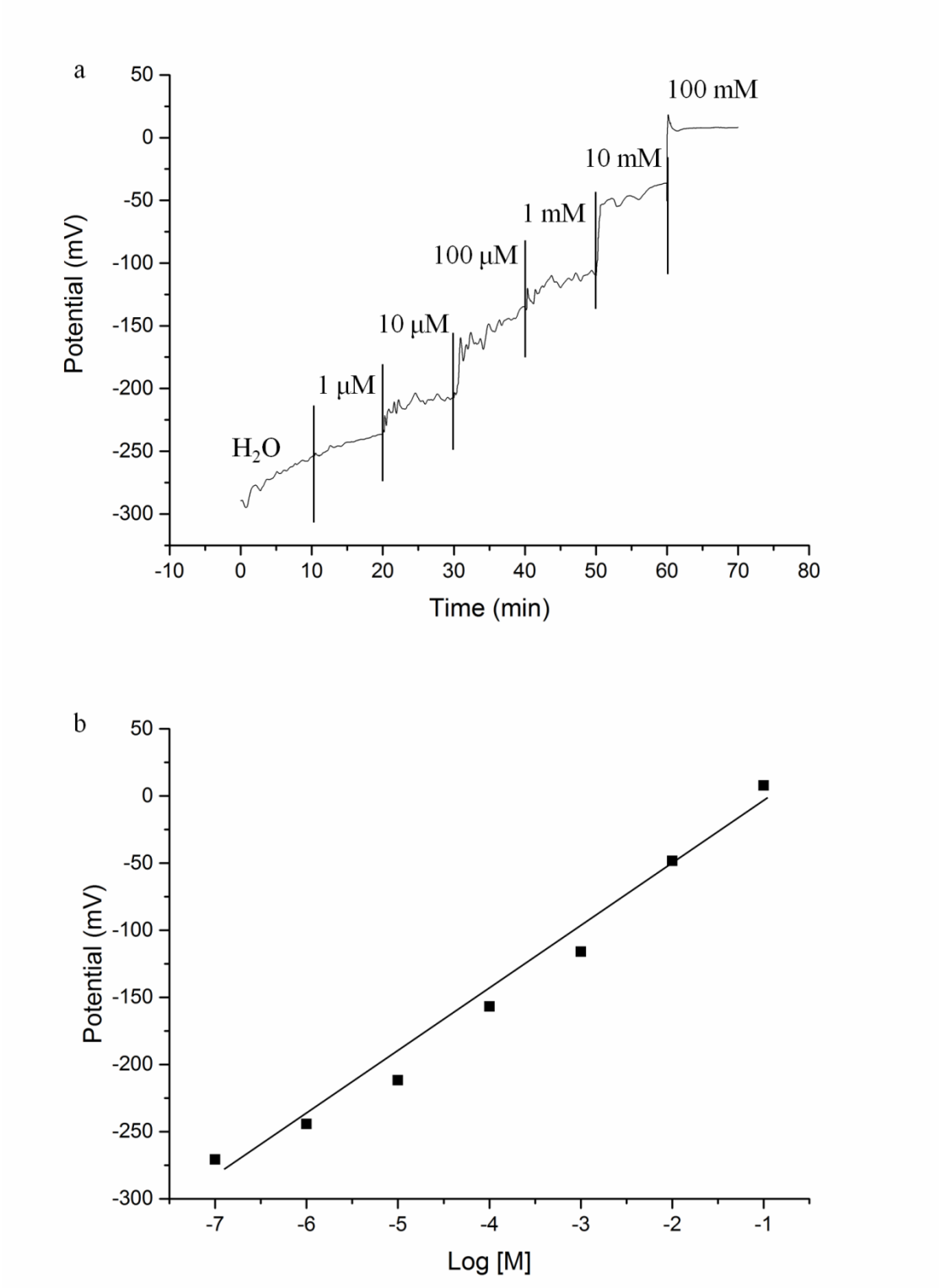

Figure 4.8 Planar calcium ISE – ionophore IV (unconditioned) calibration without background ions; (a) Calibration curve; (b) Linear fit

Figure 4.8 shows the calibration curve and linear fit for calcium ISE using ionophore IV without conditioning. Calcium concentration is increased every 10 minutes to observe any significant change in calibration. It shows 51 mV increase per decade of increase in calcium concentration (super Nernstian response). It is important to recognize that the calibration starts from H_2O without any background ions. This might not be suitable for patch clamp recording, because intracellular solution has various kinds of ions in the background. This calibration is performed to verify the basic sensor functionality and performance comparison towards other ISE calibration with presence of dominant background ions.

In order to minimize drift and stabilize the signal, calcium ISE is conditioned for 2 days before calibration: first day in high calcium concentration (100 mM) and next day in low calcium concentration (1 μM) prior to calibration. Conditioning might result improvement in reducing the drift and stabilization of signal once certain concentration is reached. If stable signal can be observed after conditioning, stabilization time can be decreased to 5 minutes from 10 minutes.

After calcium ISE is conditioned for two days, sensor is recalibrated with starting solution with 1 μM calcium ion in the background. The result is shown in Figure 4.9 with linear fit from 1 μM to 100 mM. As the calibration shows, conditioning helps stabilization of signal and drift is almost negligible compare to unconditioned calibration. So the average within 5 minutes of recording time is highly precious and accurate compare to unconditioned calcium ISE. Linear fit shows 59 mV increase per decade of increase in calcium concentration (super Nernstian behavior). After 10 mM of calcium, saturation is detected, which can be assumed as high detection limit for this ISM.

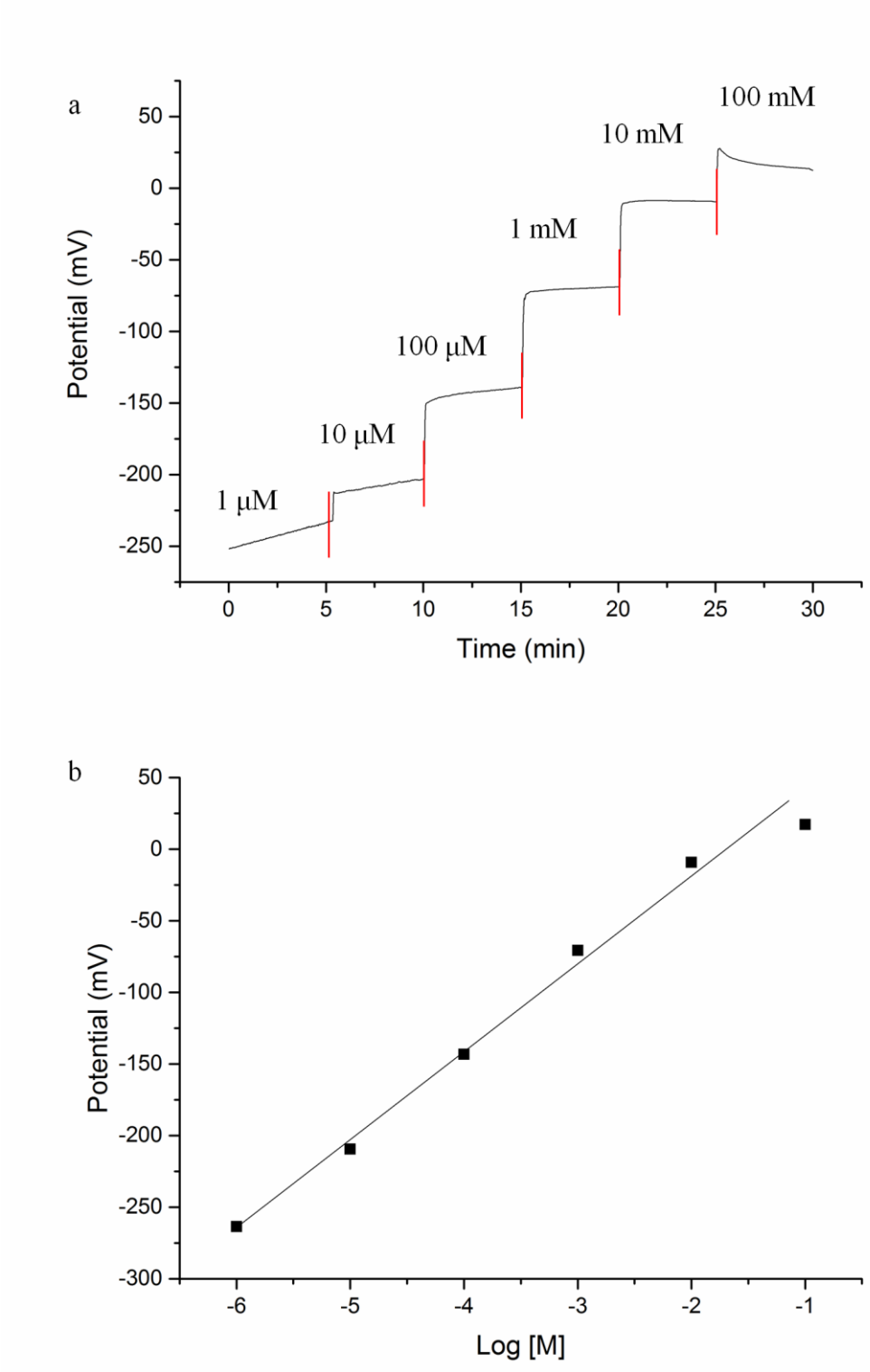

Figure 4.9 Planar calcium ISE – ionophore IV (conditioned) calibration without background ions; (a) Calibration curve; (b) Linear fit

In order to prove that this calcium ISE can perform with planar patch clamp device, sensor is calibrated with a solution with dominant background ions within intracellular solution. The dominant ions are potassium and sodium ions are included in conditioning solution for ISM. The calcium ISE is condition with solution containing 5 mM K^+, 150 mM Na^+, and 100 mM Ca^{2+} for first day. Then, the calcium ISE is transferred to the solution with 5 mM K^+, 150 mM Na^+, and 1 μM Ca^{2+} for next day. The calibration is started with a solution containing 5 mM K^+, 150 mM Na^+, and 1 μM Ca^{2+}. The solution increases its calcium concentration at every 5 minutes to observe any changes in potential.

As shown in Figure 4.10, this sensor doesn't provide predictable step increase per decade of increase in calcium concentration. This is because the ISM can't block the penetration of chloride ion. All the solutions, including conditioning solutions, have presence of potassium and sodium ions. This condition can provide constant interference to measurement [106,107]. Even though the calcium ISE is conditioned for 2 days, this membrane composition is not dependable for calcium measurement in intracellular solution. Unlike previous calibration which contained no background ions, this calibration result shows high drift level with noise. Previous calibration has slight increase-drift, but this calibration has decrease-drift with no sign of increase until 10 mM of calcium.

We have determined that this ISM cannot guarantee the performance within intracellular solution chamber in planar patch clamp device.

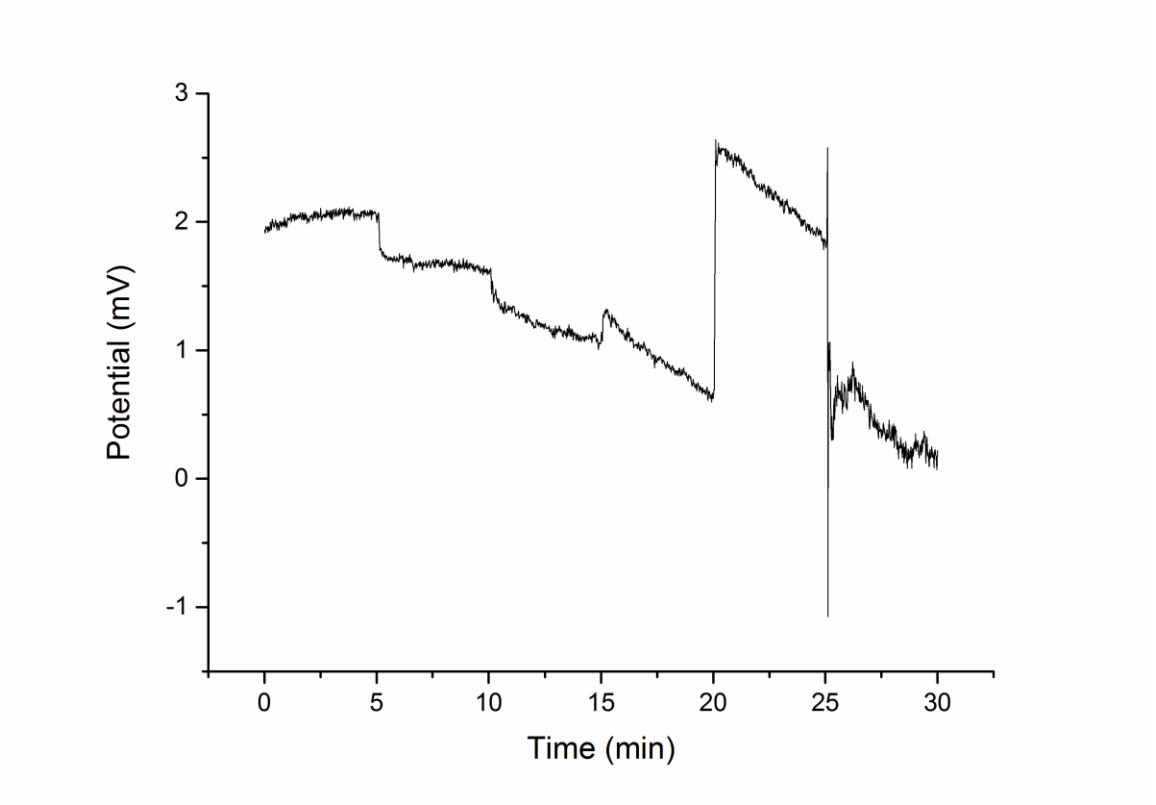

Figure 4.10 Planar calcium ISE – ionophore IV (conditioned) calibration with background ions.

ISM with Calcium Ionophore II

The ISM with calcium ionophore IV is found to misfit for planar patch clamp device. Other ISM with better selectivity and inner matrix needs to be provided for the planar platform. It is reported that polyurethane is likely to let other ions to penetrate through ISM. ISM with polyurethane and PVC mixture has lower sensitivity compares to PVC only as an inner matrix [108,109]. Membranes with ionophore II and IV used in PEDOT/PSS have polyurethane and PVC mixture as inner matrix. In order to construct predictable calcium ISE, changes are made. Table 3.1 shows the modification of the ISM with calcium ionophore II.

Figure 4.11 and 4.12 show the result of calibration of calcium ISE with newly developed ISM. Their conditioning solutions are exactly same as calcium ISE with ionophore IV.

Calcium ISE with ionophore II shows similar trends with calcium ISE with ionophore IV when it is calibrated in solution without any background ions. It shows 35 mV increases per decade increase in calcium concentration over 1 μM to 1 mM range. This is very similar to theoretical step-increase from traditional ISE with ionophore II that has inner filling solution (33.4 mV), but saturation occurs after 1 mM. In contrast, calcium ISE doesn't reach its saturation point when there are background ions are present in calibration solution.

When planar calcium ISE with ionophore II is calibrated in solution with background ions, it shows continuous step increase over 1 μM to 100 mM range. It has 1.9 mV increases per decade increase of calcium concentration. This is very predictable and repeatable over time. The resolution of this calibration is 10 μV, which is capable of detecting any difference within each decade increase.

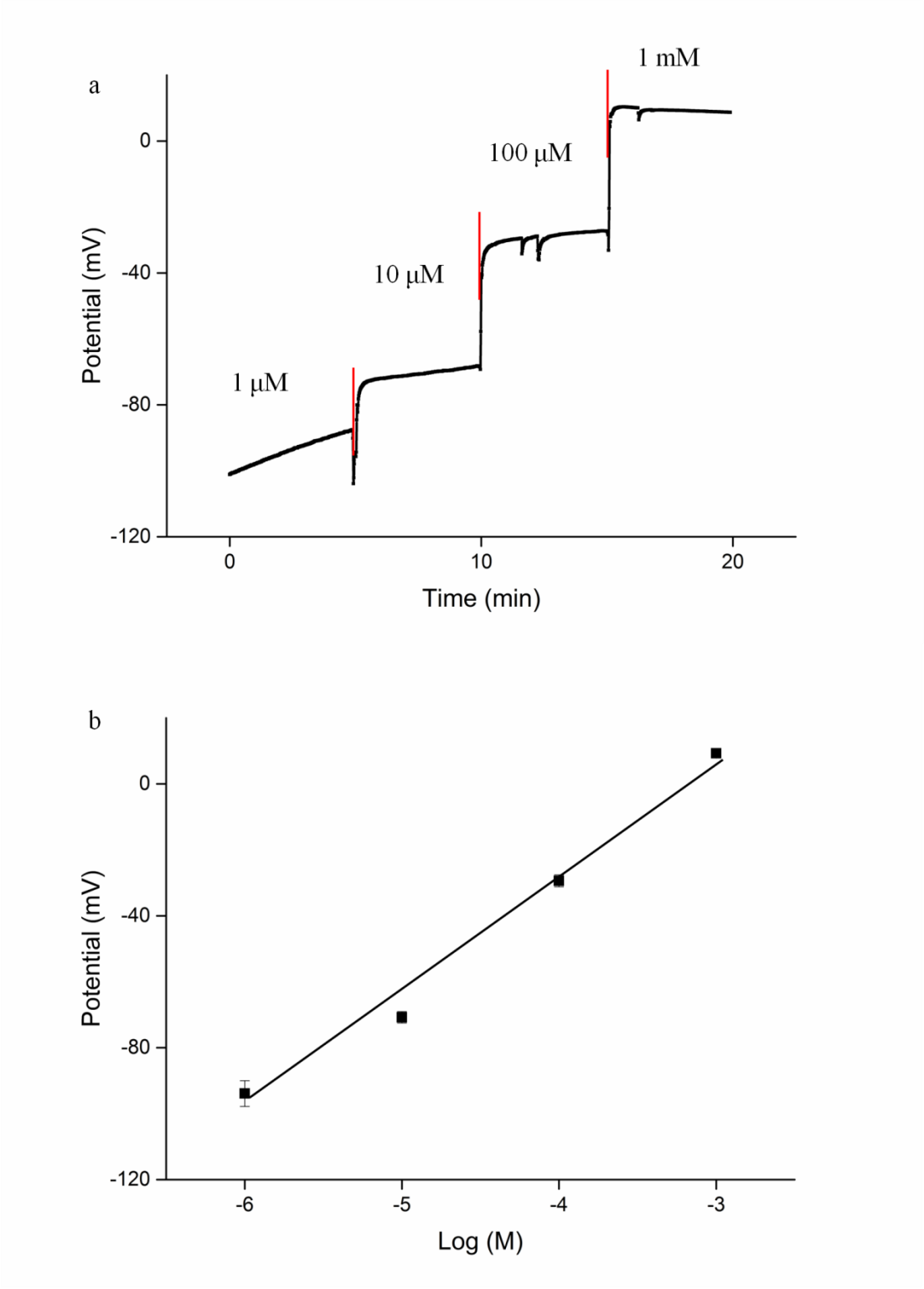

Figure 4.11 Planar calcium ISE – ionophore II (conditioned) calibration without background ions; (a) Calibration curve; (b) Linear fit.

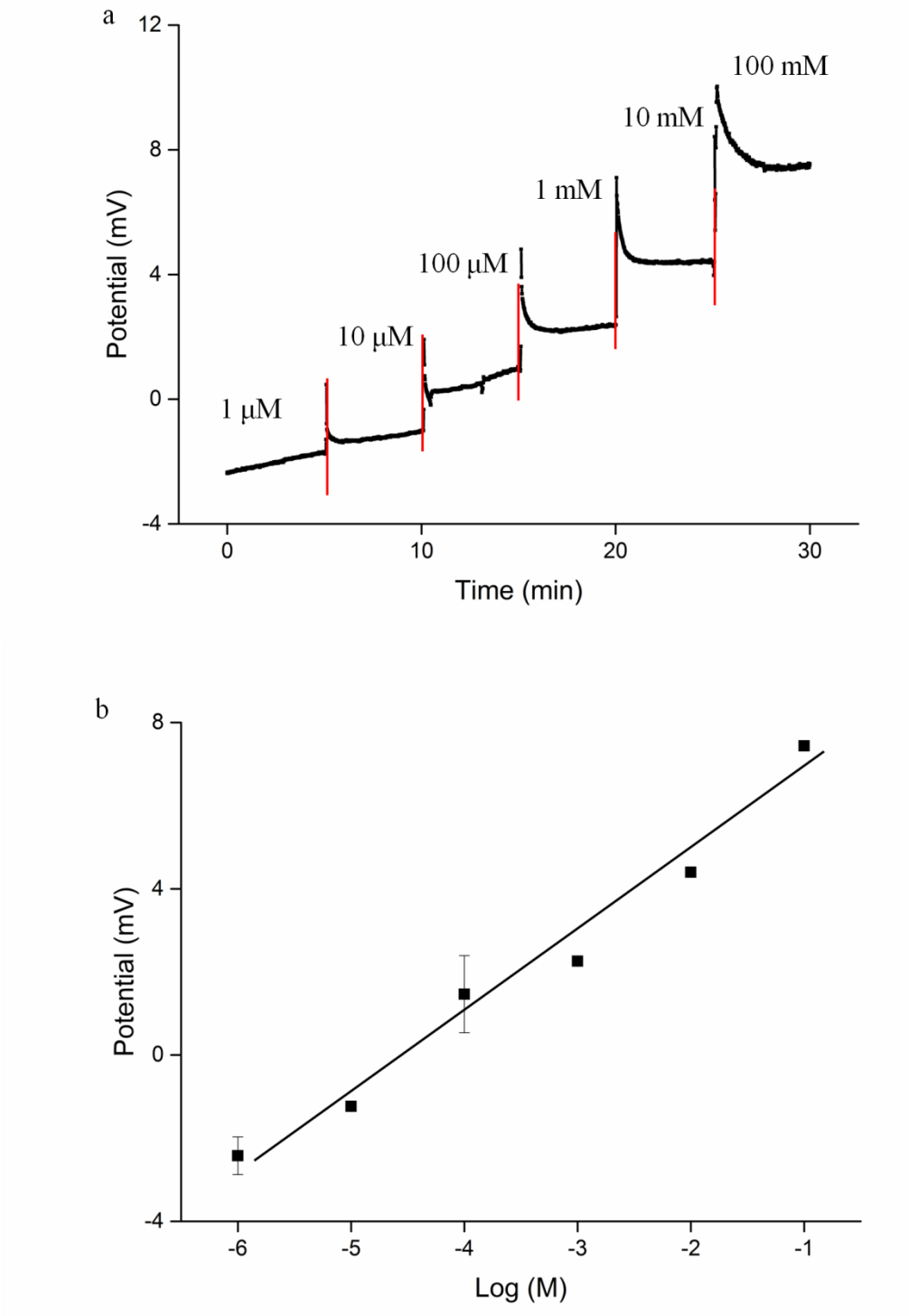

Figure 4.12 Planar calcium ISE – ionophore II (conditioned) calibration with background ions; (a) Calibration curve; (b) Linear fit.

4.2.2 Drift

Drift is inevitable in electrochemical sensor. Coated type electrode suffers from instability due to the formation of a water layer at electrode/ISM interface, responding to oxygenation of sample [94], or changes in ionic concentration [110].

In order to minimize drift, calcium ISE is allowed to stabilize for at least 15 minutes before calibration. For calcium ISE with ionophore IV calibrated without background ions (Figure 4.9a) has 1.7 mV min^{-1} of drift per decade. For calcium ISE with ionophore II calibrated without background ions (Figure 4.11a) has 1 mV min^{-1} of drift per decade. Both sensors show increase of potential much larger than drift. But calcium ISE with ionophore IV is unreliable if it is exposed to intracellular solution because it doesn't provide predictable calibration (Figure 4.10) and drift seems to be much higher with noise.

The planar calcium ISE with ionophore II has signal drift of 0.06 mV min^{-1}, which is lowest of all we have tested. Since the drift is limited, it doesn't influence in a crucial way of characterizing planar calcium ISE. Patch clamp experiment is limited to less than an hour and it also depends on the cell type, so this minor drift is not an issue. So our planar calcium ISE is a excellent sensor to monitor calcium in patch clamp technique performed on the planar device.

For long-time measurement, different type of stabilization method needs to be developed. The signal stabilization should consider both properties of electrode and environmental conditions, such as biological fouling from organic materials in the range of detection.

4.2.3 Detection Limit

At high and low ionic activities, saturations occur in ISE. Typical detection limits are shown in Figure 4.13.

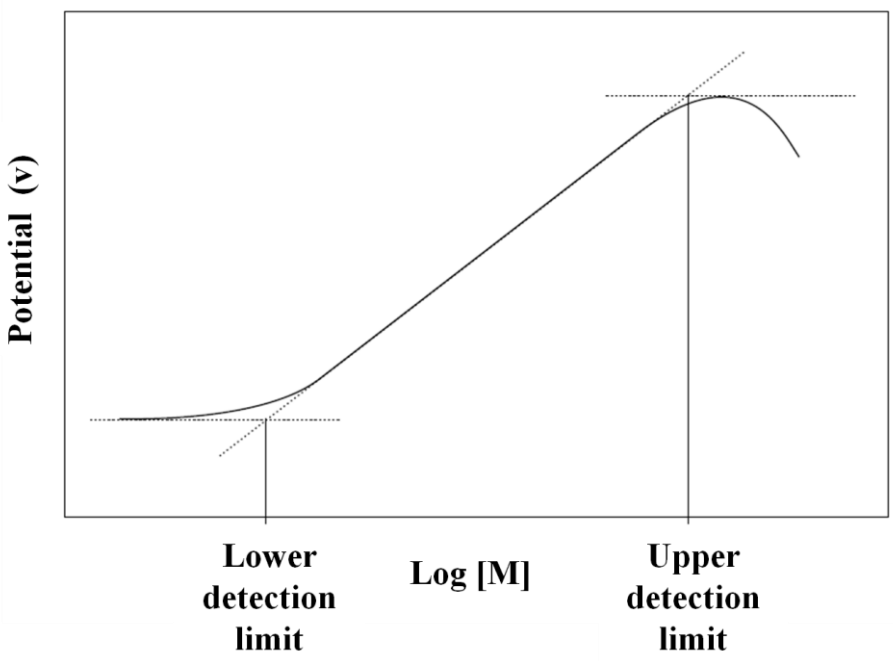

Figure 4.13 Recognizing upper and lower detection limit.

For upper detection limit, our calcium ISE only has saturation in calibration without background ions. Upper saturation limit is shown in detail in Figure 4.14 (Extension of Figure 4.11). Upper detection limit is determined by the intersection point of the linear fit and limiting high activity response [111]. In our case of Figure 4.14, upper detection limit is 5 mM.

In our calcium ISE calibration range, 1 μM to 100 mM, no lower detection limit is observed. Typical lower detection limit for calcium ISE with ionophore II is 20 nM [107], but this is for calcium ISE with inner filling solution.

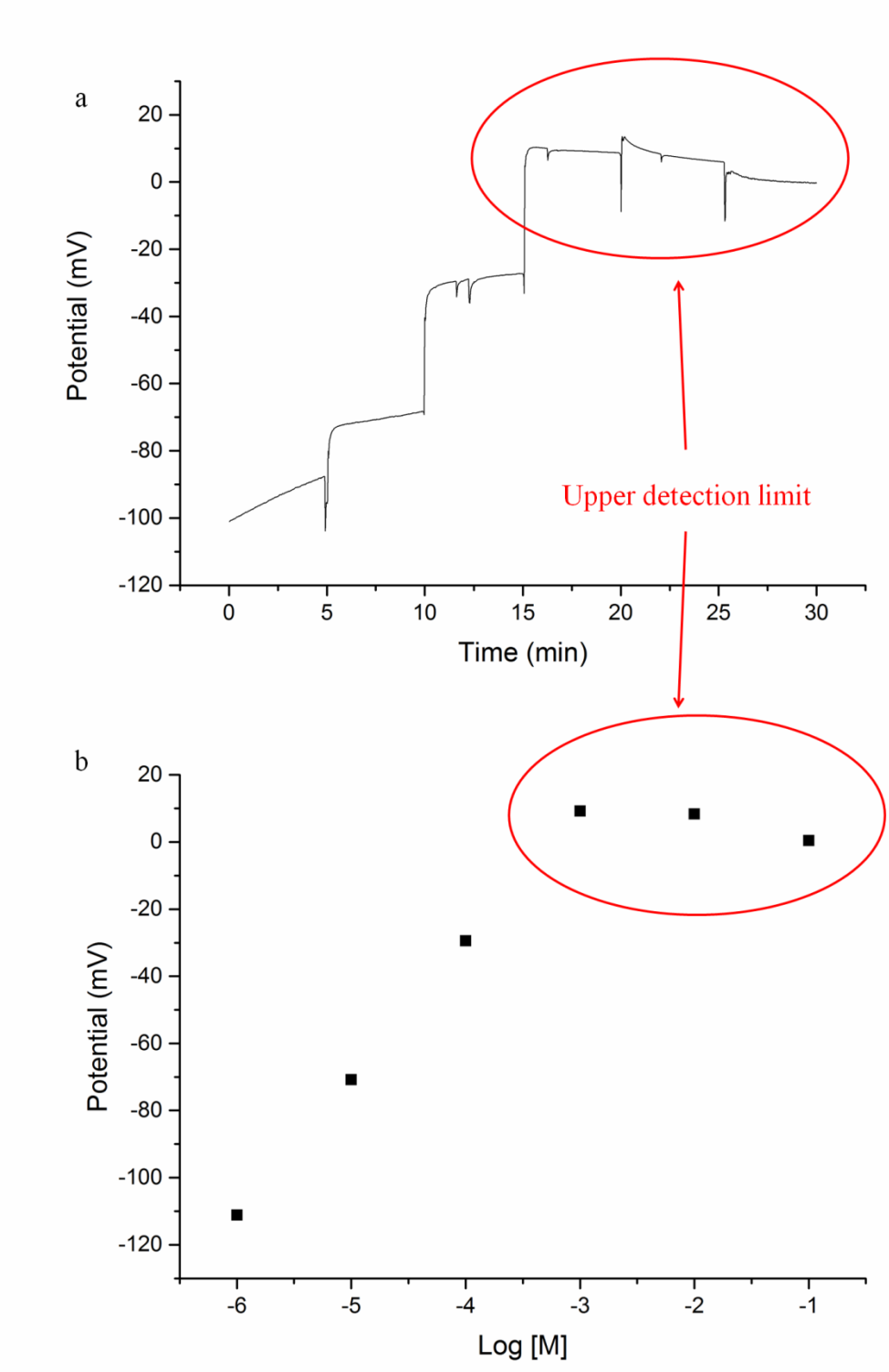

Figure 4.14 Upper detection limit at 5 mM; (a) Calibration curve; (b) Linear fit.

CHAPTER 5. CONCLUSIONS AND FUTURE RESEARCH

5.1 Accomplishments

For this Ph.D work, a planar patch clamp device with potentiometric calcium ion-selective electrode has been developed for the first time. This includes the planar transformation of patch-pore & calcium ion-selective electrode, and performance validation of the integrated device. This work could potentially lead to the intriguing prospect of planar patch clamp device. The main conclusions are outlined as follow:

1. This was the first time that planar patch-pore was fabricated using laser-drilling technique. Patch-pores < 5 μm were successfully fabricated on fused silica substrate for whole-cell recording.

2. Planar calcium ion-selective electrode without inner filling solution was fabricated on silicon substrate. This design opened up the way to monitor calcium in real-time without post data analysis.

3. Resistance and current measurements were performed for laser-drilled patch-pores. Patch-pores showed great ability to form stable gigaseal before whole-cell recording could be performed. The succession rate was

40% (8 out of 20), which could be matched with traditional glass micropipette.

4. Planar calcium ion-selective electrode calibration was performed in a range from 1μM to 100 mM of calcium ions. Calibration showed sensor's predictable linear increase per decade increase of calcium concentration.

5.2 Topics for Future Research

Although many planar patch clamps with potentiometric calcium ion-selective electrodes have been fabricated and realized in this work, there are still some critical issues that need to be solved or optimized in order to improve patching ability and sensitivity of calcium ion-selective electrode. As mentioned before, the sensitivity for planar calcium ion-selective electrode is low, because there is no inner filling solution. Author has tried to overcome the disadvantage by changing composition for ion-selective membrane. If the selectivity can be increased by putting highly stable inner filling layer in planar form, it could increase the selectivity of the sensor.

Multi-ISE setup might be realized. Since we know that there are more ISMs can be applied to this setup, multiple Ag/AgCl can be fabricated on a single substrate to monitor multi ions at single recording.

The patch-pore fabrication quality can be improved. There are continuous researches in microfabrication which involves laser. There might be an optical way to add more precision in drilling micro-sized holes. If size can be precisely controlled, planar patch clamp can do more than whole-cell recording, such as single ion channel monitoring.

Signal processing system, patch clamp amplifier, can be miniaturized for portable use of this planar patch clamp device. Since this is target ion-monitoring electrode, circuits can be simplified into and controlled by user friendly computer software.

The cell well can be bonded with patch-pore layer before patch-pore can be fabricated. This process can prevent deformation of patch-pore and provide stable cell well without a leak during patch clamp experiment.

REFERENCES

REFERENCES

[1] Lewenstam, A. (1991). "ION-SELECTIVE ELECTRODES IN CLINICAL CHEMISTRY STATE OF THE ART." Analytical Proceedings **28**(4): 106-109.

[2] Lewenstam, A. and A. Hulanicki (1990). "SELECTIVITY COEFFICIENTS OF ION-SENSING ELECTRODES." Selective Electrode Reviews **12**(2): 161-201.

[3] Widmaier, E. *Human Physiology*, 7th ed.; McGraw-Hill: New York, 1998.

[4] Xu, J., X. B. Wang, et al. (2001). "Ion-channel assay technologies: quo vadis?" Drug Discovery Today **6**(24): 1278-1287.

[5] Neher, E. and B. Sakmann (1976). "SINGLE-CHANNEL CURRENTS RECORDED FROM MEMBRANE OF DENERVATED FROG MUSCLE-FIBERS." Nature **260**(5554): 799-802.

[6] Sakmann, B. *Single-channel recording*, 2nd ed.; Plenum Press: New York, 1995.

[7] Hamill, O. P., A. Marty, et al. (1981). "IMPROVED PATCH-CLAMP TECHNIQUES FOR HIGH-RESOLUTION CURRENT RECORDING FROM CELLS AND CELL-FREE MEMBRANE PATCHES." Pflugers Archiv-European Journal of Physiology **391**(2): 85-100.

[8] Neher, E. and B. Sakmann (1992). "THE PATCH CLAMP TECHNIQUE." Scientific American **266**(3): 44-51.

[9] Sakmann, B. and E. Neher (1984). "PATCH CLAMP TECHNIQUES FOR STUDYING IONIC CHANNELS IN EXCITABLE-MEMBRANES." Annual Review of Physiology **46**: 455-472.

[10] Fertig, N., R. H. Blick, et al. (2002). "Whole cell patch clamp recording performed on a planar glass chip." Biophysical Journal **82**(6): 3056-30

[11] Stett, A., C. Burkhardt, et al. (2003). "Cytocentering: A novel technique enabling automated cell-by-cell patch clamping with the CytoPatch (TM) chip." Receptors & Channels **9**(1): 59-66.

[12] Pantoja, R., J. M. Nagarah, et al. (2004). "Silicon chip-based patch-clamp electrodes integrated with PDMS microfluidics." Biosensors & Bioelectronics **20**(3): 509-517.

[13] Sordel, T., S. Garnier-Raveaud, et al. (2006). "Hourglass SiO2 coating increases the performance of planar patch-clamp." Journal of Biotechnology **125**(1): 142-154.

[14] Matthews, B. and J. W. Judy (2006). "Design and fabrication of a micromachined planar patch-clamp substrate with integrated microfluidics for single-cell measurements." Journal of Microelectromechanical Systems **15**(1): 214-222.

[15] Li, X. H., K. G. Klemic, et al. (2006). "Microfluidic system for planar patch clamp electrode arrays." Nano Letters **6**(4): 815-819.

[16] Zhang, Z. L., T. Asano, et al. (2008). "Fabrication of Si-based planar type patch clamp biosensor using silicon on insulator substrate." Thin Solid Films **516**(9): 2813-2815.

[17] Kiss, L., P. B. Bennett, et al. (2003). "High throughput ion-channel pharmacology: Planar-array-based voltage clamp." Assay and Drug Development Technologies **1**(1): 127-135.

[18] Lehnert, T., M. A. M. Gijs, et al. (2002). "Realization of hollow SiO2 micronozzles for electrical measurements on living cells." Applied Physics Letters **81**(26): 5063-5065.

[19] Klemic, K. G., J. F. Klemic, et al. (2002). "Micromolded PDMS planar electrode allows patch clamp electrical recordings from cells." Biosensors & Bioelectronics **17**(6-7): 597-604.

[20] Fertig, N., A. Tilke, et al. (2000). "Stable integration of isolated cell membrane patches in a nanomachined aperture." Applied Physics Letters **77**(8): 1218-1220.

[21] Pantoja, R., J. M. Nagarah, et al. (2004). "Silicon chip-based patch-clamp electrodes integrated with PDMS microfluidics." Biosensors & Bioelectronics **20**(3): 509-517.

[22] Fertig, N., M. Klau, et al. (2002). "Activity of single ion channel proteins detected with a planar microstructure." Applied Physics Letters **81**(25): 4865-4867.

[23] Bruggemann, A., M. George, et al. (2003). "High quality ion channel analysis on a chip with the NPC (c) technology." Assay and Drug Development Technologies **1**(5): 665-673.

[24] Xu, J., A. Guia, et al. (2003). "A benchmark study with SealChip (TM) planar patch-clamp technology." Assay and Drug Development Technologies **1**(5): 675-684.

[25] Klemic, K. G., J. F. Klemic, et al. (2005). "An air-molding technique for fabricating PDMS planar patch-clamp electrodes." Pflugers Archiv-European Journal of Physiology **449**(6): 564-572.

[26] Seo, J., C. Ionescu-Zanetti, et al. (2004). "Integrated multiple patch-clamp array chip via lateral cell trapping junctions." Applied Physics Letters **84**(11): 1973-1975.

[27] Xu, B. J., Z. B. Liu, et al. (2009). "A PDMS PLANAR PATCH-CLAMP ARRAY CHIP WITH POLY (ETHYLENE GLYCOL)/SU-8 BASED CELL-PATCH INTERFACE." Ieee 22nd International Conference on Micro Electro Mechanical Systems (Mems 2009): 395-398.

[28] Fertig, N., M. George, et al. (2003). "Microstructured apertures in planar glass substrates for ion channel research." Receptors & Channels **9**(1): 29-40.

[29] Lamb, D. R. (1970). "SOME ELECTRICAL PROPERTIES OF SILICON-SILICON DIOXIDE SYSTEM." Thin Solid Films **5**(4): 247-&.

[30] McDonald, J. C. and G. M. Whitesides (2002). "Poly(dimethylsiloxane) as a material for fabricating microfluidic devices." Accounts of Chemical Research **35**(7): 491-499.

[31] Sylgard 184, Dow Corning Corp., Midland, Miland, MI, http://www.dowcorning.com.

[32] Levien, L., C. T. Prewitt, et al. (1980). "STRUCTURE AND ELASTIC PROPERTIES OF QUARTZ AT PRESSURE." American Mineralogist **65**(9-10): 920-930.

[33] Romashin, A. G. and Y. E. Pivinskii (1968). "Properties of fused silica ceramics." Refractories **9**(9-10): 590-595.

[34] Mathes, C. (2006). "QPatch: the past, present and future of automated patch clamp." Expert Opinion on Therapeutic Targets **10**(2): 319-327.

[35] Clare, J. J. (2010). "Targeting Ion Channels for Drug Discovery." Discovery Medicine **46**: 253-260.

[36] Kostyuk, P. G., O. A. Krishtal, et al. (1975). "EFFECT OF INTERNAL FLUORIDE AND PHOSPHATE ON MEMBRANE CURRENTS DURING INTRACELLULAR DIALYSIS OF NERVE-CELLS." Nature **257**(5528): 691-693.

[37] Dale, T. J., C. Townsend, et al. (2007). "Population patch clamp electrophysiology: a breakthrough technology for ion channel screening." Molecular Biosystems **3**(10): 714-722.

[38] Choi, K. H., C. Song, et al. (2011). "Pharmacological studies of Ca(v)3.1 T-type calcium channels using automated patch-clamp techniques." General Physiology and Biophysics **30**(1): 100-105.

[39] Vilums, M., J. Overman, et al. (2012). "Understanding of Molecular Substructures that Contribute to hERG K+ Channel Blockade: Synthesis and Biological Evaluation of E-4031 Analogues." Chemmedchem **7**(1): 107-113.

[40] Scheel, O., H. Himmel, et al. (2011). "Introduction of a Modular Automated Voltage-Clamp Platform and Its Correlation with Manual Human Ether-a-go-go Related Gene Voltage-Clamp Data." Assay and Drug Development Technologies **9**(6): 600-607.

[41] Berridge, M. J. (1993). "INOSITOL TRISPHOSPHATE AND CALCIUM SIGNALING." Nature **361**(6410): 315-325.

[42] Petersen, O. H., C. C. H. Petersen, et al. (1994). "CALCIUM AND HORMONE ACTION." Annual Review of Physiology **56**: 297-319.

[43] Clapham, D. E. (1995). "CALCIUM SIGNALING." Cell **80**(2): 259-268.

[44] Berridge, M. J. (1998). "Neuronal calcium signaling." Neuron **21**(1): 13-26.

[45] Hirota, S., P. Helli, et al. (2007). "Ionic mechanisms and Ca2+ handling in airway smooth muscle." European Respiratory Journal **30**(1): 114-133.

[46] West, D. J. and A. J. Williams (2007). "Pharmacological regulators of intracellular calcium release channels." Current Pharmaceutical Design **13**(24): 2428-2442.

[47] Feske, S. (2007). "Calcium signalling in lymphocyte activation and disease." Nature Reviews Immunology **7**(9): 690-702.

[48] Webb, S. E. and A. L. Miller (2007). "Ca2+ signalling and early embryonic patterning during zebrafish development." Clinical and Experimental Pharmacology and Physiology **34**(9): 897-904.

[49] Boelens, J., S. Lust, et al. (2007). "The endoplasmic reticulum: A target for new anticancer drugs." In Vivo **21**(2): 215-226.

[50] Ridgway, E. B. and C. C. Ashley (1967). "CALCIUM TRANSIENTS IN SINGLE MUSCLE FIBERS." Biochemical and Biophysical Research Communications **29**(2): 229-&.

[51] Grynkiewicz, G., M. Poenie, et al. (1985). "A NEW GENERATION OF CA-2+ INDICATORS WITH GREATLY IMPROVED FLUORESCENCE PROPERTIES." Journal of Biological Chemistry **260**(6): 3440-3450.

[52] Minta, A., J. P. Y. Kao, et al. (1989). "FLUORESCENT INDICATORS FOR CYTOSOLIC CALCIUM BASED ON RHODAMINE AND FLUORESCEIN CHROMOPHORES." Journal of Biological Chemistry **264**(14): 8171-8178.

[53] Tsien, R. Y. (1980). "NEW CALCIUM INDICATORS AND BUFFERS WITH HIGH SELECTIVITY AGAINST MAGNESIUM AND PROTONS - DESIGN, SYNTHESIS, AND PROPERTIES OF PROTOTYPE STRUCTURES." Biochemistry **19**(11): 2396-2404.

[54] Tsien, R. Y. (1981). "A NON-DISRUPTIVE TECHNIQUE FOR LOADING CALCIUM BUFFERS AND INDICATORS INTO CELLS." Nature **290**(5806): 527-528.

[55] Tsien, R. Y., T. Pozzan, et al. (1982). "CALCIUM HOMEOSTASIS IN INTACT LYMPHOCYTES - CYTOPLASMIC FREE CALCIUM MONITORED WITH A NEW, INTRACELLULARLY TRAPPED FLUORESCENT INDICATOR." Journal of Cell Biology **94**(2): 325-334.

[56] Williams, D. A., K. E. Fogarty, et al. (1985). "CALCIUM GRADIENTS IN SINGLE SMOOTH-MUSCLE CELLS REVEALED BY THE DIGITAL IMAGING MICROSCOPE USING FURA-2." Nature **318**(6046): 558-561.

[57] Ammann, D. (1986). Ion-selective microelectrodes: principles, design and application, Springer-Verlag, Berlin, Heidelburg etc.

[58] Wuhrmann, P., H. Ineichen, et al. (1979). "CHANGE IN NUCLEAR POTASSIUM ELECTROCHEMICAL ACTIVITY AND PUFFING OF POTASSIUM-SENSITIVE SALIVARY CHROMOSOME REGIONS DURING CHIRONOMUS DEVELOPMENT." Proceedings of the National Academy of Sciences of the United States of America **76**(2): 806-808.

[59] Schmidt, C., M. Mayer, et al. (2000). "A chip-based biosensor for the functional analysis of single ion channels." Angewandte Chemie-International Edition **39**(17): 3137-3140.

[60] Lehnert, T., D. M. T. Nguyen, et al. (2007). "Glass reflow on 3-dimensional micro-apertures for electrophysiological measurements on-chip." Microfluidics and Nanofluidics **3**(1): 109-117.

[61] Alberti, M., D. Snakenborg, et al. (2010). "Characterization of a patch-clamp microchannel array towards neuronal networks analysis." Microfluidics and Nanofluidics **9**(4-5): 963-972.

[62] Curtis, J. C., K. Baldwin, et al. (2008). "Seal formation in silicon planar patch-clamp microstructures." Journal of Microelectromechanical Systems **17**(4): 974-983.

[63] Brueggemann, A., M. George, et al. (2004). "Ion channel drug discovery and research: the automated Nano-Patch-Clamp technology." Current drug discovery technologies **1**(1): 91-96.

[64] Bruggemann, A., S. Stoelzle, et al. (2006). "Microchip technology for automated and parallel patch-clamp recording." Small **2**(7): 840-846.

[65] Fertig, N., C. Meyer, et al. (2001). "Microstructured glass chip for ion-channel electrophysiology." Physical Review E **64**(4).

[66] Dunlop, J., M. Bowlby, et al. (2008). "High-throughput electrophysiology: an emerging paradigm for ion-channel screening and physiology." Nature Reviews Drug Discovery **7**(4): 358-368.

[67] Marban, E., T. J. Rink, et al. (1980). "FREE CALCIUM IN HEART-MUSCLE AT REST AND DURING CONTRACTION MEASURED WITH CA-2+-SENSITIVE MICROELECTRODES." Nature **286**(5776): 845-850.

[68] Smith, P. J. S., K. Hammar, et al. (1999). "Self-referencing, non-invasive, ion selective electrode for single cell detection of trans-plasma membrane calcium flux." Microscopy Research and Technique **46**(6): 398-417.

[69] Kang, T. M., V. S. Markin, et al. (2003). "Ion fluxes in giant excised cardiac membrane patches detected and quantified with ion-selective microelectrodes." Journal of General Physiology **121**(4): 325-347.

[70] Bakker, E., P. Buhlmann, et al. (1997). "Carrier-based ion-selective electrodes and bulk optodes. 1. General characteristics." Chemical Reviews **97**(8): 3083-3132.

[71] Pioda, L. A. R., V. Stankova, et al. (1969). "HIGHLY SELECTIVE POTASSIUM ION RESPONSIVE LIQUID-MEMBRANE ELECTRODE." Analytical Letters **2**(12): 665-&.

[72] Meier, P. C., W. E. Morf, et al. (1984). "EVALUATION OF THE OPTIMUM COMPOSITION OF NEUTRAL-CARRIER MEMBRANE ELECTRODES WITH INCORPORATED CATION-EXCHANGER SITES." Analytica Chimica Acta **156**(JAN): 1-8.

[73] Berrocal, M. J., I. H. A. Badr, et al. (2001). "Reducing the thrombogenicity of ion-selective electrode membranes through the use of a silicone-modified segmented polyurethane." Analytical Chemistry **73**(21): 5328-5333.

[74] Lindner, E., V. V. Cosofret, et al. (1994). "ION-SELECTIVE MEMBRANES WITH LOW PLASTICIZER CONTENT - ELECTROANALYTICAL CHARACTERIZATION AND BIOCOMPATIBILITY STUDIES." Journal of Biomedical Materials Research **28**(5): 591-601.

[75] Yun, S. Y., Y. K. Hong, et al. (1997). "Potentiometric properties of ion-selective electrode membranes based on segmented polyether urethane matrices." Analytical Chemistry **69**(5): 868-873.

[76] Cha, G. S., D. Liu, et al. (1991). "ELECTROCHEMICAL PERFORMANCE, BIOCOMPATIBILITY, AND ADHESION OF NEW POLYMER MATRICES FOR SOLID-STATE ION SENSORS." Analytical Chemistry **63**(17): 1666-1672.

[77] Fouskaki, M. and N. A. Chaniotakis (2005). "Thick membrane, solid contact ion selective electrode for the detection of lead at picomolar levels." Analytical Chemistry **77**(6): 1780-1784.

[78] Zhu, Z. Q., J. Zhang, et al. (2007). "Fabrication and characterization of potassium ion-selective electrode based on porous silicon." Ieee Sensors Journal **7**(1-2): 38-42.

[79] Nagele, M., Y. M. Mi, et al. (1998). "Influence of lipophilic inert electrolytes on the selectivity of polymer membrane electrodes." Analytical Chemistry **70**(9): 1686-1691.

[80] Morf, W. E. (1981). The principles of ion-selective electrodes and of membrane transport. M. W.E, Elsevier. **Volume 2**

[81] Pandey, S., R. Mehrotra, et al. (2004). "Characterization of a MEMS BioChip for planar patch-clamp recording." Solid-State Electronics **48**(10-11): 2061-2066.

[82] Schaffer, C. B., A. Brodeur, et al. (2001). "Micromachining bulk glass by use of femtosecond laser pulses with nanojoule energy." Optics Letters **26**(2): 93-95.

[83] Glezer, E. N., M. Milosavljevic, et al. (1996). "Three-dimensional optical storage inside transparent materials." Optics Letters **21**(24): 2023-2025.

[84] Kawata, S. and H. B. Sun (2003). "Two-photon photopolymerization as a tool for making micro-devices." Applied Surface Science **208**: 153-158.

[85] Marcinkevicius, A., S. Juodkazis, et al. (2001). "Femtosecond laser-assisted three-dimensional microfabrication in silica." Optics Letters **26**(5): 277-279.

[86] Davis, K. M., K. Miura, et al. (1996). "Writing waveguides in glass with a femtosecond laser." Optics Letters **21**(21): 1729-1731.

[87] Will, M., S. Nolte, et al. (2002). "Optical properties of waveguides fabricated in fused silica by femtosecond laser pulses." Applied Optics **41**(21): 4360-4364.

[88] Li, Y., K. Itoh, et al. (2001). "Three-dimensional hole drilling of silica glass from the rear surface with femtosecond laser pulses." Optics Letters **26**(23): 1912-1914.

[89] Leong, K. H., A. A. Said, et al. (2001). Femtosecond micromachining applications for electro-optic components. 51st Electronic Components & Technology Conference. New York, Ieee**:** 210-214.

[90] Chen, X. L. and X. B. Liu (1999). "Short pulsed laser machining: How short is short enough?" Journal of Laser Applications **11**(6): 268-272.

[91] Perry, M. D., B. C. Stuart, et al. (1999). "Ultrashort-pulse laser machining of dielectric materials." Journal of Applied Physics **85**(9): 6803-6810.

[92] Chichkov, B. N., C. Momma, et al. (1996). "Femtosecond, picosecond and nanosecond laser ablation of solids." Applied Physics a-Materials Science & Processing **63**(2): 109-115.

[93] Kruger, J., W. Kautek, et al. (1998). "Laser micromachining of barium aluminium borosilicate glass with pulse durations between 20 fs and 3 ps." Applied Surface Science **127**: 892-898.

[94] Gyurcsanyi, R. E., N. Rangisetty, et al. (2004). "Microfabricated ISEs: critical comparison of inherently conducting polymer and hydrogel based inner contacts." Talanta **63**(1): 89-99.

[95] Bobacka, J. (2006). "Conducting polymer-based solid-state ion-selective electrodes." Electroanalysis **18**(1): 7-18.

[96] Michalska, A. (2006). "Optimizing the analytical performance and construction of ion-selective electrodes with conducting polymer-based ion-to-electron transducers." Analytical and Bioanalytical Chemistry **384**(2): 391-406.

[97] Wang, T. J., Y. Q. Qi, et al. (2005). "Effects of poly(ethylene glycol) on electrical conductivity of poly (3,4-ethylenedioxythiophene)-poly(styrenesulfonic acid) film." Applied Surface Science **250**(1-4): 188-194.

[98] Lindner, E., V. V. Cosofret, et al. (1993). "IN-VIVO AND IN-VITRO TESTING OF MICROELECTRONICALLY FABRICATED PLANAR SENSORS DESIGNED FOR APPLICATIONS IN CARDIOLOGY." Fresenius Journal of Analytical Chemistry **346**(6-9): 584-588.

[99] Picollet-D'hahan, N., F. Sauter, et al. (2003). Multi-Patch: A chip-based ion-channel assay system for drug screening. Los Alamitos, Ieee Computer Soc.

[100] Shah, L., J. Tawney, et al. (2001). "Femtosecond laser deep hole drilling of silicate glasses in air." Applied Surface Science **183**(3-4): 151-164.

[101] Wei, J., H. Xie, et al. (2003). "Low temperature wafer anodic bonding." Journal of Micromechanics and Microengineering **13**(2): 217-222.

[102] Gabriel, M., B. Johnson, et al. (2006). "Wafer direct bonding with ambient pressure plasma activation." Microsystem Technologies-Micro-and Nanosystems-Information Storage and Processing Systems **12**(5): 397-400.

[103] Cranny, A. W. J. and J. K. Atkinson (1998). "Thick film silver silver chloride reference electrodes." Measurement Science & Technology **9**(9): 1557-1565.

[104] Schonert, H. (1968). "A GENERALIZATION OF NERST-PLANCK MOTION EQUATIONS FOR MULTI-COMPONENT ELECTROLYTE SYSTEMS .2. STANDARD." Zeitschrift Fur Physikalische Chemie-Frankfurt **57**(3-6): 164-&.

[105] Kodandaramaiah, S. B., G. T. Franzesi, et al. (2012). "Automated whole-cell patch-clamp electrophysiology of neurons in vivo." Nature Methods **9**(6): 585-+.

[106] Bakker, E. (1997). "Determination of unbiased selectivity coefficients of neutral carrier-based cation-selective electrodes." Analytical Chemistry **69**(6): 1061-1069.

[107] Bedlechowicz-Sliwakowska, I., P. Lingenfelter, et al. (2006). "Ion-selective electrode for measuring low Ca2+ concentrations in the presence of high K+, Na+ and Mg2+ background." Analytical and Bioanalytical Chemistry **385**(8): 1477-1482.

[108] Lindner, E., V. V. Cosofret, et al. (1994). "ION-SELECTIVE MEMBRANES WITH LOW PLASTICIZER CONTENT - ELECTROANALYTICAL CHARACTERIZATION AND BIOCOMPATIBILITY STUDIES." Journal of Biomedical Materials Research **28**(5): 591-601.

[109] Liu, D., M. E. Meyerhoff, et al. (1993). "POTENTIOMETRIC ION-SELECTIVE AND BIOSELECTIVE ELECTRODES BASED ON ASYMMETRIC POLYURETHANE MEMBRANES." Analytica Chimica Acta **274**(1): 37-46.

[110] Paciorek, R., P. D. van der Wal, et al. (2003). "Optimization of the composition of interfaces in miniature planar chloride electrodes." Electroanalysis **15**(15-16): 1314-1318.

[111] Buck, R. P. and E. Lindner (1994). "RECOMMENDATIONS FOR NOMENCLATURE OF ION-SELECTIVE ELECTRODES - (IUPAC RECOMMENDATIONS 1994)." Pure and Applied Chemistry **66**(12): 2527-2536.

APPENDICES

Appendix A Silicon based planar patch clamp devices

A 1 Currently available silicon-based planar patch clamp devices

Author, Year	Passivation and thickness	Aperture diameter (µm)	Aperture depth (µm)	Aperture roughness (nm)	Seal resistance/Gigaseal success rate	Capacitance (pF)	Access resistance (MΩ)	Biological sample	Whole-cell?
Schmidt 2000 [59]	20nm PECVD SiO2 on top of 0.1-1um PECVD Si3N4	0.6 to 7	100nm	NR	1.4 to >200	<35	NR	Vesicles	No
Lehnert 2002 (Micronozzle) [60]	Thermal SiO2	>= 2.5	10 to 30 um	<10nm pp-nozzle rim; 70nm inner nozzle surface	0.1 to 0.2	150	1.4 to 2.3	Chinese hamster ovary cells (CHO)	No
Picollet D'hahan 2003 [99]	Thermal SiO2 (1 um)	2.5	1	NR	NR	NR	NR	Xenopus Oocyte	No
Panjota 2004 [12]	PECVD SiO2 (0.5 to 2)	0.7 to 1 (nanopores)	10 to 20	NR	51 Mohm (CHO-K1); 52MΩ (RAW 264.7)	>15 (with PDMS)	NR	RAW 264.7, CHO-K1, HIT-T15 and RIN m5F cells	Yes (HIT-T15 and RAW 264.7)
Panjota 2004 [12]	PECVD SiO2 (0.5 to 2)	1.5 to 2 (micropores)	20 to 40	NR	0.14 to 1.5 G-Ω (CHO-K1); 81 MΩ (RAW 264.7)	>15 (with PDMS)	3 to 5	RAW 264.7, CHO-K1, HIT-T15 and RIN m5F cells	Yes (HIT-T15 and RAW 264.7)
Pandev 2004 [81]	100 nm Si3N4/200nm SiO2	3 to 20	~0.3	NR	NR	800	1	None	No
Matthews 2006 [14]	Thermal SiO2 (2 um)	0.3 to 12	20	NR	>1	17.4pF/mm^2	0.2 to 47	CHO-K1	No
Sordel 2006 [13]	PECVD SiO2 (0.5 to 1.5 um) + Thermal SiO2	2.5	2.5 to 3.5	2.55 nm (RMS)	>1 G-Ωs; 4-9%	54	0.55 to 1.15	CHO, HEK-293	Yes
Sordel 2006 [13]	Thermal SiO2 only	2.5	2	0.24nm	0%	75	NR	CHO, HEK-293	Yes
Zhang 2008 [16]	Thermal SiO2 (0.2 um)	1.2	~5.7	NR	NR	NR	NR	TRPV1-tranfected HECK-293 cells	Yes
Curtis 2008 [62]	Thermal SiO2 (2.5um) boron doped/undoped	1.5 to 2.5	7 to 12	Undoped: 0.17nm; doped: 0.18 nm	82.3 MΩ (doped)	101-193	2.51	Neuroblastoma cell	Yes
Curtis 2008 [62]	PECVD SiO2 (1um) boron doped/undoped	1.5 to 2.5	7 to 12	Undoped: 1.13 nm; doped: 0.33 nm	34MΩ (doped)	56	1.34	Neuroblastoma cell	Yes

Appendix B Microfabrication Process & Mask Layouts

B 1 Photomask for Ti – Pt deposition

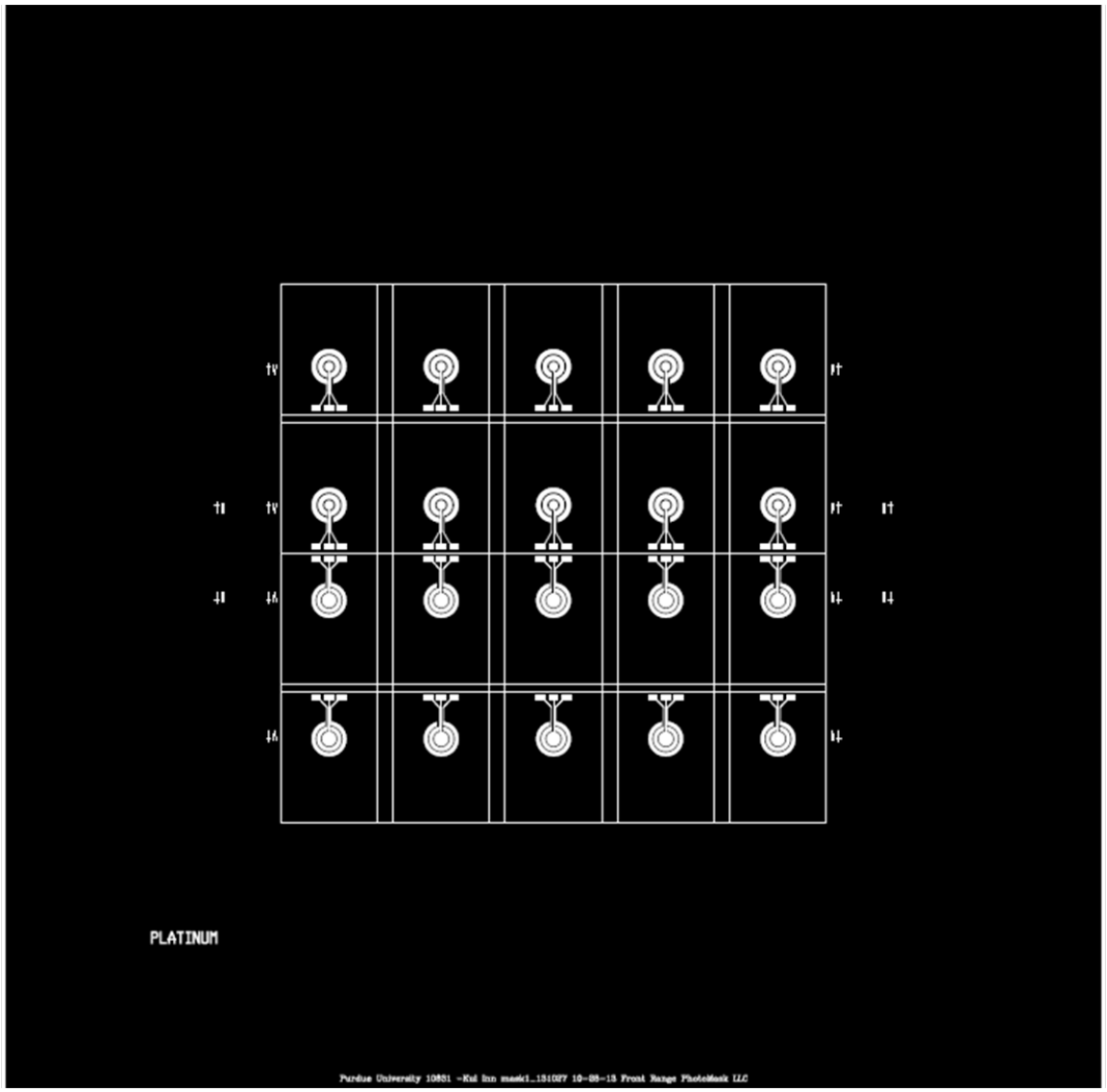

B 2 Photomask for Passivation

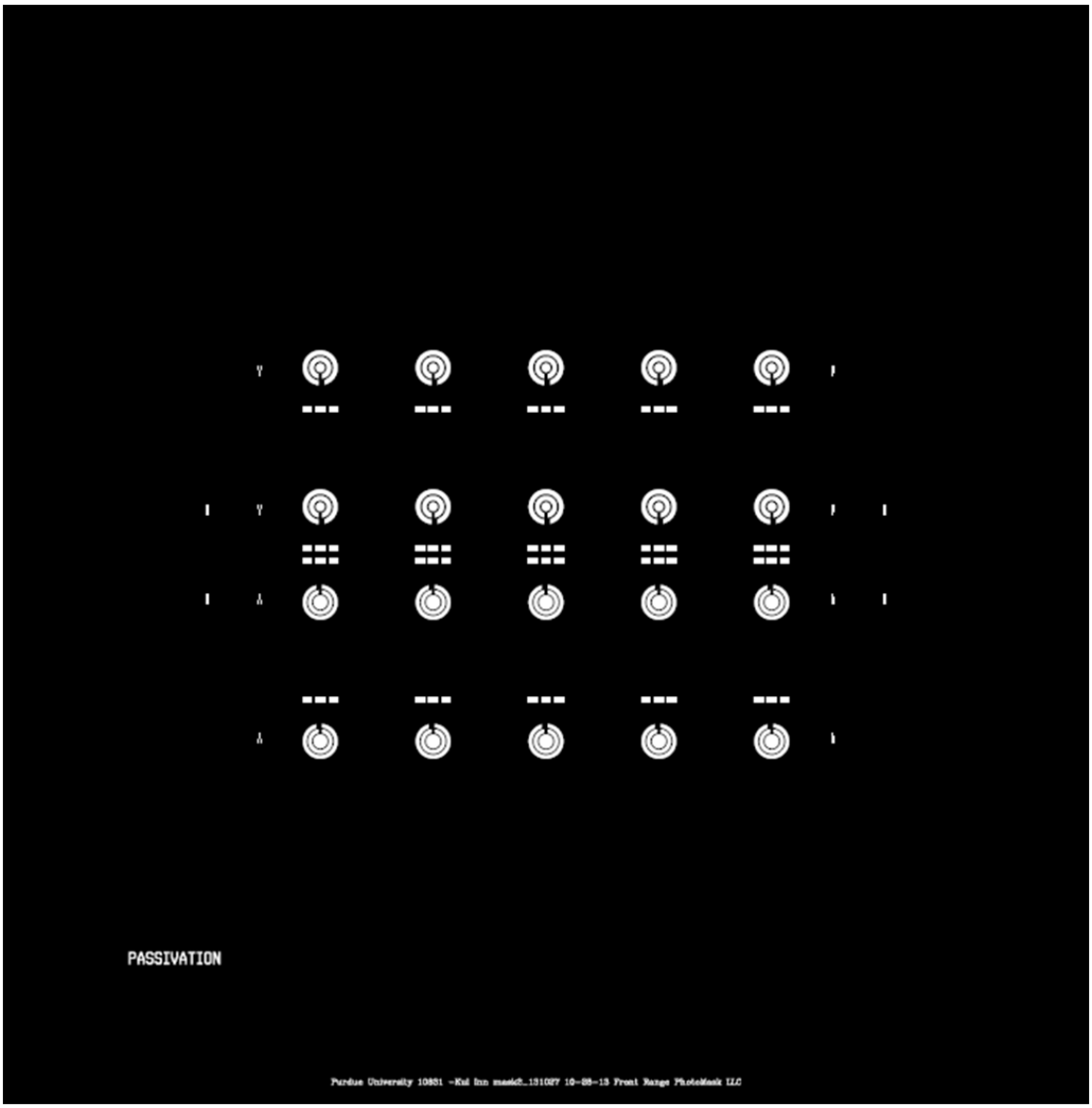

B 3 Photomask for silver deposition

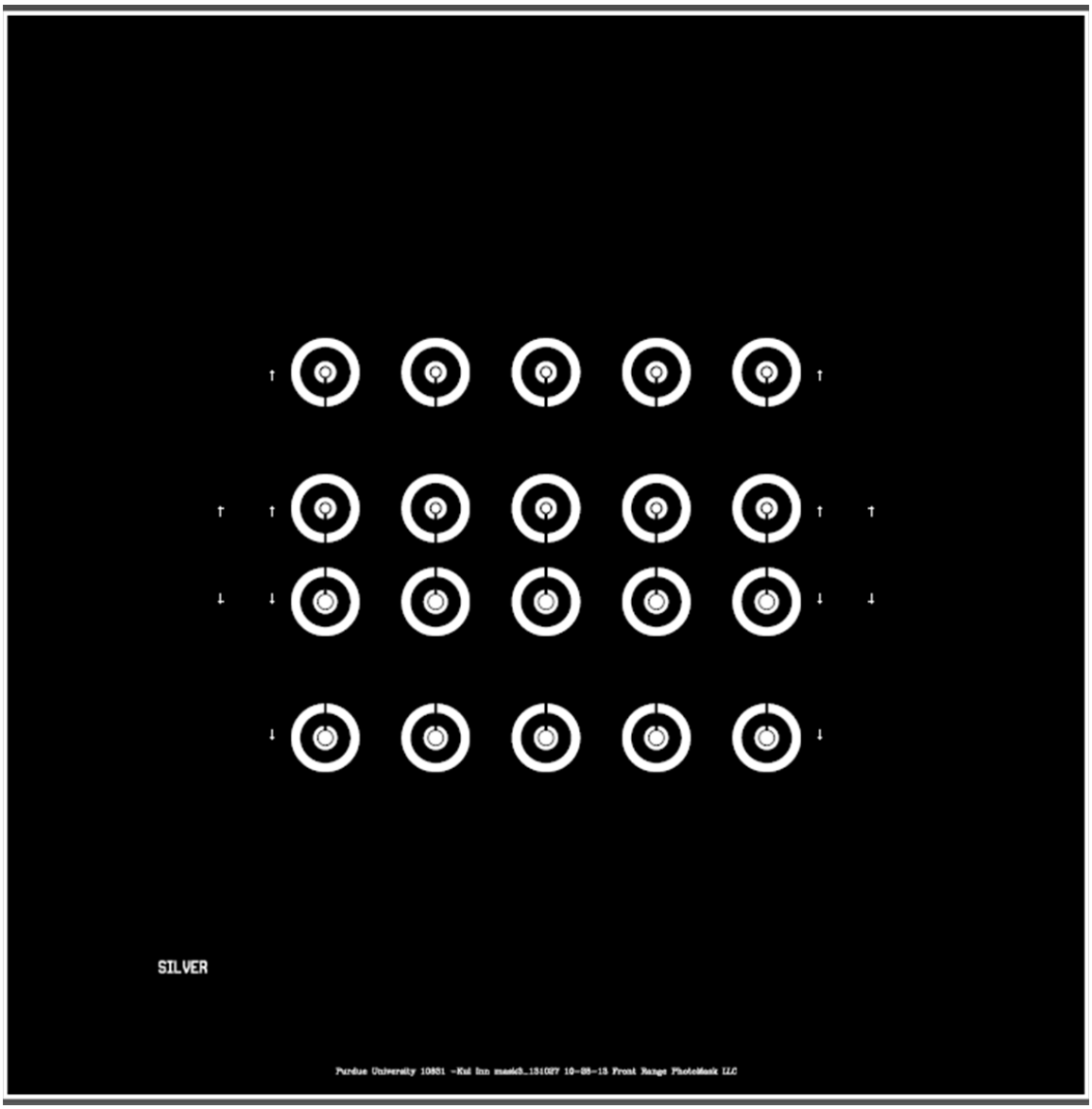

B 4 Working electrode microfabrication process

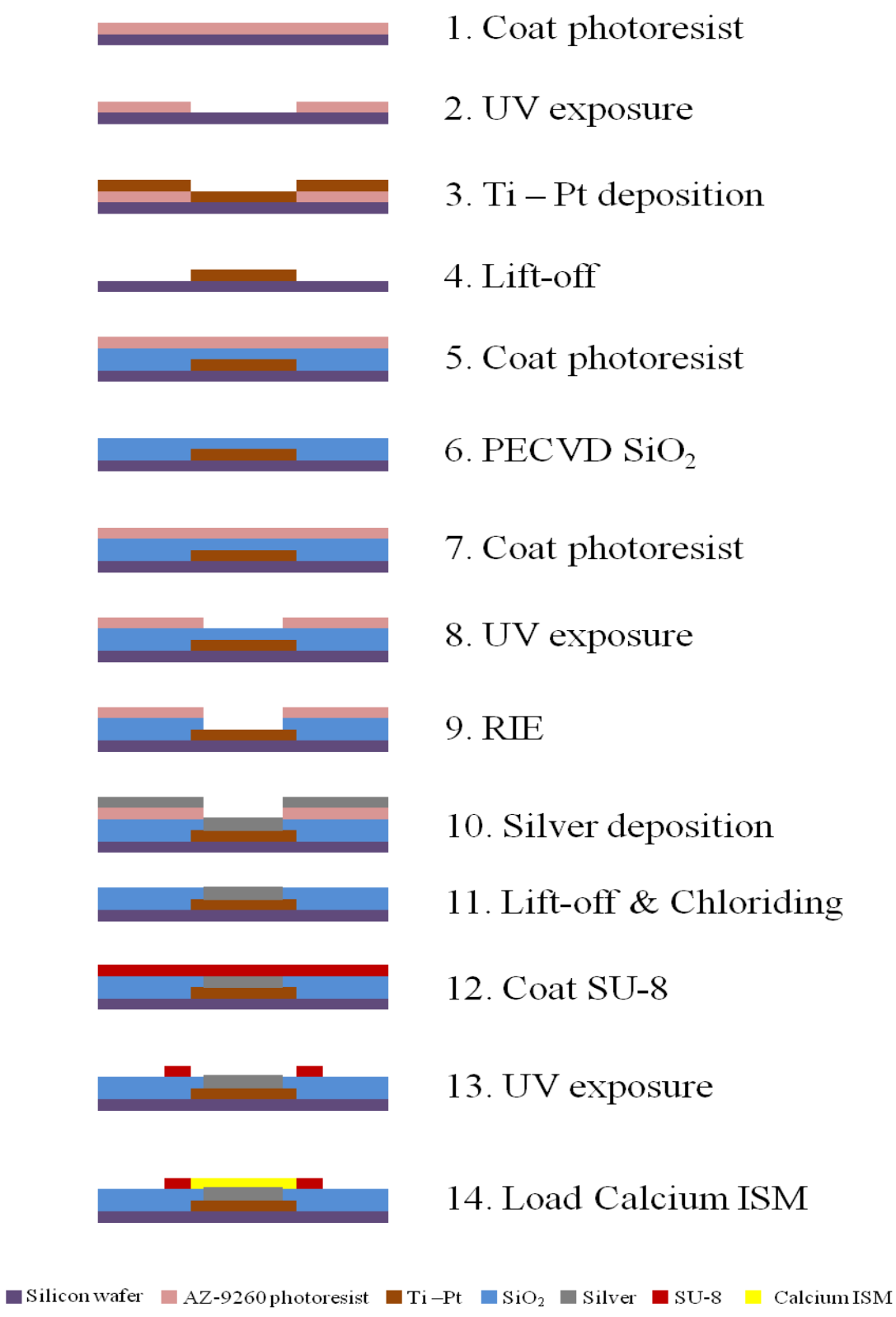

VITA

VITA

Kul Inn received his Bachelor of Science degree from the Department of Mechanical Engineering, Purdue University, West Lafayette, IN, in 2009. He completed Master of Science in Mechanical Engineering, Purdue University, West Lafayette, IN, in 2011, and transferred to the Department of Agricultural & Biological Engineering, Purdue University, West Lafayette, IN, to join Physiological Sensing Facilities as a Ph.D. student and a research assistant. His research works include Optical oxygen sensing in food packaging, hardware & software automation of diagnostic device, and development of planar patch-clamp with calcium ion-selective electrode. He will receive his Ph.D. degree in the Department of Agricultural & Biological Engineering in December of 2014.